

Global wheat production with 1.5 and 2.0°C above pre-industrial warming

Bing Liu¹ | Pierre Martre² | Frank Ewert^{3,4} | John R. Porter^{5,6,7} | Andy J. Challinor^{8,9} | Christoph Müller¹⁰ | Alex C. Ruane¹¹ | Katharina Waha¹²  | Peter J. Thorburn¹² | Pramod K. Aggarwal¹³ | Mukhtar Ahmed^{14,15} | Juraj Balkovič^{16,17}  | Bruno Basso^{18,19}  | Christian Biernath²⁰ | Marco Bindi²¹ | Davide Cammarano²²  | Giacomo De Sanctis^{23,†}  | Benjamin Dumont²⁴ | Mónica Espadafor²⁵ | Ehsan Eyshi Rezaei^{3,26} | Roberto Ferrise²¹ | Margarita Garcia-Vila²⁵ | Sebastian Gayler²⁷ | Yujing Gao²⁸ | Heidi Horan¹² | Gerrit Hoogenboom^{28,29} | Roberto C. Izaurralde^{30,31} | Curtis D. Jones³⁰  | Belay T. Kassie²⁸ | Kurt C. Kersebaum⁴ | Christian Klein²⁰ | Ann-Kristin Koehler⁸ | Andrea Maiorano^{2,32} | Sara Minoli¹⁰  | Manuel Montesino San Martin⁵ | Soora Naresh Kumar³³ | Claas Nendel⁴ | Garry J. O'Leary³⁴ | Taru Palosuo³⁵ | Eckart Priesack²⁰ | Dominique Ripoche³⁶ | Reimund P. Rötter^{37,38} | Mikhail A. Semenov³⁹ | Claudio Stöckle¹⁴ | Thilo Streck²⁷ | Iwan Supit⁴⁰ | Fulu Tao^{35,41}  | Marijn Van der Velde⁴² | Daniel Wallach⁴³ | Enli Wang⁴⁴ | Heidi Webber^{3,4}  | Joost Wolf⁴⁵ | Liujun Xiao^{1,28} | Zhao Zhang⁴⁶ | Zhigan Zhao^{44,47} | Yan Zhu¹  | Senthold Asseng²⁸ 

¹National Engineering and Technology Center for Information Agriculture, Key Laboratory for Crop System Analysis and Decision Making, Ministry of Agriculture, Jiangsu Key Laboratory for Information Agriculture, Jiangsu Collaborative Innovation Center for Modern Crop Production, Nanjing Agricultural University, Nanjing, China

²LEPSE, Université Montpellier, INRA, Montpellier SupAgro, Montpellier, France

³Institute of Crop Science and Resource Conservation INRES, University of Bonn, Bonn, Germany

⁴Leibniz Centre for Agricultural Landscape Research (ZALF), Müncheberg, Germany

⁵Plant & Environment Sciences, University Copenhagen, Taastrup, Denmark

⁶Lincoln University, Lincoln, New Zealand

⁷Montpellier SupAgro, INRA, CIHEAM-IAMM, CIRAD, University Montpellier, Montpellier, France

⁸Institute for Climate and Atmospheric Science, School of Earth and Environment, University of Leeds, Leeds, UK

⁹CGIAR-ESSP Program on Climate Change, Agriculture and Food Security, International Centre for Tropical Agriculture (CIAT), Cali, Colombia

¹⁰Potsdam Institute for Climate Impact Research, Member of the Leibniz Association, Potsdam, Germany

¹¹NASA Goddard Institute for Space Studies, New York, New York

¹²CSIRO Agriculture and Food, Brisbane, Qld, Australia

¹³CGIAR Research Program on Climate Change, Agriculture and Food Security, BISA-CIMMYT, New Delhi, India

¹⁴Biological Systems Engineering, Washington State University, Pullman, Washington

¹⁵Department of agronomy, Pir Mehr Ali Shah Arid Agriculture University, Rawalpindi, Pakistan

Authors from P.K.A. to Z.Z. are listed in alphabetical order.

[†]The views expressed in this paper are the views of the author and do not necessarily represent the views of the organization or institution, with which he is currently affiliated.

- ¹⁶International Institute for Applied Systems Analysis, Ecosystem Services and Management Program, Laxenburg, Austria
- ¹⁷Department of Soil Science, Faculty of Natural Sciences, Comenius University in Bratislava, Bratislava, Slovakia
- ¹⁸Department of Earth and Environmental Sciences, Michigan State University East Lansing, East Lansing, Michigan
- ¹⁹W.K. Kellogg Biological Station, Michigan State University, East Lansing, Michigan
- ²⁰Institute of Biochemical Plant Pathology, Helmholtz Zentrum München—German Research Center for Environmental Health, Neuherberg, Germany
- ²¹Department of Agri-food Production and Environmental Sciences (DISPAA), University of Florence, Florence, Italy
- ²²James Hutton Institute, Dundee, UK
- ²³GMO Unit, European Food Safety Authority, Parma, Italy
- ²⁴Department AgroBioChem & TERRA Teaching and Research Center, Gembloux Agro-Bio Tech, University of Liege, Gembloux, Belgium
- ²⁵IAS-CSIC, Department of Agronomy, University of Cordoba, Cordoba, Spain
- ²⁶Department of Crop Sciences, University of Göttingen, Göttingen, Germany
- ²⁷Institute of Soil Science and Land Evaluation, University of Hohenheim, Stuttgart, Germany
- ²⁸Agricultural & Biological Engineering Department, University of Florida, Gainesville, Florida
- ²⁹Institute for Sustainable Food Systems, University of Florida, Gainesville, Florida
- ³⁰Department of Geographical Sciences, University of Maryland, College Park, Maryland
- ³¹Texas A&M AgriLife Research and Extension Center, Texas A&M Univ., Temple, Texas
- ³²European Food Safety Authority, Parma, Italy
- ³³Centre for Environment Science and Climate Resilient Agriculture, Indian Agricultural Research Institute, IARI PUSA, New Delhi, India
- ³⁴Department of Economic Development, Jobs, Transport and Resources, Grains Innovation Park, Agriculture Victoria Research, Horsham, Vic., Australia
- ³⁵Natural Resources Institute Finland (Luke), Helsinki, Finland
- ³⁶US AgroClim, INRA, Avignon, France
- ³⁷University of Göttingen, Tropical Plant Production and Agricultural Systems Modelling (TROPAGS), Göttingen, Germany
- ³⁸Centre of Biodiversity and Sustainable Land Use (CBL), University of Göttingen, Göttingen, Germany
- ³⁹Rothamsted Research, Harpenden, UK
- ⁴⁰Water Systems & Global Change Group and WENR (Water & Food), Wageningen University, Wageningen, The Netherlands
- ⁴¹Institute of Geographical Sciences and Natural Resources Research, Chinese Academy of Science, Beijing, China
- ⁴²European Commission, Joint Research Centre, Ispra, Italy
- ⁴³UMRAGIR, Castanet-Tolosan, France
- ⁴⁴CSIRO Agriculture and Food, Black Mountain, ACT, Australia
- ⁴⁵Plant Production Systems, Wageningen University, Wageningen, The Netherlands
- ⁴⁶State Key Laboratory of Earth Surface Processes and Resource Ecology, Faculty of Geographical Science, Beijing Normal University, Beijing, China
- ⁴⁷Department of Agronomy and Biotechnology, China Agricultural University, Beijing, China

Correspondence

Yan Zhu, National Engineering and Technology Center for Information Agriculture, Key Laboratory for Crop System Analysis and Decision Making, Ministry of Agriculture, Jiangsu Key Laboratory for Information Agriculture, Jiangsu Collaborative Innovation Center for Modern Crop Production, Nanjing Agricultural University, Nanjing, Jiangsu, China.
Email: yanzhu@njau.edu.cn
and
Senthold Asseng, Agricultural & Biological Engineering Department, University of Florida, Gainesville, FL.
Email: sasseng@ufl.edu

Funding information

Agricultural Model Intercomparison and Improvement Project (AgMIP);
Biotechnology and Biological Sciences Research Council (BBSRC), Grant/Award Number: BB/, P016855/1

Abstract

Efforts to limit global warming to below 2°C in relation to the pre-industrial level are under way, in accordance with the 2015 Paris Agreement. However, most impact research on agriculture to date has focused on impacts of warming >2°C on mean crop yields, and many previous studies did not focus sufficiently on extreme events and yield interannual variability. Here, with the latest climate scenarios from the Half a degree Additional warming, Prognosis and Projected Impacts (HAPPI) project, we evaluated the impacts of the 2015 Paris Agreement range of global warming (1.5 and 2.0°C warming above the pre-industrial period) on global wheat production and local yield variability. A multi-crop and multi-climate model ensemble over a global network of sites developed by the Agricultural Model Intercomparison and Improvement Project (AgMIP) for Wheat was used to represent major rainfed and irrigated wheat cropping systems. Results show that projected global wheat production will change by −2.3% to 7.0% under the 1.5°C scenario and −2.4% to 10.5% under the 2.0°C scenario, compared to a baseline of 1980–2010, when considering changes in local temperature, rainfall, and global atmospheric CO₂

concentration, but no changes in management or wheat cultivars. The projected impact on wheat production varies spatially; a larger increase is projected for temperate high rainfall regions than for moderate hot low rainfall and irrigated regions. Grain yields in warmer regions are more likely to be reduced than in cooler regions. Despite mostly positive impacts on global average grain yields, the frequency of extremely low yields (bottom 5 percentile of baseline distribution) and yield interannual variability will increase under both warming scenarios for some of the hot growing locations, including locations from the second largest global wheat producer—India, which supplies more than 14% of global wheat. The projected global impact of warming $<2^{\circ}\text{C}$ on wheat production is therefore not evenly distributed and will affect regional food security across the globe as well as food prices and trade.

KEYWORDS

1.5°C warming, climate change, extreme low yields, food security, model ensemble, wheat production

1 | INTRODUCTION

The global community agreed with the Paris agreement to limiting global warming to 2.0°C , with the stated ambition to attempt to cap warming at 1.5°C (UNFCCC, 2015). While limiting the extent of climate change is critical, the more ambitious 1.5°C mitigation strategy will likely require considerable mitigation effort in the agricultural land use sector (Fujimori et al., 2018), with some studies suggesting this would actually have more negative consequence for food security than climate change impacts of 2.0°C (Frank et al., 2017; Ruane, Antle, et al., 2018; van Meijl et al., 2018). However, these economic land use studies generally only consider the average effects of climate change and not the changes in yield variability and risk of yield failure, key factors constraining intensification efforts in many developing regions (Kalkuhl, Braun, & Torero, 2016). Further such studies have generally not considered real cultivars nor typical production conditions.

Agricultural production and food security is one of many sectors already affected by climate change (Davidson, 2016; Porter, Xie, & Challinor, 2014). Wheat is one of the most important food crops, providing a substantial portion of calories for about four billion people (Shiferaw et al., 2013). Wheat production systems' response to warming can be substantial (Asseng et al., 2015; Liu et al., 2016; Rosenzweig et al., 2014), but restricted warming levels of $<2.0^{\circ}\text{C}$ global warming above pre-industrial are under-represented in previous assessments (Porter et al., 2014). Thus, assessing the impact of 1.5 and 2.0°C global warming above pre-industrial conditions on crop productivity levels, including the potential benefits of associated carbon dioxide (CO_2) fertilization, and the likelihood of extremely low-yielding wheat harvests, is critical for understanding the challenges of global warming for global food security.

Several simulation studies have assessed the changes in global wheat production due to the changes in climate and CO_2

concentration (Asseng et al., 2015, 2018; Rosenzweig et al., 2014). However, previous studies have almost all considered more extreme warming and most of current studies investigated the impact of global warming $>2.0^{\circ}\text{C}$, which means that previous impact assessments lacked details for $<2^{\circ}\text{C}$ of warming. Also, many previous studies did not focus sufficiently on extreme events and yield interannual variability (Challinor, Martre, Asseng, Thornton, & Ewert, 2014; Challinor, Watson, et al., 2014; Porter et al., 2014). Therefore, in terms of food security, it is important to analyze the effect of the new 1.5 and 2.0°C warming scenarios on the interannual variability of crop production. In particular, studies on impact of 1.5 and 2.0°C global warming on wheat production at a global and regional scale are missing.

Process-based crop simulation models, as tools to quantify the complexity of crop growth as driven by climate, soil, and management practice, have been widely used in climate change impact assessments at different spatial scales (Challinor, Martre, et al., 2014; Challinor, Watson, et al., 2014; Chenu et al., 2017; Ewert, Rötter, et al., 2015; Porter et al., 2014), including multi-model ensemble approaches (Asseng et al., 2015, 2013; Wang, Martre, et al., 2017; Wang, Lin, et al., 2017). The multi-model ensemble approach has been proven to be a reliable method in reproducing the main effects anticipated for climate change when simulations are compared with field experimental observations (including changes in temperature, heat events, rainfall, atmospheric CO_2 concentration [CO_2], and their interactions) (Asseng et al., 2015, 2013, 2018; Wallach et al., 2018; Wang, Martre, et al., 2017; Wang, Lin, et al., 2017).

Here, we applied a global network of 60 representative wheat production sites and an ensemble of 31 crop models (Asseng et al., 2015, 2018) developed by the Agricultural Model Intercomparison and Improvement Project (AgMIP) Wheat Team (Rosenzweig et al., 2013) with climate scenarios from five Global Climate Models

(GCMs) from the Half a degree Additional warming, Prognosis and Projected Impacts (HAPPI) project (Mitchell et al., 2017; Ruane, Phillips, & Rosenzweig, 2018) to evaluate the impacts of the 2015 Paris Agreement range of global warming (1.5 and 2.0°C warming above the pre-industrial period, referred hereafter as “1.5 scenario” and “2.0 scenario”) on global wheat production and yield interannual variability. We hypothesize that the mean impacts of warming may not differ greatly between the two scenarios as losses due to accelerated development are compensated by gains from elevated CO₂. However, we expect that the higher frequency of extreme events under 2.0°C (Ruane, Phillips, et al., 2018) would result in greater damages of heat and drought stress, greater inter-annual variability, and higher risk of yield failures. Such information could supply important nuance in understanding the implications of the two levels of warming and associated mitigation efforts of the two warming scenarios.

2 | MATERIALS AND METHODS

2.1 | Model inputs for global simulations

An ensemble of 31 wheat crop models was used to assess climate change impacts for 60 representative wheat-growing locations developed by the AgMIP-Wheat team (Asseng et al., 2015, 2018; Wallach et al., 2018). All models in the ensemble were calibrated for the phenology of local cultivars and used site-specific soils and crop management. The multi-model ensemble used here has been tested against observed field data and showed reliable response to changing climate in several previous studies, including responses of model ensemble to elevated CO₂, post-anthesis chronic warming and different heat shock treatments during grain filling (Asseng et al., 2018; Wallach et al., 2018). Hoffman et al. (2015) and Ruane et al. (2016) showed that a multi-model ensemble can also reproduce some of observed seasonal yield variability. The 60 locations are from key wheat-growing regions in the world (Supporting Information Table S1 in Appendix S1). Locations 1–30 are high rainfall or irrigated wheat-growing locations representing 68% of current global wheat production. These locations were simulated without water or nitrogen limitation. Details about these locations can be found in Asseng et al. (2015). Locations 31–60 are low rainfall locations with average wheat yield <4 t/ha and represent 32% of current global wheat production (Asseng et al., 2018).

Thirty-one wheat crop models (Supporting Information Table S2 in Appendix S1) within AgMIP were used for assessing impacts of 1.5 and 2.0°C global warming above pre-industrial time on global wheat production (Asseng et al., 2018). The 31 wheat crop models considered here have been described in publications. All model simulations were executed by the individual modeling groups with expertise in using the model they executed. All modeling groups were provided with daily weather data, basic physical characteristics of soil, initial soil water, and N content by layer and crop management information. One representative cultivar, either winter or spring type, was selected for each location after consulting with local experts or

literature. Different wheat types may be used at different locations in one country (e.g., China, Russia, and United States), to cover some of the possible heterogeneity in cultivar use (Supporting Information Table S1 in Appendix S1). Observed local mean sowing, anthesis, and maturity dates were supplied to modelers with qualitative information on vernalization requirements and photoperiod sensitivity for each cultivar. Observed sowing dates were used and cultivar parameters calibrated with the observed anthesis and maturity dates by considering the qualitative information on vernalization requirements and photoperiod sensitivity. More details about model inputs are provided in the supplementary methods and in Asseng et al. (2018).

2.2 | Future climate projections

Baseline (1980–2010) climate data for each wheat modeling site come from the AgMERRA climate dataset, which combines observations, reanalysis data, and satellite data products to provide daily climate forcing data for agricultural modeling (Ruane, Goldberg, & Chryssanthacopoulos, 2015). Climate scenarios here are consistent with the AgMIP Coordinated Global and Regional Assessments (CGRA) 1.5 and 2.0°C World study (Rosenzweig et al., 2018; Ruane, Antle, et al., 2018; Ruane, Phillips, et al., 2018), utilizing the methods summarized below and in the Supporting Information Appendix S1 and fully described by Ruane, Phillips, et al. (2018). Climate changes from large (83–500 member for each model) climate model ensemble projections of the +1.5 and +2.0°C scenarios from the Half a Degree Additional Warming, Prognosis and Projected Impacts project (HAPPI; Mitchell et al., 2017) are combined with the local AgMERRA baseline to generate driving climate scenarios from five GCMs (MIROC5, NorESM1-M, CanAM4 [HAPPI], CAM4-2degree [HAPPI], and HadAM3P) for each location (Ruane, Phillips, et al., 2018). Only five GCMs here were used due to data availability at the time the study was conducted. Specifically, HAPPI ensemble changes in monthly mean climate, the number of precipitation days, and the standard deviation of daily maximum and minimum temperatures are imposed upon the historical AgMERRA daily series using quantile mapping that forces the observed conditions to mimic the future distribution of daily events (Ruane, Phillips, et al., 2018; Ruane, Winter, McDermid, & Hudson, 2015). This results in climate scenarios that maintain the characteristics of local climate while also capturing major climate changes. As in previous AgMIP assessments, solar radiation changes from GCMs introduce uncertainties that can at times overwhelm the impact of temperature and rainfall changes and thus were not considered here other than small radiation effects associated with changes in the number of precipitation days (Ruane, Winter, et al., 2015).

HAPPI anticipates atmospheric [CO₂] for 1.5 scenario (1.5°C above the 1861–1880 pre-industrial period = ~0.6°C above current global mean temperature; Morice, Kennedy, Rayner, & Jones, 2012) and 2.0 scenario (2.0°C above pre-industrial = ~1.1°C above current global mean temperature) at 423 ppm and 487 ppm ([CO₂] in the center of the 1980–2010 current period is 360 ppm). Uncertainty around these CO₂ levels from climate models' transient and

equilibrium climate sensitivity is not explored here, although [CO₂] for 2.0°C warming may be slightly overestimated (Ruane, Phillips, et al., 2018).

This large climate × crop model setup enabled a robust multi-model ensemble estimate (Martre et al., 2015; Wallach et al., 2018) as well as analysis of spatial heterogeneity (Liu et al., 2016) and inter-model uncertainty. There were 11 treatments (baseline, five GCMs for 1.5 and five GCMs for 2.0 scenarios) simulated for 60 locations and 30 years (see additional detail on climate scenarios in Supporting Information Appendix S1 and in Ruane, Phillips, et al., 2018).

2.3 | Aggregation of local climate change impacts to global wheat production impacts

Simulation results were up-scaled using a stratified sampling method, a guided sampling method to improve the scaling quality (van Bussel et al., 2016), with several points per wheat mega region when necessary (Gbegbelegbe et al., 2017). During the up-scaling process, the simulation result of a location was weighted by the production the location represents as described below (Asseng et al., 2015). Liu et al. (2016) recently showed that stratified sampling with 30 locations across wheat mega regions resulted in similar temperature impact and uncertainty as aggregation of simulated grid cells at country and global scale. And Zhao et al. (2016) indicated that the uncertainty due to sampling decreases with increasing number of sampling points. We therefore doubled the 30 locations from Asseng et al. (2015) to 60 locations (Supporting Information Table S1 in Appendix S1) to cover contrasting conditions across all wheat mega regions.

Before aggregating local impacts at 60 locations to global impacts, we determined the actual production represented by each location following the procedure described by Asseng et al. (2015). The total wheat production for each country came from FAO country wheat production statistics for 2014 (www.fao.org). For each country, wheat production was classified into three categories (i.e., high rainfall, irrigated, and low rainfall). The ratio for each category was quantified based on the Spatial Production Allocation Model (SPAM) dataset (<https://harvestchoice.org/products/data>). For some countries where no data were available through the SPAM dataset, we estimated the ratio for each category based on the country-level yield from FAO country wheat production statistics. The high rainfall production and irrigated production in each country were represented by the nearest high rainfall and irrigated locations (locations 1–30). Low rainfall production in each country was represented by the nearest low rainfall locations (locations 31–60).

For each climate change scenario, we calculated the absolute regional production loss by multiplying the relative yield loss from the multi-model ensemble median (median across 31 models and five GCMs) with the production represented at each location. Global wheat production loss was determined by adding all regional production losses, and the relative impacts on global wheat production were calculated by dividing simulated global production loss by

historical global production. Similar steps with global impacts were used for calculating the impacts on country scale impacts, except that only the local impacts from corresponding locations in each country were aggregated to the country impacts.

We also tested the significance of the differences in the estimated impacts and the changes in simulated yield inter-annual variability between the two warming scenarios. More detailed steps about impact aggregation and significance tests can be found in the supplementary methods.

2.4 | Environmental clustering of the 60 global locations

The 60 global wheat-growing locations were clustered in order to analyze the results by groups of environments with similar climates (Supporting Information Figure S5 in Appendix S1). A hierarchical clustering on principal components of the 60 locations was performed based on four climate variables for 1981–2010: the growing season (sowing to maturity) mean temperature, the growing season cumulative evapotranspiration, the growing season cumulative solar radiation, and the number of heat stress days (maximum daily temperature >32°C) during the grain filling period. All data were scaled (centered and reduced to make the mean and standard deviation of data to be zero and one, respectively) prior to the principal component analysis.

After determining the wheat yield impacts for each of the 1.5 and 2.0°C scenarios, yield variability for both scenarios was assessed, including the extreme low yield probability and yield interannual variability. For each location, we determined the yield threshold of the bottom 5% from the yield series for the baseline period and calculated the cumulative probability series of simulated yields under 1.5 and 2.0°C scenarios. Next, the probability of occurrence for extreme low yield for each scenario was assessed as the corresponding cumulative probability of the yield threshold of the bottom 5% from baseline period from the cumulative probability series. Interannual yield variability was quantified as the coefficient of variation of simulated yields over the 30-year simulation period. In all cases, the multi-model median from the 31 models was employed.

3 | RESULTS

3.1 | Impacts of 2015 Paris Agreement compliant warming

Compared with the present baseline period (1980–2010; 0.67°C above pre-industrial), the HAPPI scenarios gave projected temperature increases of 1.1–1.4°C (25%–75% range of 60 locations) for the 60 wheat-growing locations spread over the globe under the 1.5 scenario and 1.6–2.0°C under the 2.0 scenario (Supporting Information Figure S1 in Appendix S1). Temperature increase during the wheat-growing season (sowing to maturity) typically warms about 0.5°C less than the annual mean under both warming scenarios: 0.7–1.0°C (25%–75% range of 60 locations) under the 1.5 scenario and

1.0°C to 1.5°C under 2.0 scenario (Supporting Information Figure S2 in Appendix S1). In the HAPPI scenarios, annual rainfall is projected to increase in most of the 60 locations under both warming scenarios (Supporting Information Figure S3 in Appendix S1; Ruane, Phillips, et al., 2018).

Based on baseline climate conditions (1980–2010), we categorized the 60 wheat production sites into three environment types (temperate high rainfall, moderately hot low rainfall, and hot irrigated; Supporting Information Figure S5 in Appendix S1). Across these environments, increasing temperatures reduce wheat crop duration due to accelerated phenology (Supporting Information Figure S22a in Appendix S1). As a consequence, the crop duration declines with future climate change scenarios compared with the baseline. For most of the locations from temperate high rainfall and moderately hot low rainfall regions, simulated cumulative growing season evapotranspiration (ET) and growing season rainfall decreased slightly under the 1.5 and 2.0 scenarios (Supporting Information Figure S20b and S21b in Appendix S1). In hot irrigated regions, simulated cumulative evapotranspiration decreased (in average by -16 and -25 mm) under both warming scenarios during the crop duration (Supporting Information Figure S20b in Appendix S1), while simulated cumulative rainfall increased slightly (usually <10 mm) in more than half of the locations (Supporting Information Figure S21b in Appendix S1) due to projected increase in annual rainfall (Supporting Information Figure S3 in Appendix S1). The decrease in cumulative ET was mostly due to shorter crop duration (in average by -4.9 and -7.2 days) due to warming, as shown with significant negative relationship between growing season cumulative ET and crop duration in all hot irrigated locations (Supporting Information Figure S23 in Appendix S1). For example, cumulative ET decreased by about 2.2 mm with a shortening of the growing season by 1 day in Aswan, Egypt. Heat stress days (daily maximum air temperature $>32^{\circ}\text{C}$; Porter & Gawith, 1999) during grain filling already occur in almost all regions, but their frequency increases under both warming scenarios, particularly in moderately hot low rainfall (in average by 1.0 and 1.6 days) and hot irrigated locations (in average by 1.8 and 2.5 days; Supporting Information Figure S22b in Appendix S1).

Simulated impacts on wheat yields for the 1.5 and 2.0 scenarios (Figure 1) are negatively correlated with baseline crop season mean temperature (Figure 2a), suggesting that cooler regions will benefit more from moderate warming. For example, most locations with crop growing season mean temperature (sowing to maturity) $<15^{\circ}\text{C}$ will have mostly positive yield changes, while for growing season mean temperature $>15^{\circ}\text{C}$, any increase in temperature will reduce grain yields (Figure 2a) despite the growth stimulation from elevated $[\text{CO}_2]$. Generally, regions which produce the largest proportion of wheat globally are projected to have small positive yield changes under both scenarios, but there are exceptions such as India, which is currently the world's second largest wheat producer (Figure 2).

The projected changes in growing season climate variables have a significant impact on simulated grain yield under the two warming scenarios at most global locations. As shown in Supporting Information Table S4 in Appendix S1, a significant negative relationship

between simulated grain yield and growing season mean temperature and the number of heat stress days during grain filling were found at most locations, especially for hot irrigated locations, while a significant positive relationship between simulated grain yields and growing season cumulative ET, solar radiation, and rainfall (only for rainfed locations) were found in almost all locations. For example, wheat grain yield at Griffith, Australia, was projected to decrease by 0.44 t/ha per $^{\circ}\text{C}$ increase in growing season mean temperature, and decrease by 0.067 t/ha per day increase in heat stress days, but increase by 0.008 t/ha per mm increase in growing season cumulative ET. In addition, shortening the growing season duration was also found to negatively impact simulated wheat yield significantly. For example, wheat yield was projected to decrease by 0.1 t/ha per day reduction in growing season duration, in Indore, India. Growing season rainfall also showed significant positive effects on projected grain yield in most rainfed locations (Supporting Information Table S4 in Appendix S1), however, projected growing season rainfall declined in most locations, except for small rainfall increases in a few hot irrigated locations (Supporting Information Figure S21b in Appendix S1).

When scaling up from the 60 locations, we found that wheat yields in about 80% of wheat production areas will increase under 1.5 scenario, but usually by $<5\%$ (Figure 3). Largest positive impacts under 1.5 scenario are projected for United States (6.4%), the third largest wheat producer in the world. Loss in wheat yields under the 1.5 scenario is projected mostly for Central Asia, Africa, and South America (Figure 3), regions with generally high growing season temperatures, shorter crop duration, and more heat stress days during grain filling (Supporting Information Figure S14 in Appendix S1). Further yield declines in these countries are expected with the 2.0 scenario, including in large wheat-producing countries such as India (-2.9% ; Figure 3).

Analysis for the three environment types projects a larger yield increase for temperate high rainfall regions (3.2% and 5.5% under 1.5 and 2.0 scenarios, respectively) than for moderately hot low rainfall (2.1% and 2.4%) but a decline in hot irrigated regions (-0.7% and 0.02%; Supporting Information Figures S9 and S10 in Appendix S1). These positive values contrast with the negative trend found across a meta-analysis, with a large uncertainty range, with local temperature change of 1.5 – 2.0°C , despite positive effects from elevated $[\text{CO}_2]$ (Challinor, Martre, et al., 2014; Challinor, Watson, et al., 2014).

Up-scaled to the globe, wheat production on current wheat-producing areas is projected to increase by 1.9% (-2.3% to 7.0%, 25th percentile to 75th percentile) under the 1.5 and by 3.3% (-2.4% to 10.5%) under the 2.0 scenario (Figure 4a and Supporting Information Figure S8a in Appendix S1). The differences in estimated ensemble median impacts between the two warming levels may be small, but significant, as indicated by a statistical test for the model ensemble median of the global impacts ($p < 0.001$). Under the Representative Concentration Pathway 8.5 (RCP8.5) for the 2050s, with a global mean temperature increase of 2.6°C above pre-industrial, global wheat production are suggested to increase by 2.7% (Asseng et al., 2018), highlighting the non-linear nature of climate change impact.

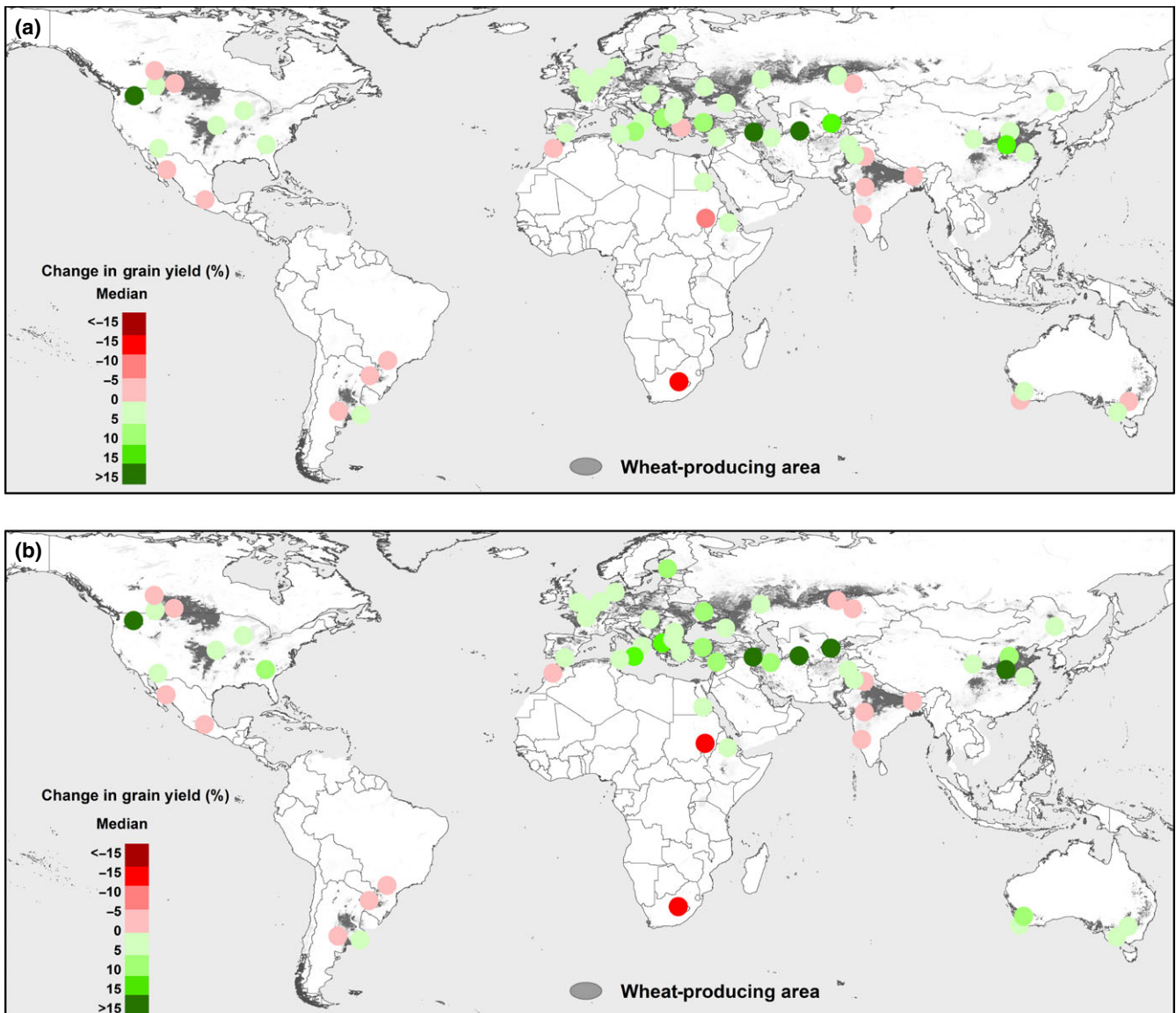


FIGURE 1 Impact of (a) 1.5 and (b) 2.0 scenarios on wheat grain yield for 60 representative global wheat-growing locations. Relative changes in grain yield were the median across 31 crop models and five GCMs, calculated with simulated 30-year mean grain yields for baseline, 1.5 and 2.0 scenarios (HAPPI), including changes in temperature, rainfall, and atmospheric $[CO_2]$, using region-specific soils, cultivars, and crop management

When up-scaling the impact for different wheat types (Supporting Information Figure S26 in Appendix S1), the impact on global wheat production of the multi-model medians was 0.76% and 1.26% for spring wheat types (planted at 39 global locations) under 1.5 and 2.0 scenarios but 3.2% and 5.7% for winter wheat types (planted at 21 global locations), respectively.

3.2 | More variable yields in hot and dry areas

While the 30-year average yield is projected to increase under the 1.5 and 2.0 scenarios across many regions, the risk of extremely low yields may increase, especially in some of the hot-dry locations. The probability of extreme low yields (yields lower than the bottom 5 percentile of the 1981–2010 distribution) will increase significantly

in more than half of the moderately hot low rainfall locations under both scenarios (Figure 5 and Supporting Information Figure S19a in Appendix S1). For the hot irrigated locations, the probability of extreme low yields will increase significantly in about half of the locations (Supporting Information Figures S13 and S19a in Appendix S1). In some hot irrigated locations, the likelihood of extreme low yields will increase by up to five times, that is from 5% under baseline to 11% and 22% under 1.5 warming and 2.0 warming scenarios, respectively, for example, in Wad Medani from Sudan. But in other hot irrigated locations (e.g., Maricopa in United States, Aswan in Egypt, and Balcarce in Argentina) and most of temperate high rainfall locations, the extreme low yield probability will decrease or remain unchanged for the two warming scenarios (Supporting Information Figures S11 and S19a in Appendix S1). The likelihood of

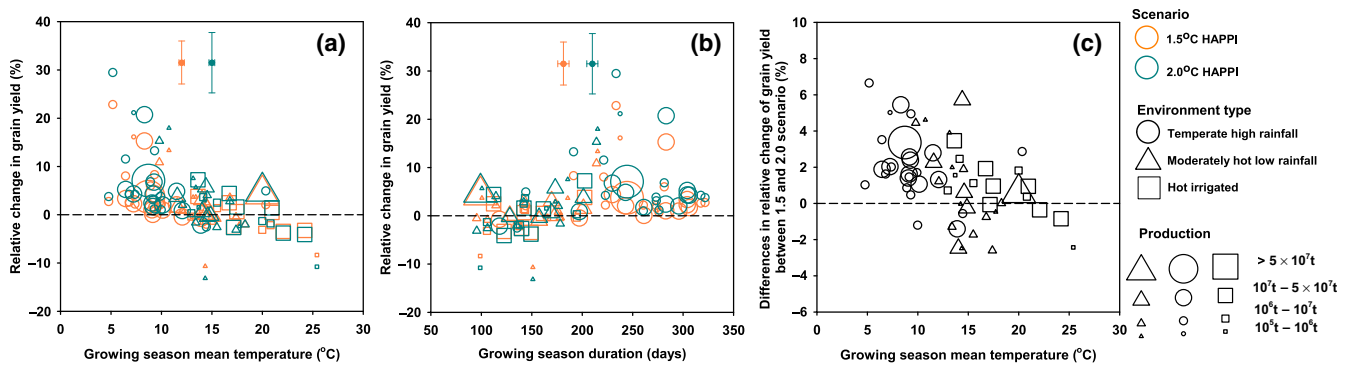


FIGURE 2 Projected Impact of the 1.5 and 2.0 scenarios on wheat grain yield and crop duration. Simulated change in grain yield vs. (a) growing season mean temperature and (b) mean growing season duration (sowing to maturity) for the 1.5 (orange) and 2.0 (dark cyan) scenarios (HAPPI). (c) Differences in relative change in grain yield between the 1.5 and 2.0 scenarios vs. growing season mean temperature for 60 representative wheat-producing global locations. Relative changes in grain yield were the median across 31 crop models and five GCMs, calculated with simulated 30-year (1981–2010) mean grain yields for baseline, the 1.5 and 2.0 scenarios (including changes in temperature, rainfall, and [CO₂]) using region-specific soils, cultivars, and crop management. The size of symbols indicates the production represented by each location (using 2014 FAO country wheat production statistics). The vertical and horizontal range crosses indicate the median 25%–75% uncertainty range of relative change in grain yields, growing season mean temperature, and crop duration across the 31 crop models and five GCMs, respectively. In (a), r^2 of linear regressions were 0.32 and 0.33 under 1.5 and 2.0 scenarios, respectively ($p < 0.001$)

extreme low yields will increase significantly from 1.5 warming to 2.0 warming scenarios only at three locations (from 11% to 22% at Wad Medani in Sudan, from 14% to 15% at Swift Current in Canada, and from 7% to 11% at Bloemfontein in South Africa) and remain to be same at all other locations.

To determine the reasons for the changes in extreme low yield probability, relationships between changes in growing season variables and changes in extreme low yield probability were quantified with linear regressions. As shown in Supporting Information Figure S24 in Appendix S1, only growing season mean temperature, maximum temperature, minimum temperature, heat stress days, and cumulative rainfall (only in rainfed locations) were found to be significantly related to changes in extreme low yield probability (all $p < 0.05$), but with relatively poor correlation (r between 0.26 and 0.61). Among these variables, growing season maximum temperature explained most of the changes in extreme low yield probability, with $r = 0.54$ and 0.61 for the 1.5 and 2.0 scenarios, respectively (Supporting Information Figure S24 in Appendix S1). The probability of extreme low yields was projected to increase by 10% and 9% per °C increase in growing season maximum temperature under 1.5 and 2.0 scenarios, respectively.

Under 1.5 warming scenario, the inter-annual variability of simulated grain yields was projected to increase significantly in only few locations (mostly in hot irrigated locations, Supporting Information Figure S19b in Appendix S1), while moderate warmings of 2.0°C above pre-industrial are projected to increase the inter-annual variability of simulated grain yields in about 50% of hot irrigated locations and parts of moderately hot low rainfall locations significantly, including Sudan, Bangladesh, Egypt, and India (Figure 6). For example, inter-annual variability of simulated grain yields is projected to increase by 23%–35% in Wad Medani from Sudan under 1.5 and 2.0 scenarios, respectively. The inter-annual variability of simulated grain yields will increase significantly from 1.5 warming to 2.0 warming

scenarios at five moderately hot low rainfall locations and four hot irrigated locations and remain to be same at all other locations. For example, the inter-annual variability of simulated grain yields will increase by 20% and 27% at Bloemfontein in South Africa under 1.5 and 2.0 scenarios, respectively. No significant changes in the inter-annual variability of simulated grain yields were found in most of the temperate high rainfall locations under two warming scenarios (Figure 6 and Supporting Information Figure S19b in Appendix S1).

The relationship between changes in growing season variables (including growing season duration, cumulative ET, cumulative solar radiation, cumulative rainfall, mean temperature, maximum temperature, minimum temperature, and heat stress days) and changes in yield interannual variability (CV) was also quantified with linear regressions. As shown in Supporting Information Figure S25 in Appendix S1, only growing season duration, cumulative ET, and heat stress days were statistically significantly related to changes in yield interannual variability ($p < 0.05$), but with relatively poor correlation coefficients ($0.24 < r < 0.38$). Among these variables, growing season heat stress days explains most of the changes in yield interannual variability, with $r = 0.38$ and 0.34 for the 1.5 and 2.0 scenarios, respectively (Supporting Information Figure S25 in Appendix S1). Yield interannual variability was projected to increase by 2.6% and 2.0% per day increase in growing season heat stress days under the 1.5 and 2.0 scenarios, respectively.

4 | DISCUSSION

With the latest climate scenarios from the HAPPI project, we used a multi-crop and multi-climate model ensemble over a global network of sites to represent major rainfed and irrigated systems to assess global wheat production and local yield interannual variability under 1.5 and 2.0°C warming above pre-industrial, which considered changes in local temperature, rainfall, and global [CO₂]. Under the

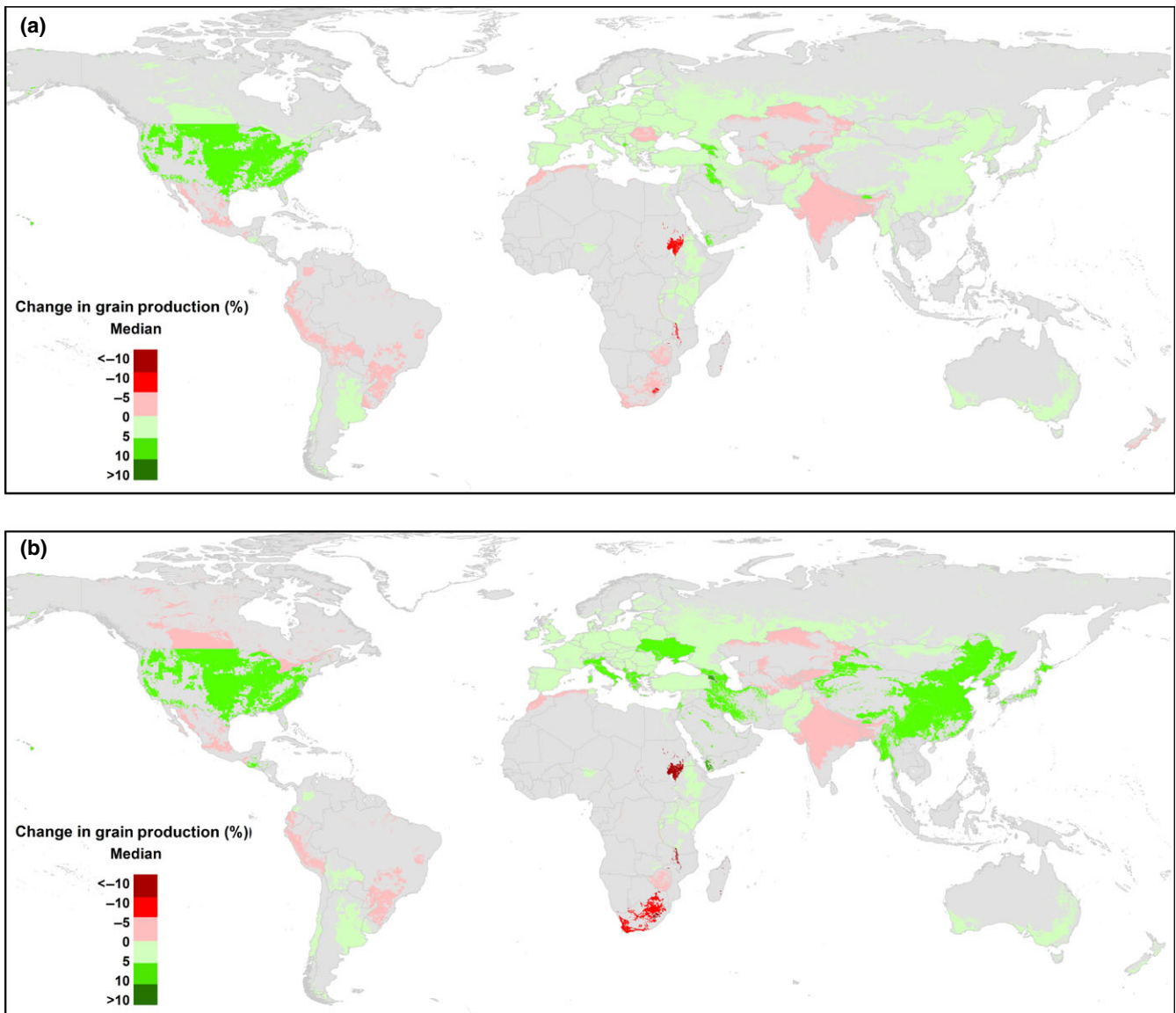


FIGURE 3 Simulated multi-model ensemble projection of global wheat grain production for wheat-growing area per country under the 1.5 and 2.0 scenarios (HAPPI). Relative climate change impacts on grain production under (a) the 1.5 and (b) 2.0 scenarios (including changes in temperature, rainfall, and $[\text{CO}_2]$) compared with the 1981–2010 baseline. Impacts were calculated using the average over 30 years of yields and the medians across 31 models and five GCMs, using region-specific soils, current cultivars, and crop management. Impacts from 60 global locations were aggregated to impacts on country production by weighting the irrigated, high rainfall, and low rainfall production, based on FAO wheat production statistics

two warming scenarios, climate impact on wheat yield can be largely attributed to elevated $[\text{CO}_2]$, shorter wheat growth duration due to increasing growing season temperature and a decrease in cumulative evapotranspiration in most of the 60 locations (Supporting Information Table S4 and Figure S20–22 in Appendix S1). In addition, even with restricted warming levels, increasing weather variability also negatively impacts projected wheat production (Supporting Information Table S4 and Figure S22 in Appendix S1). However, considering the uncertainty related to $[\text{CO}_2]$ in the 1.5 and 2.0°C scenarios (see below), the small differences in yield impact for the two scenarios do not allow concluding on the putative benefits of a limitation of global warming to 1.5°C compared with 2.0°C for global wheat yield production.

4.1 | Changes in atmospheric CO_2 concentration drive the impacts of 1.5 and 2.0°C scenarios on wheat yield

Using four independent methods (Liu et al., 2016; Zhao et al., 2017), global wheat yields had been previously projected to decline by an average of -5.0% for each increase in 1.0°C global warming, but in the absence of concomitant atmospheric $[\text{CO}_2]$ increase. Similar findings have been reported for various typical wheat cultivation regions in Europe when applying a systematic climate sensitivity analysis (Pirttioja et al., 2015). In a sensitivity analysis with the same crop model ensemble for the same 60 representative locations, global wheat production could increase by about 15.8% when CO_2

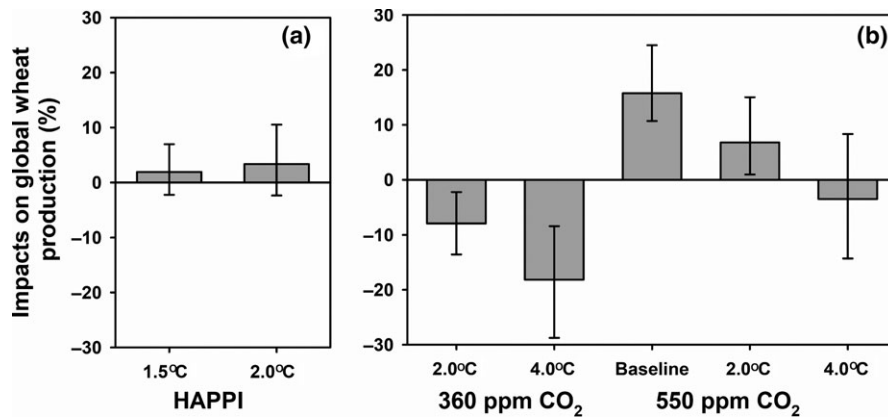


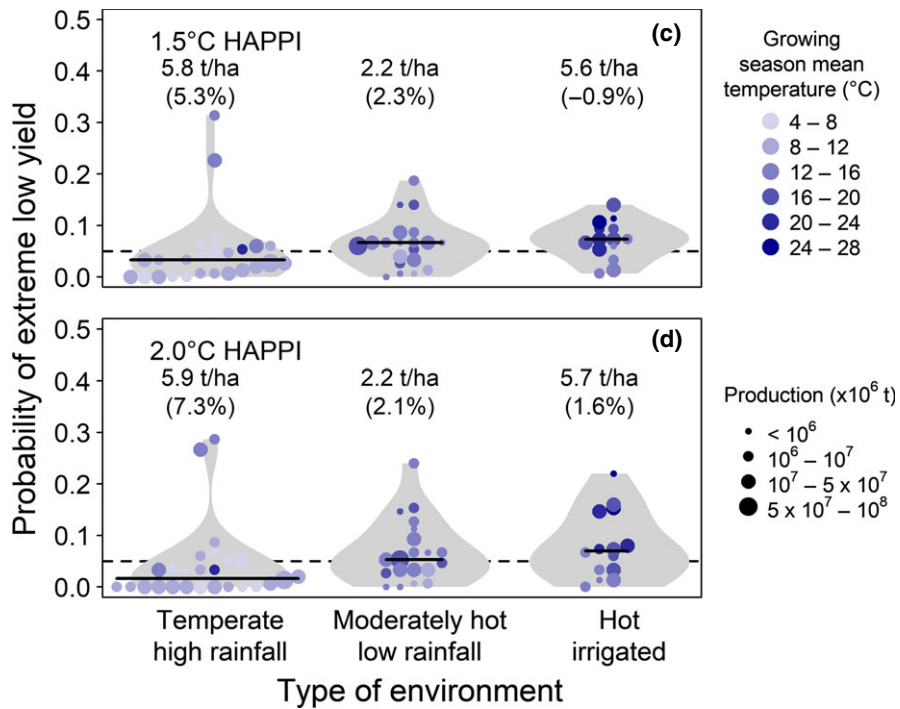
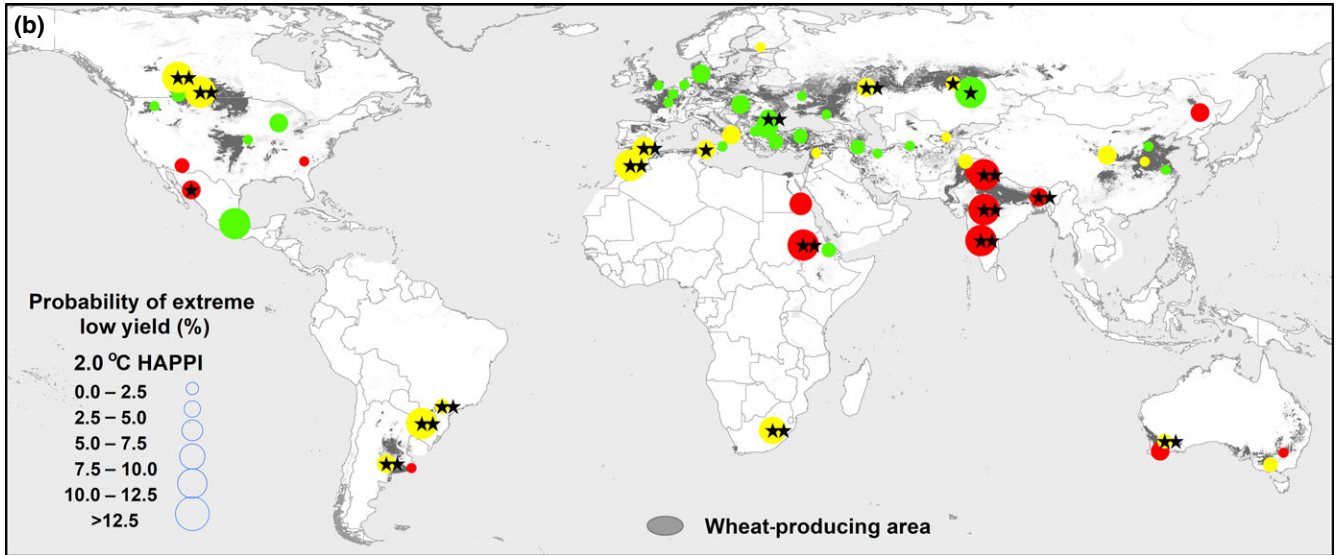
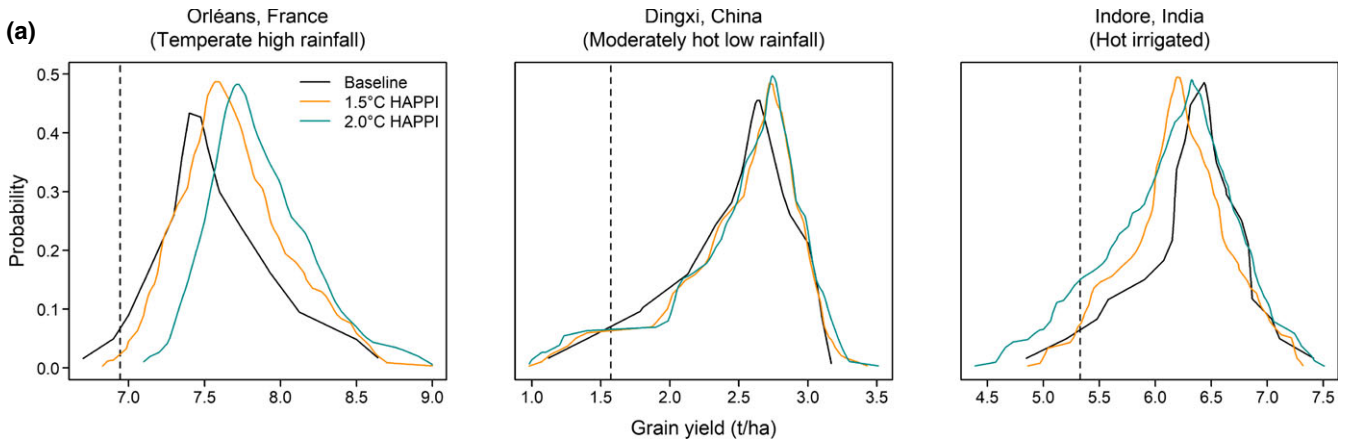
FIGURE 4 Simulated global impacts of climate change scenarios on wheat production. Relative impact on global wheat grain production for (a) 1.5 and 2.0 warming scenarios (HAPPI) with changes in temperature, rainfall, and atmospheric [CO₂]. Atmospheric [CO₂] for the 1.5 and 2.0 scenarios was 423 and 487 ppm, respectively. (b) Local temperature increase by +2°C (360 ppm CO₂ +2°C) and +4°C (360 ppm CO₂ +4°C) for the baseline period with historical [CO₂] (360 ppm) and elevated [CO₂] (550 ppm) for no temperature change (baseline), +2°C (550 ppm [CO₂] +2°C) and +4°C (550 ppm [CO₂] +4°C). Impacts were weighted by production area (based on FAO statistics). Relative change in grain yields was calculated from the mean of 30 years projected yields and the ensemble medians of 31 crop models (plus five GCMs for HAPPI scenarios) using region-specific soils, cultivars, and crop management. Error bars are the 25th and 75th percentiles across 31 crop models (plus five GCMs for HAPPI scenarios)

increased from 360 to 550 ppm. The two HAPPI scenarios include 423 and 487 ppm [CO₂], and the impacts from CO₂ fertilization under the two scenarios are a proportion of the impacts with those for 550 ppm [CO₂]. When assuming a linear response of wheat yield to elevated CO₂ (Amthor, 2001), the impacts of elevated CO₂ under 1.5 and 2.0 scenarios would be 5.2% and 10.5%, respectively, if nitrogen was not limiting. As the overall impacts of climate change under 1.5 and 2.0 scenarios were 1.9% and 3.3%, thus, we can conclude that most of the projected increases in global wheat production under the 1.5 and 2.0 scenarios can be attributed to a CO₂ fertilization effect (Figure 4b and Supporting Information Figure S8b in Appendix S1). This conclusion is consistent with field observations in a range of growing environments (Kimball, 2016; O'Leary et al., 2015) and with a rate of 0.06% yield increase per ppm [CO₂] derived from a meta-analysis of simulation results (Challinor, Martre, et al., 2014; Challinor, Watson, et al., 2014). The CO₂ fertilization effect is

often found to dominate model-based projections of future global wheat productivity (Rosenzweig et al., 2014; Ruiz-Ramos et al., 2018; Wheeler & von Braun, 2013), but with substantial uncertainties and regional differences (Deryng et al., 2016; Kersebaum & Nendel, 2014; Müller et al., 2015).

The relatively low warming levels of the HAPPI scenarios (0.6 and 1.1°C above 1980–2010 global mean temperature) but high increases in [CO₂] suggest that CO₂ fertilization effects also dominate here (Kimball, 2016; O'Leary et al., 2015), but could be less, if nitrogen is limiting growth. However, the impacts here could be slightly overoptimistic with estimates of heat stress, as most of crop models do not account for well-established canopy warming under elevated CO₂ (Kimball et al., 1999; Webber et al., 2018). Also, Schlessner et al. (2018) have shown that CO₂ uncertainties at 1.5 and 2.0°C, which is not considered here, are comparable to the effect of 0.5°C warming increments. This indicated possible differences in

FIGURE 5 Projected impacts of the 1.5 and 2.0 scenarios on the probability of extreme low wheat yields. (a) Grain yield distribution at three locations representative of the three main types of environments (see below) for the 1981–2010 baseline and for the 1.5 and 2.0 scenarios (HAPPI; including changes in temperature, rainfall, and [CO₂]). The yield distribution at the 60 global sites is given in Supporting Information Figures S11–S13 in Appendix S1. The vertical dashed lines indicate the value of extreme low yields (defined as the lower 5% of the distribution) for the baseline. (b) Probability of extreme low yield ($\leq 5\%$ of the baseline distribution) for the 2.0 scenario at 60 representative global wheat-growing locations for clusters of temperate high rainfall or irrigated locations (green; 26 locations), moderately hot low rainfall locations (yellow; 20 locations), and hot irrigated locations (red; 14 locations). In (b), ★ and ★★ indicate the changes in extreme low yield between warming scenarios and baseline was significant at $p < 0.05$ and $p < 0.01$, respectively. (c) and (d) Probability of extreme low yields for each type of environment for the 1.5 and 2.0 scenarios, respectively. Horizontal dashed lines are the probability of extreme low yield for the baseline (defined as the bottom 5% of the baseline distribution). Horizontal thick solid lines are the median probability of extreme low yield. The circles are the 60 global locations shown in (c and d), their size indicates the production represented at each location (using FAO country wheat production statistics) and their color indicated the growing season mean temperature at each location for the 1.5 and 2.0 scenarios. Within each environment type, the circles have been jiggled along the horizontal axis to make it easier to see locations with similar probability values, which means that the horizontal positions of circles in each environment type were used to avoid the overlapping of circles and have no meaning. The shaded areas show the distribution of the data. Numbers above each box are the mean yields for the baseline period and in parenthesis the average yield impacts of the 1.5 and 2.0 scenarios compared with the 1981–2010 baseline yield. See Supporting Information Material and Methods in Appendix S1 for more details on clustering of wheat-growing environments



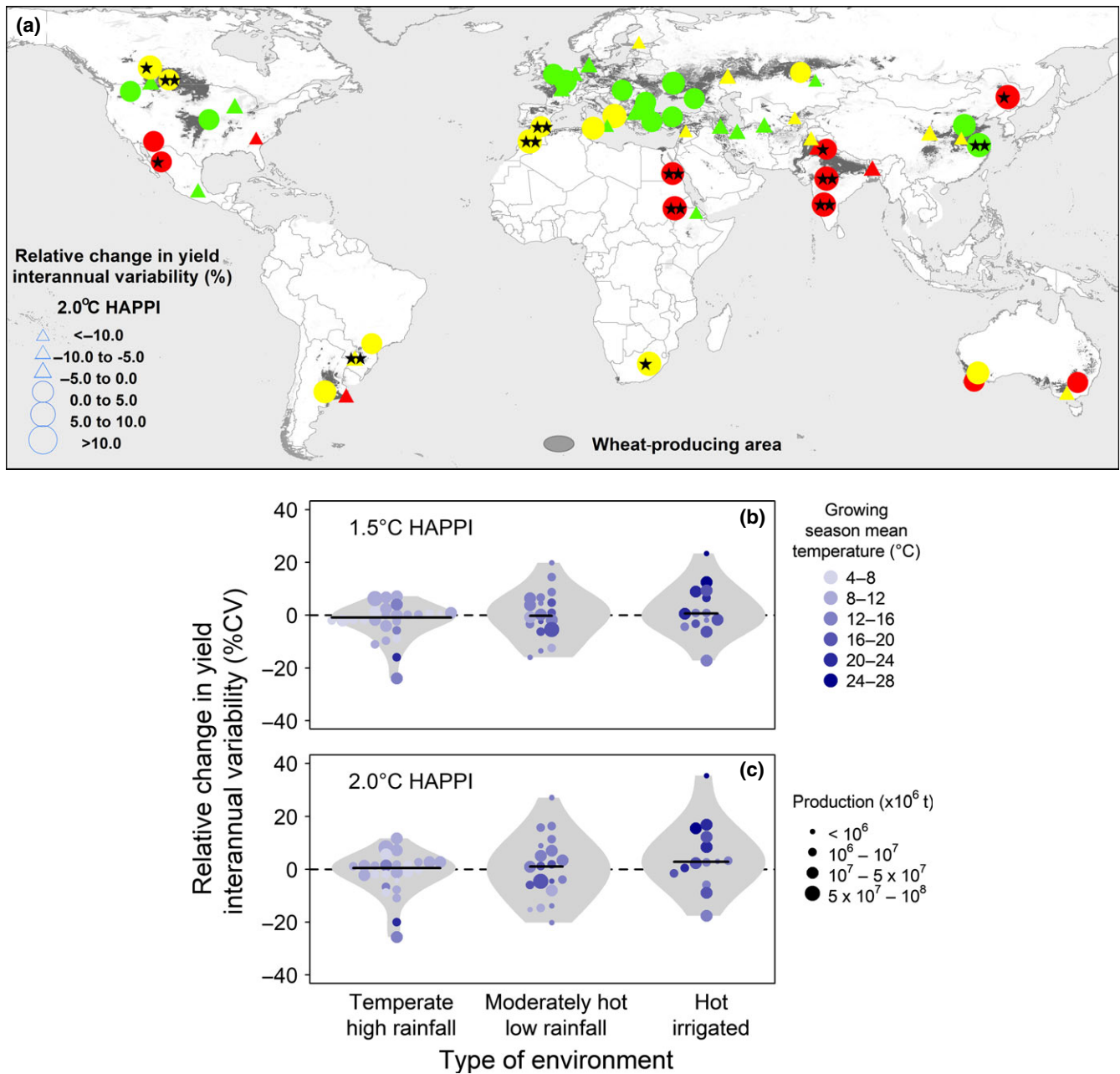


FIGURE 6 Projected impacts of 1.5 and 2.0 scenarios on wheat yield interannual variability. (a) Relative climate change impacts for the 2.0°C warming scenarios (HAPPI) compared with the 1981–2010 baseline on interannual yield variability (coefficient of variation) at 60 representative global wheat-growing locations for clusters of temperate high rainfall or irrigated locations (green; 26 locations), moderately hot low rainfall locations (yellow; 20 locations), and hot irrigated locations (red; 14 locations). In (a), \star and $\star\star$ indicate the changes in interannual yield variability between warming scenarios and baseline was significant at $p < 0.05$ and $p < 0.01$, respectively. The circles and triangles showed increased and decreased interannual variability, respectively. (b) and (c) Relative climate change impacts for the 1.5 and 2.0 scenarios compared with the 1981–2010 baseline on interannual yield variability (coefficient of variation) in temperate high rainfall or irrigated (26 locations), moderately hot low rainfall (20 locations), and hot irrigated (14 locations) locations. Horizontal thick solid lines are the median change in interannual yield variability for each environment type. The circles are the 60 global locations shown in (a), their size indicates the production represented at each location (using FAO country wheat production statistics) and their color indicated the growing season mean temperature at each location under the 1.5 and 2.0 scenarios. Within each environment type, the circles have been jiggled along the horizontal axis to make it easier to see locations with similar probability values, which means that the horizontal positions of circles in each environment type were used to avoid the overlapping of circles, and have no meaning. The shaded areas show the distribution of the data

impacts on wheat production in the simulated 1.5 or 2.0°C worlds (Seneviratne et al., 2018), as a transient 1.5 or 2.0°C world may see higher CO₂ concentrations because of the lagged response of the

climate system (peak warming around 10 years after zero CO₂ emissions are reached) and differences in aerosol loadings (Wang, Lin, et al., 2017). Ruane, Phillips, et al. (2018) also noted uncertainties

related to CO₂ impacts in the 1.5 and 2.0°C worlds, as well as peculiarities in the definition of CO₂ concentrations in HAPPI. CO₂ is also identified as the primary cause of increases between 1.5 and 2.0°C worlds in Rosenzweig et al. (2018). Our study focused on stabilized 1.5 and 2.0°C worlds rather than the transient pathways that get us there, which will include gradually increasing CO₂ concentrations even as some scenarios include an overshoot in global mean temperatures. Elevated CO₂ concentrations are expected to have a particularly strong initial effect, although the benefits will saturate as CO₂ concentrations increase in RCP8.5 or other higher emission pathways.

4.2 | The interannual yield variability and the risk of extreme low yields will increase in a 1.5 and 2.0°C world

Unlike the simulated grain yield impacts, aggregating the simulated yield variability from representative locations to regions or globally with a multi-model ensemble approach has not been tested with observed data. Different aggregation method may result in different characteristics of climate-forced crop yield variance at different spatial scales. Therefore, the simulated yield variability at local scale was not aggregated to region or global scale.

The fraction of yield interannual variability accounted for by weather-forced yield variability may vary substantially depending on the region (Ray, Gerber, & Macdonald, 2015; Ruane et al., 2016); therefore, comparing simulated and observed yield interannual yield variability is critical to analyze changes in yield variability. However, there are no time series data which would allow a scientific model-observation comparison for all the 60 global locations and even for regions where historical yield records are available, they usually do not allow an evaluation of model performance due to missing information on sowing date, cultivar use, crop management of fertilizer N and irrigation, soil characteristics, initial soil conditions, and bias in the reported yields (Guarin, Bliznyuk, Martre, & Asseng, 2018). While for these reasons, it is not possible for us to project meaningfully how interannual yield variability will change at regional or global scale, our study supplies important information on how the additional half degree of warming will impact on yield variability, considering the parallel changes in mean yield levels associated with the combined warming and elevated CO₂ levels. This information is urgently required by national governments and international policy makers in assessing the relative risks and costs of mitigating to 1.5°C warming vs. 2.0°C warming.

Here, we compared our simulated interannual yield variability for the 60 global locations with the estimated global interannual yield variability from statistic yield data in Ray et al. (2015) (Supporting Information Figure S27 in Appendix S1) and we found that the spatial patterns of interannual yield variability were similar for the two studies. For example, both studies showed interannual yield variability and estimated climate-induced yield variability were high at locations in southern Russia, Spain, and Kazakhstan, and were small at locations in western Europe, India, and some locations in China.

Climate-driven yield variability is generally higher in more intensive cropping systems, and many regions around the world now actively pursue intensification of currently low-yielding smallholder cropping systems. Therefore, our current projections of estimates of climate-driven yield variability under the two warming scenarios may be conservative, if some regions will experience intensification and climate change simultaneously.

Extreme low-yielding seasons can impact the livelihood of many farmers (Morton, 2007), but also disturb global markets (e.g., Russian heat wave in 2010; Welton, 2011), or even destabilize entire regions of the world (e.g., Arab Spring in 2011; Gardner et al., 2015). Climate scenarios used for this study included monthly mean changes and shifts in the distribution of daily events within a season but did not include changes in interannual variability; these changes are therefore largely the result of warmer average conditions pushing wheat closer to damaging biophysical thresholds. A recent study based on the HAPPI 1.5 and 2.0 scenarios also identified an increased frequency of interannual drought conditions in regions with declining or constant total precipitations (Ruane, Phillips, et al., 2018), although skewness toward drought in the interannual distribution was small and highly geographically variable.

Despite mostly positive impacts on average yields, projections suggest that the frequency of extreme low yields will increase under both scenarios for some of the hot growing locations (for both low rainfall and irrigated sites), including India, that currently supply more than 14% of global wheat (FAO, 2014). Similarly, an increase in the frequency of crop failures has been shown with 1.5°C global warming above the pre-industrial period for maize, millet, and sorghum in West Africa (Parkes, Defrance, Sultan, Ciais, & Wang, 2018). On the other hand, Faye et al. (2018) did not detect a change in yield variability for the same three crops in West African between the 1.5 and 2.0°C warming scenarios using HAPPI climate data. In our study, the change in climate extremes occurs due to projected shifts in mean temperatures (which bring wheat cropping systems closer to heat stress thresholds) as well as shifts in the distribution of daily temperatures, which can increase or decrease the frequency of future heat waves. Coupled changes in projected precipitation may also exacerbate drought and heat stress yield damage.

4.3 | Impact of 1.5 and 2.0°C scenarios on wheat production and food security

Wheat yields have been stagnating in many agricultural regions (Brisson et al., 2010; Lin & Huybers, 2012; Ray, Ramankutty, Mueller, West, & Foley, 2012). Shifting agriculture polewards has been considered elsewhere, but might not be always possible or feasible for adapting to increasing temperature due to land use and land suitability constraints. Measures such as change in sowing date and irrigation management, improved heat- and drought-resistant cultivars, reduced trade barriers, and increased storage capacity (Schewe, Otto, & Frieler, 2017) will be necessary to adapt to changes in temperature and precipitation for improving food security. However, since the largest estimated yield losses and increased probability of

extreme low yields occur in tropical areas (that is, in hot environment with low-temperature seasonality) and under irrigated systems, the above-mentioned measures would probably not be sufficient. Therefore, it will be challenging to find effective incremental solutions and might need to consider transformation of the agricultural systems in some regions (Asseng et al., 2013; Challinor, Martre, et al., 2014; Challinor, Watson, et al., 2014). In this study, the extreme low yield probability and inter-annual yield variability of simulated yield were projected to increase significantly in parts of hot irrigated locations and moderately hot low rainfall locations, and further increase could be expected from 1.5 scenario to 2.0 scenario, especially for inter-annual yield variability. This indicated that more efforts will be needed for adaptation for food security in these locations.

4.4 | Uncertainties

Here, we up-scaled the climate warming impacts from 60 representative global locations to country and global scales, following the approach by Asseng et al. (2015). The 60 locations were selected with local experts to be representative of each region, and high-quality model inputs for each location were obtained (Supporting Information Table S1 in Appendix S1). Liu et al. (2016) and Zhao et al. (2017) recently showed that up-scaled simulations for representative locations, as suggested by van Bussel et al. (2015), have similar temperature impacts to $0.5^\circ \times 0.5^\circ$ global grid simulations or statistical approaches. The projected impact for spring wheat reported here is similar to that reported by Iizumi et al. (2017), who reported global spring wheat production to increase by 1.43%–1.60% and 1.43%–1.61% under 1.5 and 2.0 scenarios using a global gridded simulation approach under different Shared Socioeconomic Pathways.

To analyze risks of the extreme low yields, we used a well-tested multi-model ensemble (Asseng et al., 2015, 2013, 2018; Ruane et al., 2016; Wallach et al., 2018) instead of individual wheat models, as the model ensemble has shown to reproduce observed yields and observed yield interannual variability. In Asseng et al. (2015), the multi-model ensemble median reproduced observed wheat yield under different warming treatments, with wheat-growing season temperature ranging from 15 to 32°C, including extreme heat conditions. Asseng et al. (2018) recently demonstrated that a multi-model ensemble could also simulate the impact of heat shocks and extreme drought on wheat yield.

Global warming will also affect weeds, pests, and diseases, which are not considered in our analysis, but could significantly impact crop production (Jones et al., 2017; Juroszek & von Tiedemann, 2013; Stratonovitch, Storkey, & Semenov, 2012). Possible agricultural land use changes were not considered here, which could increase production (Nelson et al., 2014), but also accelerate further greenhouse gas emissions (Porter, Howden, & Smith, 2017), adding to the uncertainty of future impact projections.

Projections in this study were designed to be consistent with the AgMIP Coordinated Global and Regional Assessments (CGRA) of 1.5 and 2.0°C warming and therefore add additional detail and context

to linked analysis of climate, crop, and economic implications for agriculture across scales (Ruane, Antle, et al., 2018). Here, the mean impact of 1.5 and 2.0°C warming above preindustrial on global wheat production is projected to be small but positive. In addition, the significant differences between estimated ensemble median impacts from the two warming scenarios indicate a potential yield benefit from higher global warming level. However, in our study, the uneven distribution of impacts across regions, including projected average yield reductions in locations with rapid population growth (e.g., India), the increased probability of extreme low yields and a higher inter-annual yield variability, will be more challenging for food security and markets in a 2.0°C world than in 1.5°C world, particularly in hot growing locations.

ACKNOWLEDGEMENTS










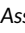

We thank the Agricultural Model Intercomparison and Improvement Project (AgMIP) for support. B.L., L.X., and Y.Z. were supported by the National Science Foundation for Distinguished Young Scholars (31725020), the National Natural Science Foundation of China (31801260, 51711520319, and 31611130182), the Natural Science Foundation of Jiangsu province (BK20180523), the 111 Project (B16026), and the Priority Academic Program Development of Jiangsu Higher Education Institutions (PAPD). S.A. and B.K. received support from the International Food Policy Research Institute (IFPRI) through the Global Futures and Strategic Foresight project, the CGIAR Research Program on Climate Change, Agriculture and Food Security (CCAFS), and the CGIAR Research Program on Wheat. P.M., D.R., and D.W. acknowledge support from the FACCE JPI MACSUR project (O31A103B) through the metaprogram Adaptation of Agriculture and Forests to Climate Change (AAFCC) of the French National Institute for Agricultural Research (INRA). F.T. and Z.Z. were supported by the National Natural Science Foundation of China (41571088, 41571493, 31761143006, and 31561143003). R.R. acknowledges support from the German Federal Ministry for Research and Education (BMBF) through project “Limpopo Living Landscapes” project (SPACES program; grant number O1LL1304A). Rothamsted Research receives grant-aided support from the Biotechnology and Biological Sciences Research Council (BBSRC) Designing Future Wheat project [BB/P016855/1]. L.X. and Y.G. acknowledge support from the China Scholarship Council. M.B. and R.F. were funded by JPI FACCE MACSUR2 through the Italian Ministry for Agricultural, Food and Forestry Policies and thank A. Soltani from Gorgan Univ. of Agric. Sci. & Natur. Resour for his support. K.C.K. and C.N. received support from the German Ministry for Research and Education (BMBF) within the FACCE JPI MACSUR project. S.M. and C.M. acknowledge financial support from the MACMIT project (O1LN1317A) funded through BMBF. G.J.O. acknowledges support from the Victorian Department of Economic Development, Jobs, Transport and Resources, the Australian Department of Agriculture and Water Resources. P.K.A. was supported by the multiple donors contributing to the CGIAR Research Program on Climate Change, Agriculture and Food Security (CCAFS). B.B. received financial

support from USDA NIFA-Water Cap Award 2015-68007-23133. F.E. acknowledges support from the FACCE JPI MACSUR project through the German Federal Ministry of Food and Agriculture (2815ERA01J) and from the German Science Foundation (project EW 119/5-1). J.R.P. acknowledges the support of the Labex Agro (Agropolis no. 1501-003). La. T.P. and F.T. received financial support from the Academy of Finland through the project PLUMES (decision nos. 277403 and 292836) and from Natural Resources Institute Finland through the project ClimSmartAgri.

CONFLICT OF INTERESTS

The authors declare no competing interests.

ORCID

Katharina Waha  <https://orcid.org/0000-0002-8631-8639>
 Juraj Balkovič  <https://orcid.org/0000-0003-2955-4931>
 Bruno Basso  <https://orcid.org/0000-0003-2090-4616>
 Davide Cammarano  <https://orcid.org/0000-0003-0918-550X>
 Giacomo De Sanctis  <https://orcid.org/0000-0002-3527-8091>
 Curtis D. Jones  <https://orcid.org/0000-0002-4008-5964>
 Sara Minoli  <https://orcid.org/0000-0001-7920-3107>
 Fulu Tao  <https://orcid.org/0000-0001-8342-077X>
 Heidi Webber  <https://orcid.org/0000-0001-8301-5424>
 Yan Zhu  <https://orcid.org/0000-0002-1884-2404>
 Senthold Asseng  <https://orcid.org/0000-0002-7583-3811>

REFERENCES

- Amthor, J. S. (2001). Effects of atmospheric CO₂ concentration on wheat yield: Review of results from experiments using various approaches to control CO₂ concentration. *Field Crops Research*, 73, 1–34. [https://doi.org/10.1016/S0378-4290\(01\)00179-4](https://doi.org/10.1016/S0378-4290(01)00179-4)
- Asseng, S., Ewert, F., Martre, P., Rötter, R. P., Lobell, D. B., Cammarano, D., ... Zhu, Y. (2015). Rising temperatures reduce global wheat production. *Nature Climate Change*, 5, 143–147.
- Asseng, S., Ewert, F., Rosenzweig, C., Jones, J. W., Hatfield, J. L., Ruane, A. C., ... Wolf, J. (2013). Uncertainty in simulating wheat yields under climate change. *Nature Climate Change*, 3, 827–832. <https://doi.org/10.1038/nclimate1916>
- Asseng, S., Martre, P., Maiorano, A., O'Leary, G. J., Fitzgerald, G. J., ... Ewert, F. (2018). Climate change impact and adaptation for wheat protein. *Global Change Biology*, 25, 155–173.
- Brisson, N., Gate, P., Gouache, D., Charmet, G., Oury, F. X., & Huard, F. (2010). Why are wheat yields stagnating in Europe? A comprehensive data analysis for France. *Field Crops Research*, 119, 201–212. <https://doi.org/10.1016/j.fcr.2010.07.012>
- Challinor, A., Martre, P., Asseng, S., Thornton, P., & Ewert, F. (2014). Making the most of climate impacts ensembles. *Nature Climate Change*, 4(4), 77–80. <https://doi.org/10.1038/nclimate2117>
- Challinor, A. J., Watson, J., Lobell, D. B., Howden, S. M., Smith, D. R., & Chhetri, N. (2014). A meta-analysis of crop yield under climate change and adaptation. *Nature Climate Change*, 4, 287–291. <https://doi.org/10.1038/nclimate2153>
- Chenu, K., Porter, J. R., Martre, P., Basso, B., Chapman, S. C., Ewert, F., ... Asseng, S. (2017). Contribution of crop models to adaptation in wheat. *Trends in Plant Science*, 22, 472–490. <https://doi.org/10.1016/j.tplants.2017.02.003>
- Davidson, D. (2016). Gaps in agricultural climate adaptation research. *Nature Climate Change*, 6, 433–435.
- Deryng, D., Elliott, J., Folberth, C., Müller, C., Pugh, T. A. M., & Boote, K. J., ... Rosenzweig, C. (2016). Regional disparities in the beneficial effects of rising CO₂ concentrations on crop water productivity. *Nature Climate Change*, 6, 786–790.
- Ewert, F., Rötter, R. P., Bindi, M., Webber, H., Trnka, M., Kersebaum, K. C., ... Asseng, S. (2015). Crop modelling for integrated assessment of risk to food production from climate change. *Environmental Modelling and Software*, 72, 287–303.
- FAO (2014). Asian wheat producing countries-Uzbekistan-Central Zone. Retrieved from http://www.fao.org/ag/agp/agpc/doc/field/Wheat/asia/Uzbekistan/agroeco_central.htm
- Faye, B., Webber, H., Naab, J., MacCarthy, D. S., Adam, M., Ewert, F., ... Gaiser, T. (2018). Impacts of 1.5 versus 2.0°C on cereal yields in the West African Sudan Savanna. *Environmental Research Letters*, 13, 034014.
- Frank, S., Havlik, P., Soussana, J. F., Levesque, A., Valin, H., Wollenberg, E., ... Obersteiner, M. (2017). Reducing greenhouse gas emissions in agriculture without compromising food security? *Environmental Research Letters*, 12(10), 105004. <https://doi.org/10.1088/1748-9326/aa8c83>
- Fujimori, S., Hasegawa, T., Rogelj, J., Su, X., Havlik, P., Krey, V., ... Riahi, K. (2018). Inclusive climate change mitigation and food security policy under 1.5 °C climate goal. *Environmental Research Letters*, 13, 074033. <https://doi.org/10.1088/1748-9326/aad0f7>
- Gardner, G., Prugh, T., Renner, M., Gardner, G., Prugh, T., & Renner, M. (2015). *State of the World 2015: confronting hidden threats to sustainability*. Washington, DC: Island Press.
- Gbegbelegbe, S., Cammarano, D., Asseng, S., Robertson, R., Chung, U., Adam, M., ... Nelson, G. (2017). Baseline simulation for global wheat production with CIMMYT mega-environment specific cultivars. *Field Crops Research*, 202, 122–135. <https://doi.org/10.1016/j.fcr.2016.06.010>
- Guarin, J., Bliznyuk, N., Martre, P., & Asseng, S. (2018). Testing a crop model with extreme low yields from historical district records. *Field Crops Research*. (In press).
- Hoffmann, H., Zhao, G., van Bussel, L. G. J., Enders, A., Specka, X., Sosa, C., ... Ewert, F. (2015). Variability of aggregation effects of climate data on regional yield simulation by crop models. *Climate Research*, 65, 53–69.
- Iizumi, T., Furuya, J., Shen, Z., Kim, W., Okada, M., Fujimori, S., ... Nishimori, M. (2017). Responses of crop yield growth to global temperature and socioeconomic changes. *Scientific Reports*, 7(1), 7800. <https://doi.org/10.1038/s41598-017-08214-4>
- Jones, L. M., Koehler, A. K., Trnka, M., Balek, J., Challinor, A. J., Atkinson, H. J., & Urwin, P. E. (2017). Climate change is predicted to alter the current pest status of *Globodera pallida* and *G. rostochiensis* in the United Kingdom. *Global Change Biology*, 23, 4497–4507.
- Juroszek, P., & von Tiedemann, A. (2013). Climate change and potential future risks through wheat diseases: A review. *European Journal of Plant Pathology*, 136, 21–33. <https://doi.org/10.1007/s10658-012-0144-9>
- Kalkuhl, M., von Braun, J., & Torero, M. (2016). Volatile and extreme food prices, food security, and policy: An overview. In M. Kalkuhl, J. von Braun, & M. Torero (Eds.), *Food price volatility and its implications for food security and policy* (pp. 3–31). Cham, Switzerland: Springer.
- Kersebaum, K. C., & Nendel, C. (2014). Site-specific impacts of climate change on wheat production across regions of Germany using different CO₂ response functions. *European Journal of Agronomy*, 52, 22–32. <https://doi.org/10.1016/j.eja.2013.04.005>
- Kimball, B. A. (2016). Crop responses to elevated CO₂ and interactions with H₂O, N, and temperature. *Current Opinion in Plant Biology*, 31, 36–43. <https://doi.org/10.1016/j.pbi.2016.03.006>

- Kimball, B. A., Lamorte, R. L., Pinter, P. J., Wall, G. W., Hunsaker, D. J., Adamsen, F. J., ... Brooks, T. J. (1999). Free-air CO₂ enrichment and soil nitrogen effects on energy balance and evapotranspiration of wheat [J]. *Water Resources Research*, 35(1), 1179–1190.
- Lin, M., & Huybers, P. (2012). Reckoning wheat yield trends. *Environmental Research Letters*, 7, 024016. <https://doi.org/10.1088/1748-9326/7/2/024016>
- Liu, B., Asseng, S., Muller, C., Ewert, F., Elliott, J., & Lobell, D. B., ... Zhu, Y. (2016). Similar estimates of temperature impacts on global wheat yield by three independent methods. *Nature Climate Change*, 6, 1130–1136.
- Martre, P., Wallach, D., Asseng, S., Ewert, F., Jones, J. W., Rötter, R. P., ... Wolf, J. (2015). Multimodel ensembles of wheat growth: Many models are better than one. *Global Change Biology*, 21, 911–925. <https://doi.org/10.1111/gcb.12768>
- Mitchell, D., Achutarao, K., Allen, M., Bethke, I., Beyerle, U., Ciavarella, A., ... Zaaboul, R. (2017). Half a degree additional warming, prognosis and projected impacts (HAPPI): Background and experimental design. *Geoscientific Model Development*, 10, 571–583. <https://doi.org/10.5194/gmd-10-571-2017>
- Morice, C. P., Kennedy, J. J., Rayner, N. A., & Jones, P. D. (2012). Quantifying uncertainties in global and regional temperature change using an ensemble of observational estimates: The HadCRUT4 data set. *Journal of Geophysical Research Atmospheres*, 117, 8101. <https://doi.org/10.1029/2011JD017187>
- Morton, J. F. (2007). The impact of climate change on smallholder and subsistence agriculture. *Proceedings of the National Academy of Sciences of the United States of America*, 104, 19680–19685. <https://doi.org/10.1073/pnas.0701855104>
- Müller, C., Elliott, J., Chrystanthopoulos, J., Deryng, D., Folberth, C., Pugh, T. A. M., & Schmid, E. (2015). Implications of climate mitigation for future agricultural production. *Environmental Research Letters*, 10, 125004. <https://doi.org/10.1088/1748-9326/10/12/125004>
- Nelson, G. C., Valin, H., Sands, R. D., Havlik, P., Ahammad, H., Deryng, D., ... Willenbockel, D. (2014). Climate change effects on agriculture: Economic responses to biophysical shocks. *Proceedings of the National Academy of Sciences*, 111, 3274–3279. <https://doi.org/10.1073/pnas.1222465110>
- O'Leary, G. J., Christy, B., Nuttall, J., Huth, N., Cammarano, D., Stöckle, C., ... Asseng, S. (2015). Response of wheat growth, grain yield and water use to elevated CO₂ under a free-air CO₂ enrichment (FACE) experiment and modelling in a semi-arid environment. *Global Change Biology*, 21, 2670–2686.
- Parkes, B., Defrance, D., Sultan, B., Ciais, P., & Wang, X. (2018). Projected changes in crop yield mean and variability over West Africa in a world 1.5 K warmer than the pre-industrial. *Earth System Dynamics Discussions*, 9(1), 119–134.
- Pirttioja, N., Carter, T. R., Fronzek, S., Bindi, M., Hoffmann, H., Palosuo, T., ... Rötter, R. P. (2015). Temperature and precipitation effects on wheat yield across a European transect: A crop model ensemble analysis using impact response surfaces. *Climate Research*, 65, 87–105. <https://doi.org/10.3354/cr01322>
- Porter, J. R., & Gawith, M. (1999). Temperatures and the growth and development of wheat: A review. *European Journal of Agronomy*, 10, 23–36. [https://doi.org/10.1016/S1161-0301\(98\)00047-1](https://doi.org/10.1016/S1161-0301(98)00047-1)
- Porter, J. R., Howden, M., & Smith, P. (2017). Considering agriculture in IPCC assessments. *Nature Climate Change*, 7, 680–683.
- Porter, J. R., Xie, L., Challinor, A. J., Cochrane, K., Howden, S. M., Iqbal, M. M., ... Travasso, M. I. (2014). Food security and food production systems. In V. R. Barros, C. B. Field, D. J. Dokken, M. D. Mastrandrea, K. J. Mach, T. E. Bilir, ... L. L. White (Eds.), *Climate change 2014: Impacts, adaptation, and vulnerability. Part A: Global and sectoral aspects. Contribution of Working Group II to the Fifth Assessment Report of the Intergovernmental Panel on Climate Change* (pp. 485–533). Cambridge, United Kingdom and New York, NY: Cambridge University Press.
- Ray, D. K., Gerber, J. S., Macdonald, G. K., & West, P. C. (2015). Climate variation explains a third of global crop yield variability. *Nature Communications*, 6(5989), 5989. <https://doi.org/10.1038/ncomms6989>
- Ray, D. K., Ramankutty, N., Mueller, N. D., West, P. C., & Foley, J. A. (2012). Recent patterns of crop yield growth and stagnation. *Nature Communications*, 3, 1293. <https://doi.org/10.1038/ncomms2296>
- Rosenzweig, C., Elliott, J., Deryng, D., Ruane, A. C., Müller, C., Arneth, A., ... Jones, J. W. (2014). Assessing agricultural risks of climate change in the 21st century in a global gridded crop model intercomparison. *Proceedings of the National Academy of Sciences*, 111, 3268–3273. <https://doi.org/10.1073/pnas.1222463110>
- Rosenzweig, C., Jones, J. W., Hatfield, J. L., Ruane, A. C., Boote, K. J., Thorburn, P., ... Winter, J. M. (2013). The agricultural model intercomparison and improvement project (AgMIP): Protocols and pilot studies. *Agricultural and Forest Meteorology*, 170, 166–182. <https://doi.org/10.1016/j.agrformet.2012.09.011>
- Rosenzweig, C., Ruane, A. C., Antle, J., Elliott, J., Ashfaq, M., Chatta, A. A., ... Wiebe, K. (2018). Coordinating AgMIP data and models across global and regional scales for 1.5°C and 2.0°C assessments. *Philosophical Transactions of the Royal Society A: Mathematical, Physical and Engineering Sciences*, 376(2119), 20160455. <https://doi.org/10.1098/rsta.2016.0455>
- Ruane, A. C., Antle, J., Elliott, J., Folberth, C., Hoogenboom, G., Mason-D'Croz, D., ... Rosenzweig, C. (2018). Biophysical and economic implications for agriculture of +1.5° and +2.0°C global warming using AgMIP Coordinated Global and Regional Assessments. *Climate Research*, 76(1), 17–39. <https://doi.org/10.3354/cr01520>
- Ruane, A. C., Goldberg, R., & Chrystanthopoulos, J. (2015). Climate forcing datasets for agricultural modeling: Merged products for gap-filling and historical climate series estimation. *Agricultural and Forest Meteorology*, 200, 233–248.
- Ruane, A. C., Hudson, N. I., Asseng, S., Camarrano, D., Ewert, F., Martre, P., ... Wolf, J. (2016). Multi-wheat-model ensemble responses to interannual climate variability. *Environmental Modelling & Software*, 81, 86–101. <https://doi.org/10.1016/j.envsoft.2016.03.008>
- Ruane, A. C., Phillips, M. M., & Rosenzweig, C. (2018). Climate shifts for major agricultural seasons in +1.5 and +2.0°C worlds: HAPPI projections and AgMIP modeling scenarios. *Agricultural and Forest Meteorology*, 259, 329–344. <https://doi.org/10.1016/j.agrformet.2018.05.013>
- Ruane, A. C., Winter, J. M., McDermid, S. P., & Hudson, N. I. (2015). AgMIP climate data and scenarios for integrated assessment. In C. Rosenzweig, & D. Hillel (Eds.), *Handbook of climate change and agroecosystems: The agricultural model intercomparison and improvement project (AgMIP)* (pp. 45–78). London, UK: Imperial College Press.
- Ruiz-Ramos, M., Ferrise, R., Rodríguez, A., Lorite, I. J., Bindi, M., Carter, T. R., ... Rötter, R. P. (2018). Adaptation response surfaces for managing wheat under perturbed climate and CO₂ in a Mediterranean environment. *Agricultural Systems*, 159, 260–274. <https://doi.org/10.1016/j.agsy.2017.01.009>
- Schewe, J., Otto, C., & Frieler, K. (2017). The role of storage dynamics in annual wheat prices. *Environmental Research Letters*, 12, 054005. <https://doi.org/10.1088/1748-9326/aa678e>
- Schleussner, C.-F., Deryng, D., Müller, C., Elliott, J., Saeed, F., Folberth, C., ... Rogelj, J. (2018). Crop productivity changes in 1.5°C and 2°C worlds under climate sensitivity uncertainty. *Environmental Research Letters*, 13, 064007. <https://doi.org/10.1088/1748-9326/aab63b>
- Seneviratne, S. I., Rogelj, J., Séférian, R., Wartenburger, R., Allen, M. R., Cain, M., ... Warren, R. F. (2018). The many possible climates from the Paris Agreement's aim of 1.5 °C warming. *Nature*, 558, 41–49. <https://doi.org/10.1038/s41586-018-0181-4>
- Shiferaw, B., Smale, M., Braun, H. J., Duveiller, E., Reynolds, M., & Muricho, G. (2013). Crops that feed the world 10. Past successes and future challenges to the role played by wheat in global food security. *Food Security*, 5, 291–317. <https://doi.org/10.1007/s12571-013-0263-y>

- Stratonovitch, P., Storkey, J., & Semenov, M. A. (2012). A process-based approach to modelling impacts of climate change on the damage niche of an agricultural weed. *Global Change Biology*, 18, 2071–2080. <https://doi.org/10.1111/j.1365-2486.2012.02650.x>
- UNFCCC (2015). Draft decision CP 21. Retrieved from <http://unfccc.int/resource/docs/2015/cop21/eng/I09r01.pdf>
- van Bussel, L. G. J., Ewert, F., Zhao, G., Hoffmann, H., Enders, A., Wallach, D., ... Tao, F. (2016). Spatial sampling of weather data for regional crop yield simulations. *Agricultural and Forest Meteorology*, 220, 101–115. <https://doi.org/10.1016/j.agrformet.2016.01.014>
- van Bussel, L. G. J., Grassini, P., VanWart, J., Wolf, J., Claessens, L., Yang, H. ... vanIttersum, M. K. (2015). From field to atlas: Upscaling of location-specific yield gap estimates. *Field Crops Research*, 177, 98–108.
- van Meijl, H., Havlik, P., Lotze-Campen, H., Stehfest, E., Witzke, P., Dominguez, I. P., ... van Zeist, W.-J. (2018). Comparing impacts of climate change and mitigation on global agriculture by 2050. *Environmental Research Letters*, 13, 064021. <https://doi.org/10.1088/1748-9326/aabdc4>
- Wallach, D., Martre, P., Liu, B., Asseng, S., Ewert, F., Thorburn, P. J., ... Zhang, Z. (2018). Multimodel ensembles improve predictions of crop–environment–management interactions. *Global Change Biology*, 24, 5072–5083. <https://doi.org/10.1111/gcb.14411>
- Wang, E., Martre, P., Zhao, Z., Ewert, F., Maiorano, A., Rötter, R. P., ... Asseng, S. (2017). The uncertainty of crop yield projections is reduced by improved temperature response functions. *Nature Plants*, 3, 17102. <https://doi.org/10.1038/nplants.2017.102>
- Wang, Z., Lin, L., Zhang, X., Zhang, H., Liu, L., & Xu, Y. (2017). Scenario dependence of future changes in climate extremes under 1.5°C and 2°C global warming. *Scientific Reports*, 7, 46432.
- Webber, H., White, J. W., Kimball, B. A., Ewert, F., Asseng, S., Eyshi Rezaei, E., ... Martre, P. (2018). Physical robustness of canopy temperature models for crop heat stress simulation across environments and production conditions. *Field Crops Research*, 216, 75–88. <https://doi.org/10.1016/j.fcr.2017.11.005>
- Welton, G. (2011). The impact of Russia's 2010 grain export Ban. *Oxfam Policy & Practice Agriculture*, 11, 76–107(132).
- Wheeler, T., & von Braun, J. (2013). Climate change impacts on global food security. *Science*, 341, 508–513. <https://doi.org/10.1126/science.1239402>
- Zhao, C., Liu, B., Piao, S., Wang, X., Lobell, D. B., Huang, Y., ... Asseng, S. (2017). Temperature increase reduces global yields of major crops in four independent estimates. *Proceedings of the National Academy of Sciences of the United States of America*, 114, 9326–9331. <https://doi.org/10.1073/pnas.1701762114>
- Zhao, G., Hoffmann, H., Yeluripati, J., Xenia, S., Nendel, C., & Coucheney, E., ... Ewert, F. (2016). Evaluating the precision of eight spatial sampling schemes in estimating regional mean of simulated yields for two crops. *Environmental Modelling and Software*, 80, 100–112.

SUPPORTING INFORMATION

Additional supporting information may be found online in the Supporting Information section at the end of the article.

How to cite this article: Liu B, Martre P, Ewert F, et al. Global wheat production with 1.5 and 2.0°C above pre-industrial warming. *Glob Change Biol*. 2019;25:1428–1444. <https://doi.org/10.1111/gcb.14542>

1 **Supporting Information for**

2 **Global wheat production with 1.5 and 2.0°C above pre-industrial warming**

3

4 Bing Liu, Pierre Martre, Frank Ewert, John R. Porter, Andy J. Challinor, Christoph Müller, Alex
5 C. Ruane, Katharina Waha, Peter J. Thorburn, Pramod K. Aggarwal, Mukhtar Ahmed, Juraj
6 Balkovič, Bruno Basso, Christian Biernath, Marco Bindi, Davide Cammarano, Giacomo De
7 Sanctis, Benjamin Dumont, Mónica Espadafor, Ehsan Eyshi Rezaei, Roberto Ferrise, Margarita
8 Garcia-Vila, Sebastian Gayler, Yujing Gao, Heidi Horan, Gerrit Hoogenboom, Roberto C.
9 Izaurralde, Curtis D. Jones, Belay T. Kassie, Kurt C. Kersebaum, Christian Klein, Ann-Kristin
10 Koehler, Andrea Maiorano, Sara Minoli, Manuel Montesino San Martin, Soora Naresh Kumar,
11 Claas Nendel, Garry J. O’Leary, Taru Palosuo, Eckart Priesack, Dominique Ripoche, Reimund
12 P. Rötter, Mikhail A. Semenov, Claudio Stöckle, Thilo Streck, Iwan Supit, Fulu Tao, Marijn Van
13 der Velde, Daniel Wallach, Enli Wang, Heidi Webber, Joost Wolf, Liujun Xiao, Zhao Zhang,
14 Zhigan Zhao, Yan Zhu*, and Senthold Asseng*

15

16 **SI Materials and Methods**

17

18 **Model inputs for global simulations.** Sixty locations from key wheat growing regions in the
19 world were used for a global impact assessment (Table S1). Locations 1 to 30 are high rainfall or
20 irrigated wheat growing locations representing 68% of current global wheat production. These
21 locations were simulated without water or nitrogen limitation. Details about these locations can
22 be found in Asseng *et al.* (2015) and in Table S1. Locations 31 to 60 are low rainfall locations
23 with average wheat yield < 4 t ha⁻¹. These locations represent 32% of current global wheat
24 production. In contrast to the high-rainfall locations 1 to 30, soil types and N management vary
25 among the low-rainfall locations 31 to 60 according region-specific practices.

26 To carry out the global impact assessment and exclusively focus on climate change, region-
27 specific cultivars were used in all 60 locations. Observed local mean sowing, anthesis, and
28 maturity dates were supplied to modelers with qualitative information on vernalization
29 requirements and photoperiod sensitivity for each cultivar. Modelers were asked to sow at the

30 supplied sowing dates and calibrate their cultivar parameters against the observed anthesis and
31 maturity dates by considering the qualitative information on vernalization requirements and
32 photoperiod sensitivity.

33 For locations 1 to 30 sowing dates were fixed at specific dates. For locations 31 to 60, sowing
34 windows were defined and a sowing rule was used. The sowing window was based on sowing
35 dates reported in literature (Table S1). For locations 41, 43, 46, 53, 54, and 59, sowing dates
36 were not reported in literature and estimates from a global cropping calendar were used
37 (Portmann *et al.*, 2010). The cropping calendar provided a month (the 15th of the month was used)
38 in which wheat is usually sown in the region of the location. The start of the sowing window was
39 the reported sowing date and the end of the sowing window was set two months later. Sowing
40 dates and windows are listed in Table S1. Sowing was triggered in the simulations on the day
41 after cumulative rainfall reached or exceeds 10 mm over a 5-day period during the predefined
42 sowing window. Rainfall from up to 5 days before the start of the sowing window was
43 considered. If these criteria were not met by the end of the sowing window, wheat was sown on
44 the last day of the sowing window.

45 For locations 35, 39, 47, 49, and 55 to 57, anthesis dates were reported in literature. For the
46 remaining sites, anthesis dates were estimated with the APSIM-Wheat model (Fig.S27).

47 Maturity dates were estimated from a cropping calendar for sites 31 to 32, 37 to 38, 41 to 46,
48 49 to 54, and 58 to 59 where no information from literature was available. For locations 31 to 60,
49 observed grain yields from the literature (Table S1) were provided to modelers with the aim to
50 set up wheat models to have similar yield levels, as well as similar anthesis and maturity dates.
51 No yields were reported for sites 49 and 56, so APSIM-Wheat yields were estimated and used as
52 a guide (Fig.S28).

53 Locations 1 to 30 (no water or N limitations) were simulated using the same soil information
54 from Maricopa, USA. Soil information for locations 31 to 60 were obtained from a global soil
55 database (Romero *et al.*, 2012). The soil closest to a location was used, but for locations 39 and
56 59, soil carbon was decreased after consulting local experts. Soil profile hydrological parameters
57 and soil organic carbon used for locations 1 to 60.

58 Initial soil nitrogen was set to 25 kg N ha NO₃ and 5 kg N ha NH₄ per meter soil depth and
59 reset each year for locations 31 to 60. Initial soil water for spring wheat sown after winter at
60 locations 31 to 60 was set to 100 mm of plant available water, starting from 10 cm depth down to

61 100 mm was filled in between permanent wilting point and field capacity. The first 10 cm were
62 kept at permanent wilting point and reset each year. If wheat was sown after summer, initial soil
63 water was set to 50 mm plant available water, starting from 10 cm depth down to 50 mm was
64 filled in between permanent wilting point and field capacity. The first 10 cm were kept at the
65 permanent wilting point and reset each year.

66 For locations 31 to 60, fertilizer rates were determined from Gbegbelegbe *et al.* (2017) except
67 for site 59 (Ethiopia) where N fertilizer was set to 60 kg N ha⁻¹. Fertilizer rates were set low (20
68 to 50 kg N ha⁻¹) at locations 31 to 32, 48, 51, 53, 60; medium (60 kg N ha⁻¹) at locations 33 to 43,
69 45 to 47, 49 to 50, 52, 54, 57 to 59; and relatively high (100 to 120 kg N ha⁻¹) at locations 44, 55
70 to 56. All fertilizer was applied at sowing.

71

72

73 **Future climate projections.** In this assessment, baseline (1980-2010) climate data are from the
74 AgMERRA climate dataset (Ruane *et al.*, 2015), which combines observations, reanalysis data,
75 and satellite data products to provide daily maximum and minimum temperatures, solar
76 radiation, precipitation, wind speed, vapor pressure, dew point temperatures, and relative
77 humidity corresponding to the maximum temperature time of day for each location. Climate
78 projections for 1.5 and 2.0°C global warming scenarios were taken from five global climate
79 models (GCMs) [MIROC5, NorESM1-M, CanAM4 (HAPPI), CAM4-2degree (HAPPI), and
80 HadAM3P], which were selected from the Half a degree Additional warming, Prognosis and
81 Projected Impacts project (HAPPI; Mitchell *et al.*, 2017). Large (83-500 member) ensembles of
82 each simulation model were analyzed to produce grid cell ensemble mean change information
83 for each grid cell (Ruane *et al.*, 2018). Climate scenarios were then created by adjusting the
84 distribution of observed climate events to mimic projected climate changes for monthly mean
85 precipitation and minimum and maximum daily temperatures, the standard deviation of daily
86 maximum and minimum temperatures, and the number of rainy days (Ruane *et al.*, 2018).
87 Atmospheric carbon dioxide concentrations ([CO₂]) of 360, 423, and 487 ppm CO₂ were used for
88 baseline conditions and scenarios where global warming is +1.5 and +2.0 °C above pre-industrial
89 conditions to be consistent with HAPPI protocols (Ruane *et al.*, 2018). There were 11 treatments

90 (baseline, five GCMs for 1.5, and five GCMs for 2.0 scenario) simulated for 60 locations and 30
91 years:

- 92 1. Baseline (with 360ppm CO₂)
- 93 2. GCM MIROC5 (1.5°C with 423 ppm CO₂)
- 94 3. GCM NorESM1-M (1.5°C with 423 ppm CO₂)
- 95 4. GCM CanAM4 (HAPPI) (1.5°C with 423 ppm CO₂)
- 96 5. GCM CAM4-2degree (HAPPI) (1.5°C with 423 ppm CO₂)
- 97 6. GCM HadAM3P (1.5°C with 423 ppm CO₂)
- 98 7. GCM MIROC5 (2.0°C with 487 ppm CO₂)
- 99 8. GCM NorESM1-M (2.0°C with 487 ppm CO₂)
- 100 9. GCM CanAM4 (HAPPI) (2.0°C with 487 ppm CO₂)
- 101 10. GCM CAM4-2degree (HAPPI) (2.0°C with 487 ppm CO₂)
- 102 11. GCM HadAM3P (2.0°C with 487 ppm CO₂)

103 **Climate response tests.** The impacts of temperature and CO₂ were further analyzed using a
104 simple delta method that identifies fundamental biophysical responses. The 60 global locations
105 were simulated over 30 years of baseline climate (1981-2010) using 6 variations; three
106 temperature scenarios (with main daily temperature increased by 0, 2, or 4°C), each with two
107 atmospheric [CO₂] (360 for baseline and an elevated 550 ppm). The Baseline+2°C and
108 Baseline+4°C scenarios were created by adjusting each day's maximum and minimum
109 temperatures upward by that amount and then adjusting vapor pressures and related parameters
110 to maintain the original relative humidity at the maximum temperature time of day given that this
111 quantity is not expected to change dramatically with climate change (Allen and Ingram, 2002).

112

113 **Aggregation of local climate change impacts to global wheat production impacts.** Before
114 aggregating local impacts at 60 locations to global impacts, we determined the actual production
115 represented by each location following the procedure described by Asseng *et al.* (2015). The
116 total wheat production for each country came from FAO country wheat production statistics for
117 2014 (www.fao.org). For each country, wheat production was classified into three categories
118 (i.e., high rainfall, irrigated, and low rainfall). The ration for each category was quantified based

119 on the Spatial Production Allocation Model (SPAM) dataset
120 (<https://harvestchoice.org/products/data>). For some countries where no data was available
121 through the SPAM dataset, we estimated the ratio for each category based on the country-level
122 yield from FAO country wheat production statistics. The high rainfall production and irrigated
123 production in each country were represented by the nearest high rainfall and irrigated locations
124 (locations 1 to 30). Low rainfall production in each country was represented by the nearest low
125 rainfall locations (locations 31 to 60).

126 The global wheat grain production impact was calculated using the following steps:

- 127 1) Calculate the relative simulated mean yield impact for climate change scenarios for 30
128 growing seasons (1981-2010) per single model at each location.
- 129 2) Calculate the median across 31 models and five GCMs per location (multi-crop models
130 [CMs] and GCMs ensemble median). Note that CMs and GCMs simulation results were
131 kept separate only for calculating the separate CM and GCM uncertainties (expressed as
132 range between 25th and 75th percentiles).
- 133 3) Calculate the absolute regional production loss by multiplying the relative yield loss from
134 the multi-model ensemble median with the production represented at each location (using
135 FAO country wheat production statistics of 2014 (FAO, 2014)). Calculate separately for
136 high rainfall/irrigated and low input rainfed production. This assumes that the selected
137 simulated location is representative of the entire wheat-growing region surrounding this
138 location.
- 139 4) Add all regional production losses to the total global loss.
- 140 5) Calculate the relative change in global production (i.e., global production loss divided by
141 current global production).
- 142 6) Repeat the above steps for the 25th and 75th percentile relative global yield impact from
143 the 31model ensemble.

144 Similar steps with global impacts were used for calculating the impacts on country scale
145 impacts, except that only the local impacts from corresponding locations in each country were
146 aggregated to the country impacts. The upscaling method used has been shown to give similar
147 temperature impacts than global-gridded and regression- model based approach (Liu *et al.*, 2016,
148 Zhao *et al.*, 2017).

149 To test whether the estimated impacts from two warming scenarios is significantly different, we
150 assume that we have a random sample (31 wheat models) from a population of wheat models. As
151 we use the median as the best estimate of the impacts in this study, so the hypothesis for
152 statistical test was that whether the median of the differences between two warming scenarios
153 statistically different than 0. Here, we did not compare the impacts of 1.5°C and 2°C directly,
154 because the variability in impacts between two warming scenarios came from warming level and
155 wheat models together, but first calculate the difference for each model and test the significance
156 of the differences between two scenarios from 31 models. For each wheat model, the difference
157 can be either >0 or ≤ 0 . So we can treat the differences of impacts from each model as a
158 binomial distribution, with those two categories. Let b be the probability of difference > 0 . If
159 $b=0.5$, then in expectation there are as many values >0 as values ≤ 0 , so the median of delta is 0.
160 If $b>0.5$, then the median is >0 . Therefore, the hypothesis here is whether b is significantly
161 different than 0.5.

162 Let n be the number of crop models. Suppose that n' is the observed number of differences
163 between two warming levels >0 . The probability of observing n' if $b=0.5$, using R, is $dbinom(n',$
164 $size=n, prob=0.5)$. The cumulative probability of $n'-1$ or fewer values >0 is $x=pbinom(n'-1,$
165 $size=n, prob=0.5)$. The p value (for significance) is $p=1-x$, the probability of getting a value as
166 large or larger than n' , if in fact the median is 0.

167 Similar statistical tests were conducted for the changes of extreme low yield probability and
168 interannual yield variability between warming scenario and baseline for each location.

169

170 **Environmental clustering of the 60 global locations.** The 60 global wheat growing locations
171 were clustered in order to analysis the results by group of environments with similar climates. A
172 hierarchical clustering on principal components of the 60 locations was performed based on four
173 climate variables for 1981-2010: the growing duration (sowing to maturity) mean temperature,
174 the growing duration cumulative evapotranspiration, the growing duration cumulative solar
175 radiation, and the number of heat stress days (maximum daily temperature $> 32^{\circ}\text{C}$) during the
176 grain filling period. All data were scaled (centered and reduced) prior to the principal component
177 analysis.

178

179 **Data analysis.** All data were analyzed and plotted using the R language and environment for
180 statistical analysis version 3.4.1 (R Core Team, 2017). The principal component and hierarchical
181 clustering analyses were done with the R package FactoMineR (Le *et al.*, 2008).

182

Table S1. Details of the 60 locations used in this study

Location number	Country	Location	Latitude / longitude (decimal)	Elevation (m a.s.l)	Irrigation (Y/N)	Name	Cultivar			Sowing date or window	Mean 50%-anthesis date	Mean maturity date	Reference used for choosing anthesis date	Environment type [§]
							Growth habit ^a	Vernalization requirement ^b	Photoperiod sensitivity ^b					
01	USA, AZ	Maricopa	33.06 / -112.05	358	Y	Yecora Rojo	S	2	1	25 Dec.	5 Apr.	15 May	-	3
02	Mexico	Obregon	27.33 / -109.9	41	Y	Tacupeto C2001	S	2	2	1 Dec.	15 Feb.	30 Apr.	-	3
03	Mexico	Toluca	19.40 / -99.68	2,667	Y	Tacupeto C2001	S	2	2	10 May	5 Aug.	20 Sep.	-	1
04	Brazil	Londrina	-23.31 / -51.13	610	Y	Atilla	S	3	3	20 Apr.	10 Jul.	1 Sep.	-	2
05	Egypt	Aswan	24.10 / 32.90	193	Y	Seri M 82	S	3	2	20 Nov.	20 Mar.	30 Apr.	-	3
06	The Sudan	Wad Medani	14.40 / 33.50	413	Y	Debeira	S	3	2	20 Nov.	25 Jan.	25 Feb.	-	3
07	India	Dharwar	15.43 / 75.12	751	Y	Debeira	S	3	2	25 Oct.	15 Jan.	25 Feb.	-	3
08	Bangladesh	Dinajpur	25.65 / 88.68	40	Y	Kanchan	S	2	2	1 Dec.	15 Feb.	15 Mar.	-	3
09	The Netherland	Wageningen	51.97 / 5.63	12	N	Aminda	W	6	6	5 Nov.	25 Jun.	5 Aug.	-	1
10	Argentina	Balcarce	-37.75 / -58.3	122	N	Oasis	W	5	5	5 Aug.	25 Nov.	25 Dec.	-	3
11	India	Ludhiana	30.90 / 75.85	244	Y	HD 2687	S	1	1	15 Nov.	5 Feb.	5 Apr.	-	3
12	India	Indore	22.72 / 75.86	58	Y	HI 1544	S	0	1	25 Oct.	25 Jan.	25 Mar.	-	3
13	USA, WI	Madison	43.03 / -89.4	267	N	Brigadier	W	6	6	15 Sep.	15 Jun.	30 Jul.	-	1
14	USA, KS	Manhattan	39.14 / -96.63	316	N	Fuller	W	4	4	1 Oct.	15 May	01 Jul.	-	1
15	UK	Rothamsted	51.82 / -0.37	128	N	Avalon	W	3	3	15 Oct.	10 Jun.	20 Aug.	-	1
16	France	Estrées-Mons	49.88 / 3.00	87	N	Bermude	W	6	6	5 Oct.	31 May	15 Jul.	-	1
17	France	Orleans	47.83 / 1.91	116	N	Apache	W	5	4	20 Oct.	25 May	7 Jul.	-	1
18	Germany	Schleswig	54.53 / 9.55	13	N	Dekan	W	5	2	25 Sep.	15 Jun.	25 Jul.	-	1
19	China	Nanjing	32.03 / 118.48	13	N	NM13	W	4	4	5 Oct.	5 May	5 Jun.	-	1
20	China	Luancheng	37.53 / 114.41	54	Y	SM15	W	6	4	5 Oct.	5 May	5 Jun.	-	1
21	China	Harbin	45.45 / 126.46	118	Y	LM26	S	1	5	5 Apr.	15 Jun.	25 Jul.	-	3
22	Australia	Kojonup	-33.84 / 117.15	324	N	Wyallkatchem	S	2	4	15 May	5 Oct.	25 Nov.	-	3
23	Australia	Griffith	-34.17 / 146.03	193	Y	Avocet	S	2	4	15 Jun.	15 Oct.	25 Nov.	-	3
24	Iran	Karaj	35.92 / 50.90	1,312	Y	Pishtaz	S	2	2	1 Nov.	1 May	20 Jun.	-	1

Table S1. Continued

25	Pakistan	Faisalabad	31.42 / 73.12	192	Y	Faisalabad-2008	S	0	2	15 Nov.	5 Mar.	5 Apr.	-	3
26	Kazakhstan	Karagandy	50.17 / 72.74	356	Y	Steklov-24	S	2	4	20 May	1 Aug.	15 Sep.	-	1
27	Russia	Krasnodar	45.02 / 38.95	30	Y	Brigadier	W	6	6	15 Sep.	20 May	10 Jul.	-	1
28	Ukraine	Poltava	49.37 / 33.17	161	Y	Brigadier	W	6	6	15 Sep.	20 May	15 Jul.	-	1
29	Turkey	Izmir	38.60 / 27.06	14	Y	Basri Bey	S	4	4	15 Nov.	1 May	1 Jun.	-	1
30	Canada	Lethbridge	49.70 / -112.83	904	Y	AC Radiant	W	6	6	10 Sept.	10 Jun.	25 July.		1
31	Paraguay	Itapúa	-27.33 / -55.88	216	N	Based on Atilla	S	3	3	25 May – 25 Jul.	- ^d	15 Oct. ^e	(Ramirez-Rodrigues <i>et al.</i> , 2014)	2
32	Argentina	Santa Rosa	-36.37 / -64.17	177	N	Based on Avocet	S	2	4	5 Jun. – 5 Aug.	- ^d	15 Dec. ^e	(Asseng <i>et al.</i> , 2013)	2
33	USA, GA	Watkinsville	34.03 / -83.41	220	N	Based on Brigadier	W	6	6	25 Nov. – 25 Jan.	- ^d	22 Jun.	(Franzuebbers and Stuedemann, 2014)	3
34	USA, WA	Lind	47.00 / -118.56	522	N	Based on AC Radiant	W	4	4	28 Aug. – 28 Oct.	- ^d	31 Jul.	(Al-Mulla <i>et al.</i> , 2009, Donaldson <i>et al.</i> , 2001, Schillinger <i>et al.</i> , 2008)	1
35	Canada	Swift Current	50.28 / -107.78	10	N	Based on Steklov-24	S	2	4	18 May. – 18 Jul.	16 Jul.	28 Aug.	(Hu <i>et al.</i> , 2015)	2
36	Canada	Josephburg	53.7 / -113.06	631	N	Based on Steklov-24	S	2	4	15 May. – 15 Jul.	- ^d	28 Aug.	(Izaurrealde <i>et al.</i> , 1998)	2
37	Spain	Ventas Huelma	37.16 / -3.83	848	N	Based on Basri Bey	S	4	4	18 Dec. – 18 Feb.	- ^d	15 Jun. ^e	(Royo <i>et al.</i> , 2006)	2
38	Italy	Policoro	40.2 / 16.66	14	N	Based on Basri Bey	S	4	4	17 Nov. – 17 Jan.	- ^d	15 May ^e	(Steduto <i>et al.</i> , 1995)	2
39	Italy	Libertinia	37.5 / 14.58	267	N	Based on Basri Bey	S	4	4	26 Nov. – 26 Jan.	4 May	30 May	(Pecetti and Hollington, 1997)	1

40	Greece	Thessaloniki	41.08 / 22.15	36	N	Based on Basri Bey	S	4	4	15 Nov. – 15 Jan.	- ^d	22 Jun.	(Lithourgi dis <i>et al.</i> , 2006)	1
41	Hungary	Martonvásár	47.35 / 18.81	113	N	Based on Apache	S	5	4	15 Nov. – 15 Jan. ^c	- ^d	15 Jun. ^e	(Berzsenyi <i>et al.</i> , 2000)	1
42	Romania	Alexandria	43.98 / 25.35	73	N	Based on Brigadier	W	6	6	7 Oct. – 7 Dec.	- ^d	15 Aug. ^e	(Cuculean u <i>et al.</i> , 1999)	1
43	Bulgaria	Sadovo	42.13 / 24.93	154	N	Based on Brigadier	W	6	6	15 Oct. – 15 Dec. ^c	- ^d	15 Jul. ^e	(Islam, 1991)	1
44	Finland	Jokioinen	60.80 / 23.48	107	N	Based on Steklov-24	S	2	2	1 May – 1 Jul.	- ^d	15 Aug. ^e	(Rötter <i>et al.</i> , 2012)	2
45	Russia	Yershov	51.36 / 48.26	102	N	Based on Steklov-24	S	2	4	6 May – 6 Jul.	- ^d	15 Sep. ^e	(Pavlova <i>et al.</i> , 2014)	2
46	Kazakhstan	Altbasar	52.33 / 68.58	289	N	Based on Steklov-24	S	2	4	15 Mar. – 15 May ^c	- ^d	15 Sep. ^e	(Pavlova <i>et al.</i> , 2014)	2
47	Uzbekistan	Samarkand	39.70 / 66.98	742	N	Based on SM15	W	6	4	5 Nov. – 5 Jan.	7 May	5 Jul.	(FAO, 2010)	2
48	Morocco	Sidi El Aydi / Jemaa Riah	33.07 / -7.00	648	N	Based on Yecora	S	1	1	5 Nov. – 5 Jan.	- ^d	1 Jun.	(Heng <i>et al.</i> , 2007)	2
49	Tunisia	Nabeul / Tunis	36.75 / 10.75	167	N	Based on Pishtaz	S	2	2	1 Dec. – 1 Feb.	29 Mar.	15 Jun. ^e	(Latiri <i>et al.</i> , 2010)	2
50	Syria	Tel Hadya / Aleppo	36.01 / 36.56	263	N	Based on Pishtaz	S	2	2	20 Nov. – 20 Jan.	- ^d	15 Jun. ^e	(Sommer <i>et al.</i> , 2012)	2
51	Iran	Maragheh	37.38 / 46.23	1,472	N	Based on SM15	W	6	4	13 Oct. – 13 Dec.	- ^d	15 Jun. ^e	(Tavakkoli and Oweis, 2004)	1
52	Turkey	Ankara	39.92 / 32.85	895	N	Based on Fuller	W	4	4	1 Sep. – 1 Nov	- ^d	15 Jul. ^e	(Ilbeyi <i>et al.</i> , 2006)	1
53	Iran	Ghoochan / Quchan	37.66 / 58.50	1,555	N	Based on Pishtaz	S	2	2	15 Oct. – 15 Dec. ^c	- ^d	15 Jun. ^e	(Bannaya n <i>et al.</i> , 2010)	1
54	Pakistan	Urmar	34.00 / 71.55	340	N	Based on Yecora	S	1	1	15 Nov. – 15 Jan. ^c	- ^d	15 May	(Iqbal <i>et al.</i> , 2005)	2
55	China	Dingxi	35.46 / 104.73	2,009	N	Based on Pishtaz	S	2	2	15 Mar. – 15 May.	15 Jun.	2 Aug.	(Huang <i>et al.</i> , 2008)	2

Table S1. Continued

56	China	Xuchang	34.01 / 113.51	110	N	Based on Wenmai	W	4	4	10 Oct. – 10 Dec.	25 Apr.	1 Jun.	^f	2
57	Australia	Merredin	-31.50 / 118.2	3000	N	Based on Wyalkatchem	S	2	4	15 May – 25 Jul.	5 Oct.	25 Nov.	(Asseng <i>et al.</i> , 1998)	2
58	Australia	Rupanyup / Wimmera	-37.00 / 143.00	219	N	Based on Avocet	S	2	4	1 May – 1 Jul.	- ^d	15 Nov. ^e	(van Rees <i>et al.</i> , 2014)	2
59	Ethiopia	Adi Gudom	13.25 / 39.51	2,090	N	Based on Debeira	S	2	4	15 Jun. – 15 Aug. ^c	- ^d	15 Dec. ^e	(Araya <i>et al.</i> , 2015)	1
60	South Africa	Glen / Bloemfontein	-28.95 / 26.33	1,290	N	Based on Wyalkatchem	S	2	4	15 May – 15 Jul.	- ^d	15 Nov.	(Singels and De Jager, 1991)	2

Location, name and characteristics of the cultivars, sowing date (locations 1-30) or sowing window (locations (31-60), and mean anthesis and physiological maturity date for the 30 locations (1-30) from high rainfall or irrigated wheat regions and thirty locations from low rainfall (low input) regions (31-60) of the world used in this study.

^a S, spring type; W, winter type.

^b Vernalization requirement and photoperiod sensitivity of the cultivars range from nil (0) to high (6).

^c Sowing date estimated using global cropping calendar.

^d See from Fig.S5 in Asseng *et al.*, 2018.

^e Maturity date estimated using global cropping calendar.

^f Yan Zhu, personal communication, August 4, 2015.

^g 1, 2, 3 in environment type indicated temperate high rainfall, moderately hot low rainfall, and hot irrigated, respectively.

Table S2. List of the 31 wheat crop models used in the AgMIP Wheat study

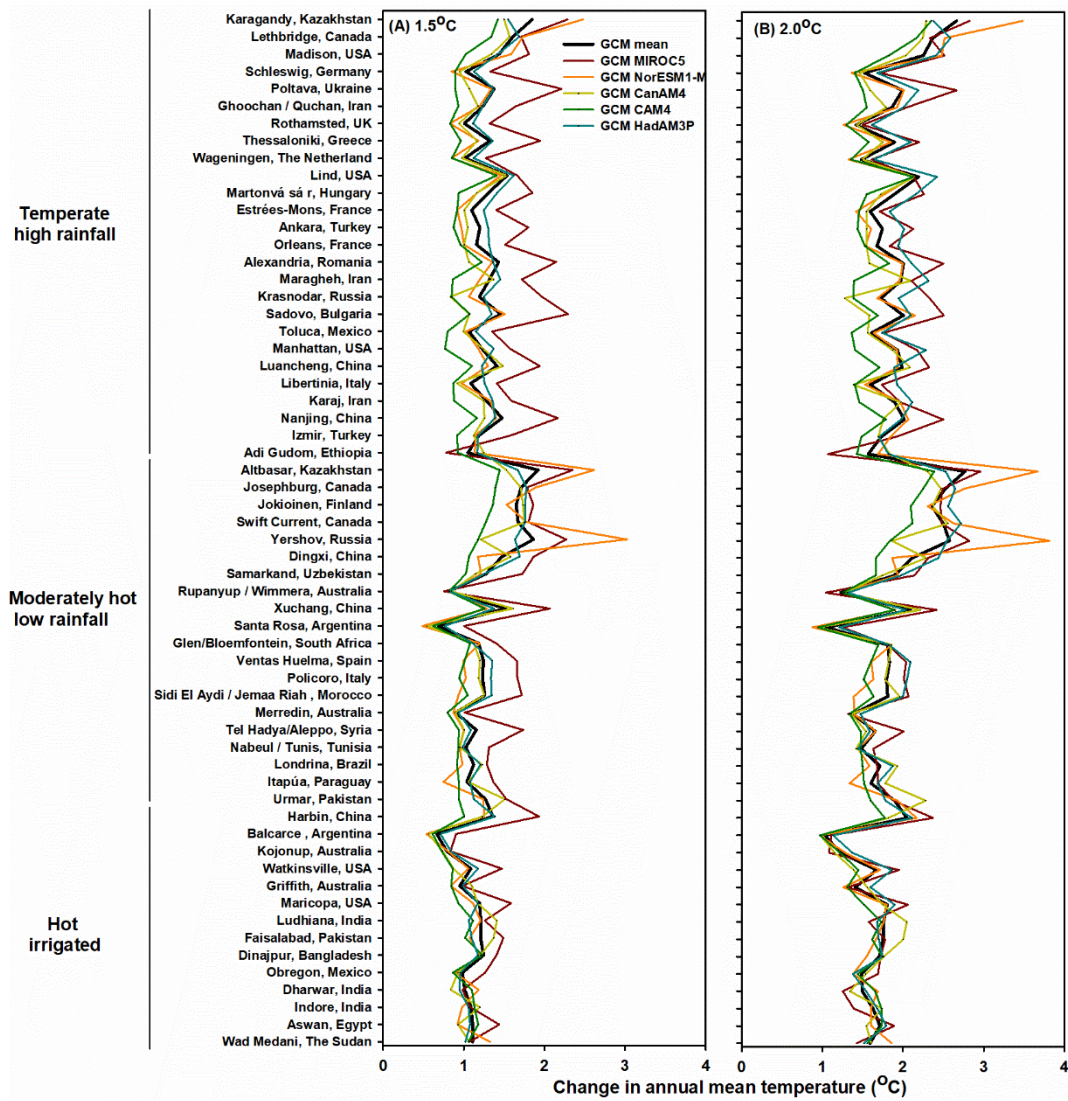
Code	Name (version)	Reference	Documentation
AE	APSIM-E	(Chen <i>et al.</i> , 2010, Keating <i>et al.</i> , 2003, Wang <i>et al.</i> , 2002)	http://www.apsim.info/Wiki
AF	AFRCWHEAT2	(Porter, 1984, Porter, 1993, Weir <i>et al.</i> , 1984)	Request from John Porter: jrp@plen.ku.dk
AQ	AQUACROP (V.4.0)	(Steduto <i>et al.</i> , 2009)	http://www.fao.org/nr/water/aquacrop.html
AW	APSIM-Wheat (V.7.3)	(Keating <i>et al.</i> , 2003)	http://www.apsim.info/Wiki
CS	CropSyst (V.3.04.08)	(Stockle <i>et al.</i> , 2003)	http://modeling.bsye.wsu.edu/CS_Suite_4/CropSyst/index.html
DC	DSSAT-CERES-Wheat (V.4.0.1.0)	(Hoogenboom and White, 2003, Jones <i>et al.</i> , 2003, Ritchie <i>et al.</i> , 1985)	http://dssat.net/
DN	DSSAT-Nwheat	(Asseng, 2004, Kassie <i>et al.</i> , 2016)	http://dssat.net/
DR	DSSAT-CROPSIM (V4.5.1.013)	(Hunt and Pararajasingham, 1995, Jones <i>et al.</i> , 2003)	http://dssat.net/
EI	EPIC-I (V0810)	(Balkovič <i>et al.</i> , 2013, Balkovič <i>et al.</i> , 2014, Kiniry <i>et al.</i> , 1995, Williams, 1995, Williams <i>et al.</i> , 1989)	http://epicapex.tamu.edu/epic
EW	EPIC-Wheat(V1102)	(Izaurrealde <i>et al.</i> , 2006, Izaurrealde <i>et al.</i> , 2012, Kiniry <i>et al.</i> , 1995, Williams, 1995, Williams <i>et al.</i> , 1989)	http://epicapex.brc.tamus.edu
GL	GLAM (V.2 updated)	(Challinor <i>et al.</i> , 2004, Li <i>et al.</i> , 2010)	https://www.see.leeds.ac.uk/research/ic-as/research-themes/climate-change-and-impacts/climate-impacts/glam
HE	HERMES (V.4.26)	(Kersebaum, 2007, Kersebaum, 2011)	http://www.zalf.de/en/forschung/institute/lsa/forschung/oekomod/hermes
IC	INFOCROP (V.1)	(Aggarwal <i>et al.</i> , 2006)	http://infocrop.iari.res.in/wheatmodel/UserInterface/HomeModule/Default.aspx
LI	LINTUL4 (V.1)	(Shibu <i>et al.</i> , 2010, Spitters and Schapendonk, 1990)	http://models.pps.wur.nl/node/950
L5	SIMPLACE<Lintul-5 SlimWater3,FAO-56, CanopyT,HeatStressHourly	(Gaiser <i>et al.</i> , 2013, Shibu <i>et al.</i> , 2010, Spitters and Schapendonk, 1990, Webber <i>et al.</i> , 2016)	http://www.simplace.net/Joomla/
LP	LPJmL (V3.2)	(Beringer <i>et al.</i> , 2011, Bondeau <i>et al.</i> , 2007, Fader <i>et al.</i> , 2010, Gerten <i>et al.</i> , 2004, Müller <i>et al.</i> , 2007, Rost <i>et al.</i> , 2008)	http://www.pik-potsdam.de/research/projects/lpjweb
MC	MCWLA-Wheat (V.2.0)	(Tao <i>et al.</i> , 2009a, Tao and Zhang, 2010, Tao and Zhang, 2013, Tao <i>et al.</i> , 2009b)	Request from taofl@igsnr.ac.cn
MO	MONICA (V.1.0)	(Nendel <i>et al.</i> , 2011)	http://monica.agrosystem-models.com
NC	Expert-N (V3.0.10) – CERES (V2.0)	(Biernath <i>et al.</i> , 2011, Priesack <i>et al.</i> , 2006, Ritchie <i>et al.</i> , 1987, Stenger <i>et al.</i> , 1999)	http://www.helmholtz-muenchen.de/en/iboe/expertn
NG	Expert-N (V3.0.10) – GECROS (V1.0)	(Biernath <i>et al.</i> , 2011, Stenger <i>et al.</i> , 1999)	http://www.helmholtz-muenchen.de/en/iboe/expertn

NP	Expert-N (V3.0.10) – SPASS (2.0)	(Biernath <i>et al.</i> , 2011, Priesack <i>et al.</i> , 2006, Stenger <i>et al.</i> , 1999, Wang and Engel, 2000, Yin and van Laar, 2005)	http://www.helmholtz-muenchen.de/en/iboe/expertn
NS	Expert-N (V3.0.10) – SUCROS (V2)	(Biernath <i>et al.</i> , 2011, Goudriaan and Van Laar, 1994, Priesack <i>et al.</i> , 2006, Stenger <i>et al.</i> , 1999)	http://www.helmholtz-muenchen.de/en/iboe/expertn
OL	OLEARY (V.8)	(Latta and O'Leary, 2003, OLeary and Connor, 1996a, OLeary and Connor, 1996b, OLeary <i>et al.</i> , 1985)	Request from gjoleary@yahoo.com
S2	Sirius (V2014)	(Jamieson and Semenov, 2000, Jamieson <i>et al.</i> , 1998, Lawless <i>et al.</i> , 2005, Semenov and Shewry, 2011)	http://www.rothamsted.ac.uk/mas-models/sirius.php
SA	SALUS (V.1.0)	(Basso <i>et al.</i> , 2010, Senthilkumar <i>et al.</i> , 2009)	http://salusmodel.glg.msu.edu
SP	SIMPLACE<Lintul-2 CC,Heat,CanopyT,Re-Translocation	(Angulo <i>et al.</i> , 2013)	http://www.simplace.net/Joomla/
SQ	<i>SiriusQuality</i> (V3.0)	(Ferrise <i>et al.</i> , 2010, He <i>et al.</i> , 2010, Maiorano <i>et al.</i> , 2017, Martre <i>et al.</i> , 2006, Wang <i>et al.</i> , 2017)	http://www1.clermont.inra.fr/siriusquality
SS	SSM-Wheat	(Soltani <i>et al.</i> , 2013)	Request from afshin.soltani@gmail.com
ST	STICS (V.1.1)	(Brisson <i>et al.</i> , 2003, Brisson <i>et al.</i> , 1998)	http://www6.paca.inra.fr/stics_eng
WG	WheatGrow (V3.1)	(Cao <i>et al.</i> , 2002, Cao and Moss, 1997, Hu <i>et al.</i> , 2004, Li <i>et al.</i> , 2002, Pan <i>et al.</i> , 2007, Pan <i>et al.</i> , 2006, Yan <i>et al.</i> , 2001)	Request from yanzhu@njau.edu.cn
WO	WOFOST (V.7.1)	(Boogaard and Kroes, 1998)	http://www.wofost.wur.nl

Table S3. Variability of simulated grain yields for different environments under baseline, 1.5°C and 2.0°C warming scenarios

Type of environment	Scenario	Coefficient of variation (%)			
		Location	Year	Model	GCM
All locations	Baseline	56.1	1.5	22.4	
	1.5°C HAPPI	55.4	1.6	22.7	1.1
	2.0°C HAPPI	55.4	1.6	23.3	1.2
Temperate high rainfall or irrigated	Baseline	47.9	1.6	23.7	
	1.5°C HAPPI	46.4	1.7	23.3	1.2
	2.0°C HAPPI	46.1	1.7	23.9	1.3
Moderately hot low rainfall	Baseline	37.8	5.3	27.7	
	1.5°C HAPPI	37.0	5.4	28.1	1.9
	2.0°C HAPPI	36.9	5.5	28.7	1.9
Hot irrigated	Baseline	26.5	2.7	27.8	
	1.5°C HAPPI	27.1	2.8	28.5	0.6
	2.0°C HAPPI	27.4	2.9	29.2	0.9

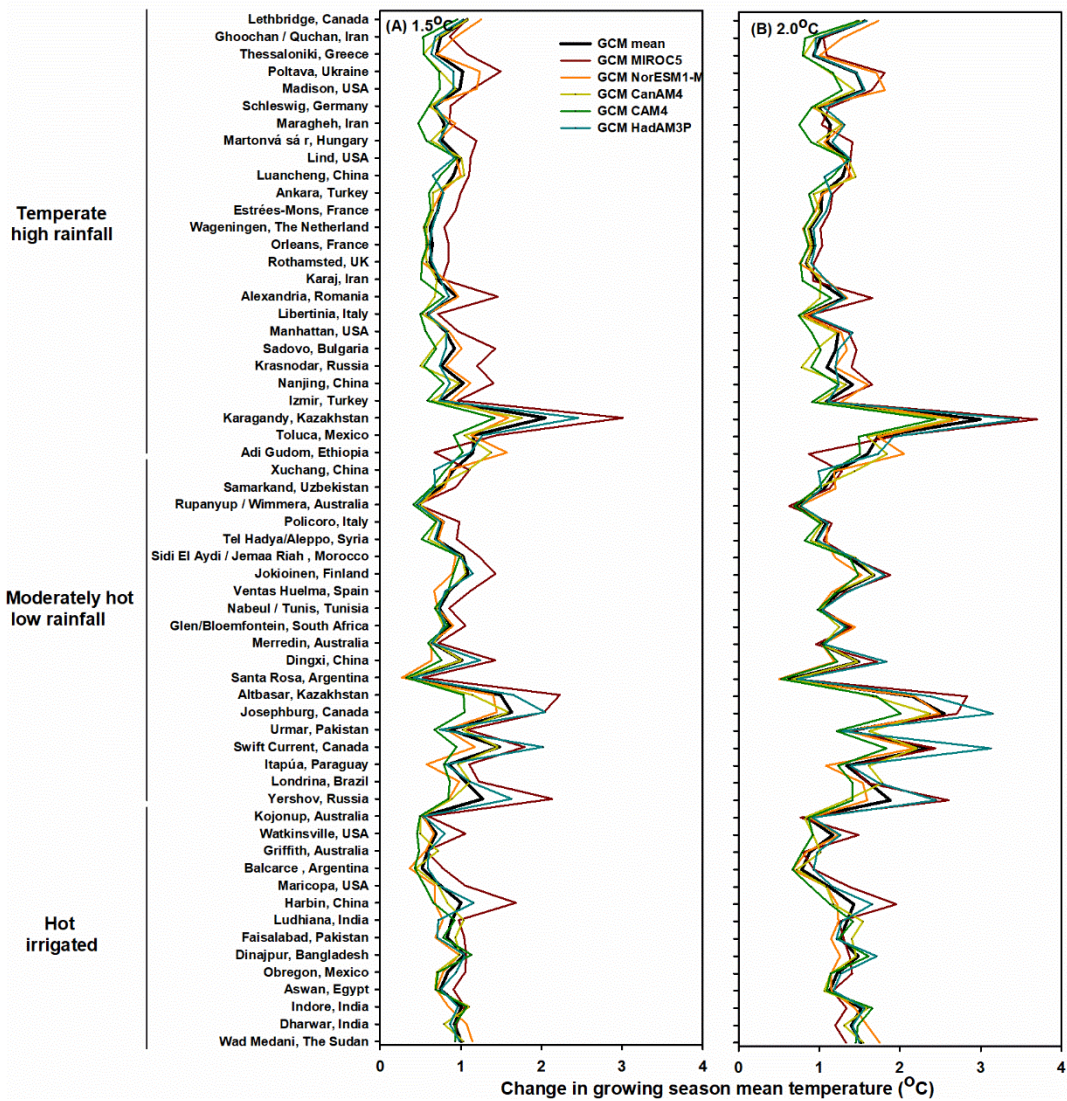
Variability due to location was calculated as coefficient of variation (CV) of simulated grain yields for corresponding locations (mean of 30 years, 31 models, and five global climate models [GCMs]). Variability due to year was calculated as CVs of simulated grain yields for 31 years (mean of corresponding locations, 31 models, and five GCMs). Variability due to model was calculated as CVs of simulated grain yields for 31 locations (mean of 30 years, corresponding locations and five GCMs). Variability due to GCM was calculated as CVs of simulated grain yields for five GCMs (mean of 30 years, 31 models and corresponding locations).



3

4 **Fig. S1. Projected changes in annual mean temperature with the five global climate models (GCMs) for the 60**
5 **representative global wheat growing locations under (A) 1.5 and (B) 2.0 scenarios (HAPPI).** The locations in each
6 environment type were ordered by the annual mean temperature for the baseline period.

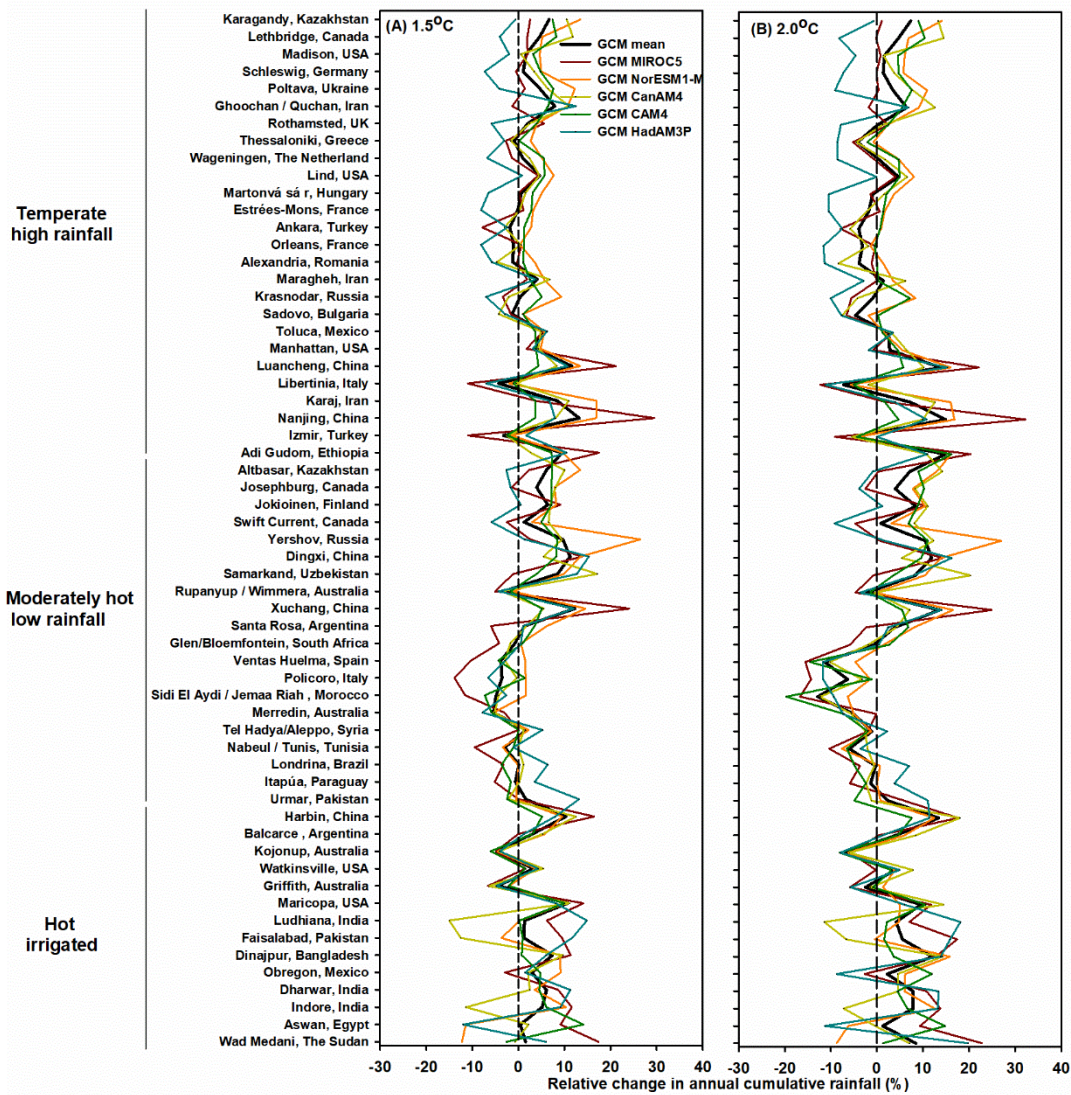
7



9

10 **Fig. S2. Projected changes in growing season (sowing to maturity) mean temperature with the five global**
 11 **climate models (GCMs) for the 60 representative global wheat growing locations under (A) 1.5 and (B) 2.0**
 12 **scenarios (HAPPI). The locations in each environment type were ordered by the growing season mean**
 13 **temperature for the baseline period.**

14



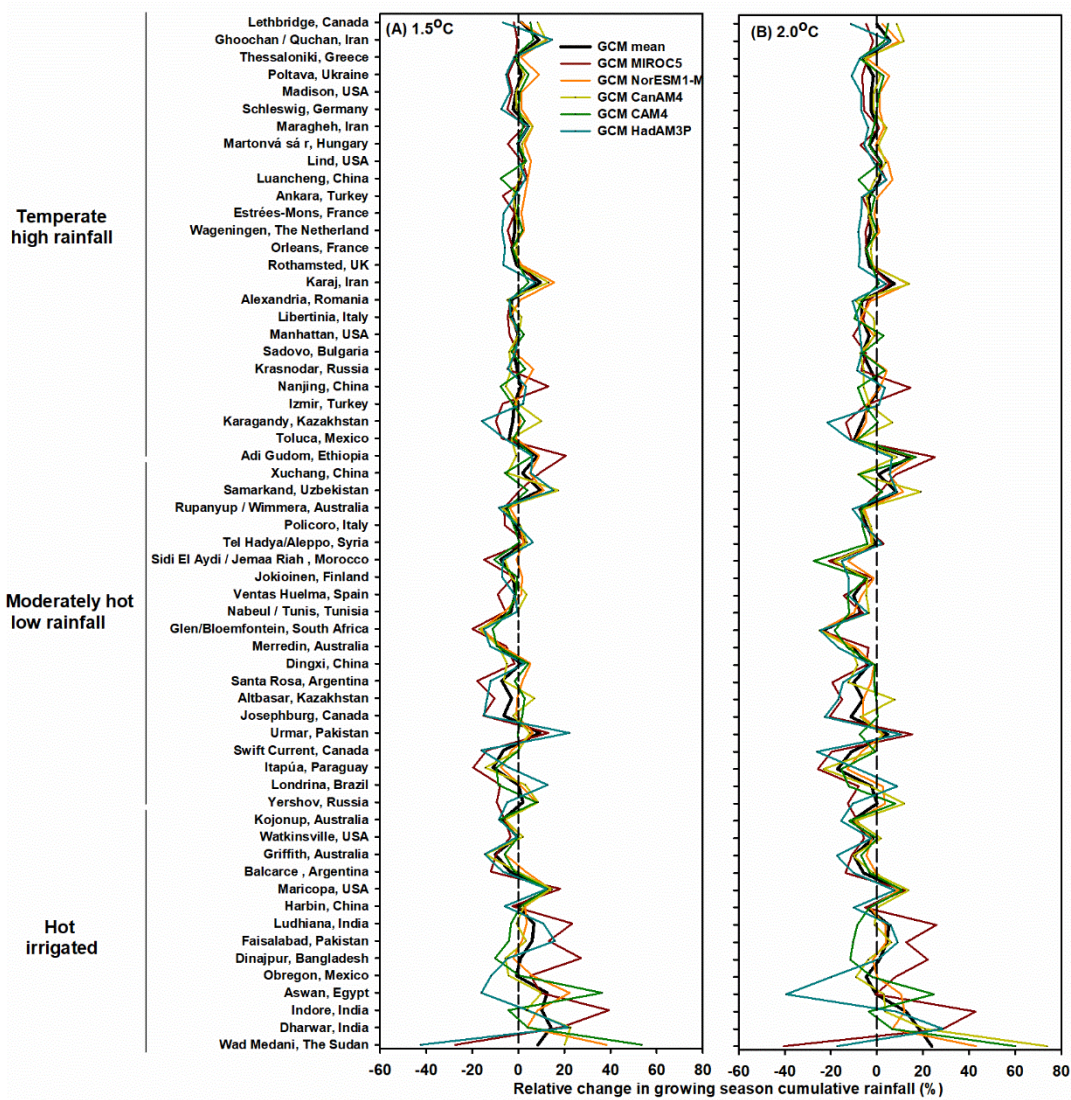
16

17 **Fig. S3. Projected relative changes in annual cumulative rainfall with the five global climate models (GCMs) for**
 18 **the 60 representative global wheat growing locations under (A) 1.5 and (B) 2.0 scenarios (HAPPI). The locations**
 19 **in each environment type were ordered by the annual mean temperature for the baseline period.**

20

21

22

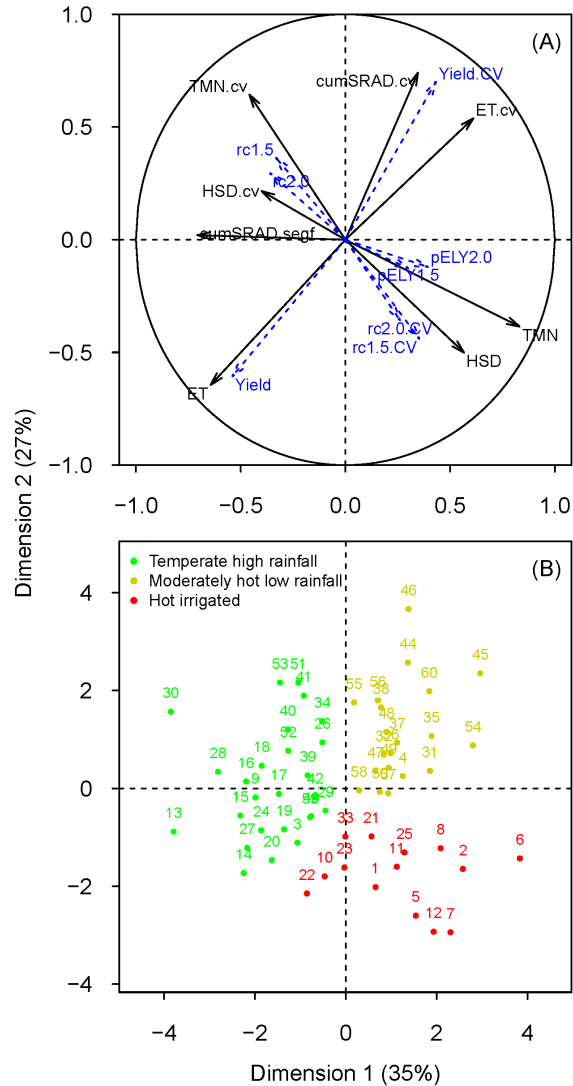


23

24 **Fig. S4.** Projected relative changes in growing season (sowing to maturity) cumulative rainfall with the five global
 25 climate models (GCMs) for the 60 representative global wheat growing locations under (A) 1.5 and (B) 2.0
 26 scenarios (HAPPI). The locations in each environment type were ordered by the growing season mean temperature
 27 for the baseline period.

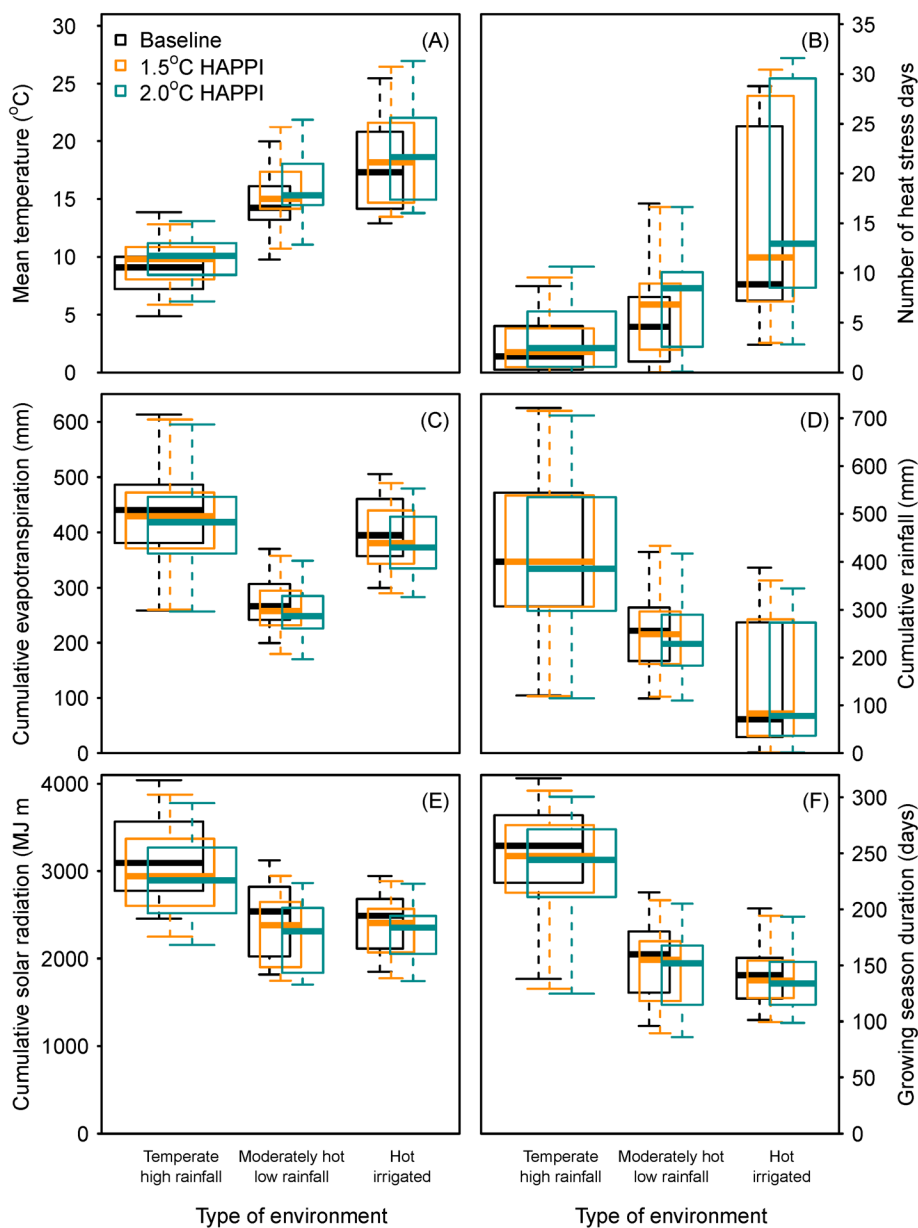
28

29



30

31 **Fig. S5. Hierarchical clustering on principal components of 60 representative global wheat growing**
 32 **locations based on climate variables for 1981-2010. (A)** Individual factor map with 30-years average
 33 and coefficient of variation for four climate variables (TMN, growing season [sowing to maturity] mean
 34 temperature; ET, growing season cumulative evapotranspiration; SRAD, growing season cumulative
 35 solar radiation; HSD, number of heat stress days [maximum daily temperature > 32°C] during the grain
 36 filling period). Blue, variables (Yield, average yield for the 1981-2010 baseline; Yield.cv, interannual yield
 37 variability [coefficient of variation] of yield for the 1981-2010 baseline; rc1.5 and rc2.0, relative changes
 38 in average yield for the 1.5 and 2.0 scenarios [HAPPI], respectively; rc1.5.CV and rc2.0.CV, relative
 39 changes in interannual yield variability for the 1.5 and 2.0°C warming scenarios, respectively; and
 40 pELY1.5 and pELY2.0, probabilities of extreme low yield [< 5% of baseline yield distribution] under the
 41 1.5 and 2.0 scenarios, respectively) projected onto the same factorial plan but not used to construct the
 42 axes. **(B)** Location/cluster map of the principal component analysis. The numbers refer to the location ID
 43 given in Table S1.



44

45 **Fig. S6. Weather variables during wheat growing season (sowing to maturity) and crop duration in the**
 46 **three main types of environments for the 1981-2010 baseline and under 1.5 and 2.0 scenario. (A)**

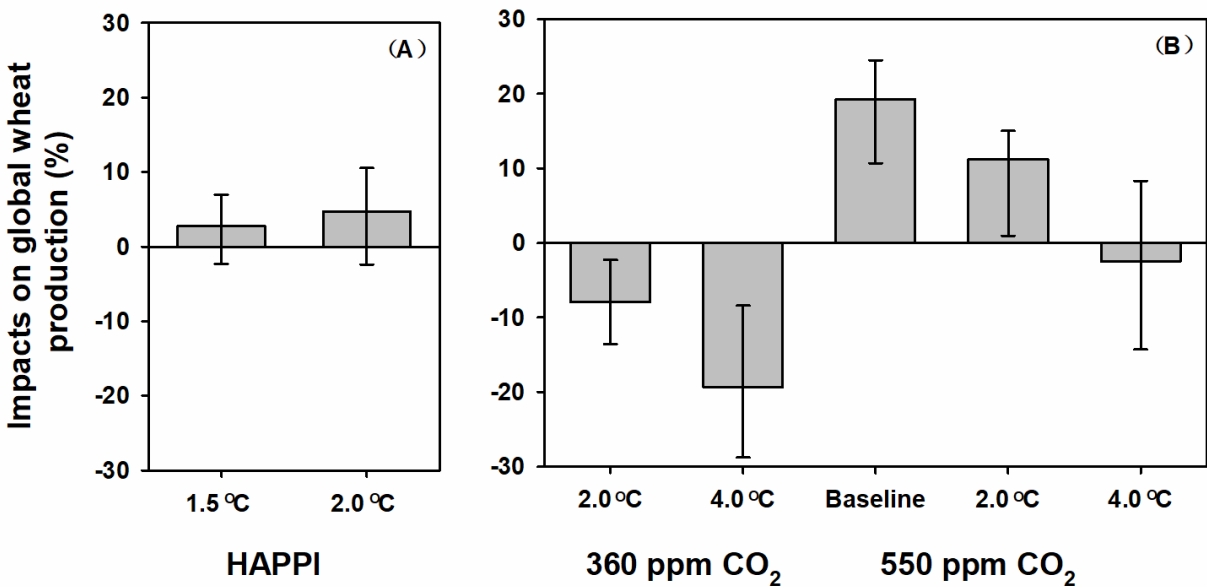
47 Growing season mean temperature, (B) Number of heat stress days (maximum daily temperature >
 48 32°C) during the post-flowering period. (C) Cumulative growing season evapotranspiration. (D)

49 Cumulative growing season rainfall. (E) Cumulative growing season solar radiation. (F) Growing season
 50 duration. The width of the boxes is proportional to the percentage of global wheat production of each

51 type of environment. The 60 global locations were clustered using 30-year means and coefficient of
 52 variability of the weather variables shown in this Figure S5. In each box plot, horizontal lines represent,

53 from top to bottom, the 10th percentile, 25th percentile, median, 75th percentile and 90th percentile. In
 54 hot irrigated locations, growing season rainfall does not include the irrigation amount.

55 **Note: Similar with Fig.3 in the main text, but show the means across crop models and GCMs.**

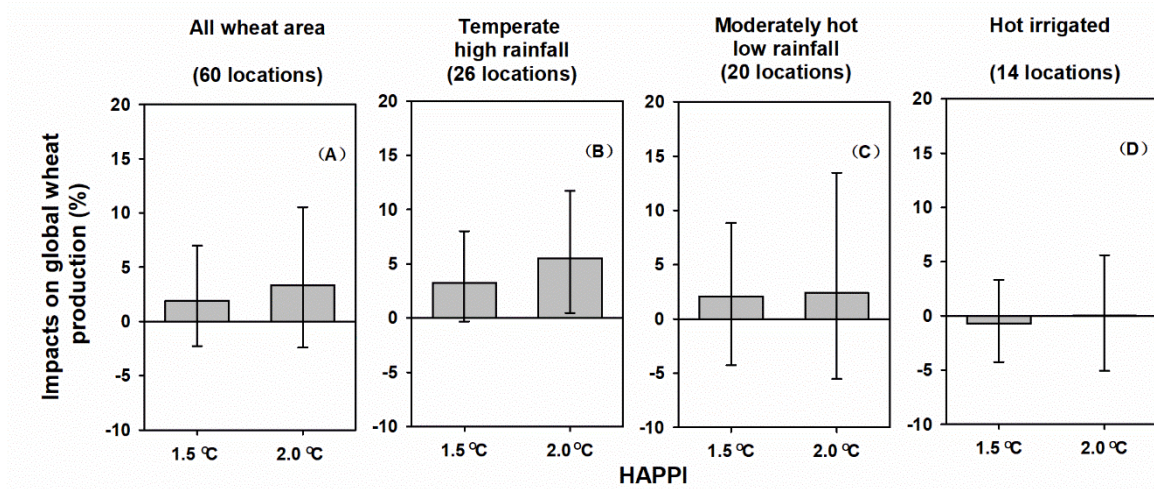


56

57 **Fig. S8. Simulated global impacts of climate change scenarios on wheat production.** Relative impact on global
58 wheat grain production for (A) 1.5 and 2.0 warming scenarios (HAPPI) with changes in temperature, rainfall and
59 atmospheric CO₂ concentration. Atmospheric CO₂ concentration for the 1.5 and 2.0 scenario were 423 and 487
60 ppm, respectively. (B) +2°C (360 ppm CO₂ +2°C) and +4°C (360 ppm CO₂ +4°C) temperature increase for the
61 baseline period with historical atmospheric CO₂ concentration (360 ppm CO₂) and elevated CO₂ (550 ppm CO₂)
62 for no temperature change (Baseline), +2°C (550 ppm CO₂ +2°C) and +4°C (550 ppm CO₂ +4°C). Impacts were
63 weighted by production area (based on FAO statistics). Relative change in grain yields were calculated from the
64 mean of 30 years projected yields and the ensemble **means** of 31 crop models (plus five GCMs for HAPPI
65 scenarios) using region-specific soils, cultivars, and crop management. Error bars are the 25th and 75th
66 percentiles across 31 crop models (plus five GCMs for HAPPI scenarios).

67

68

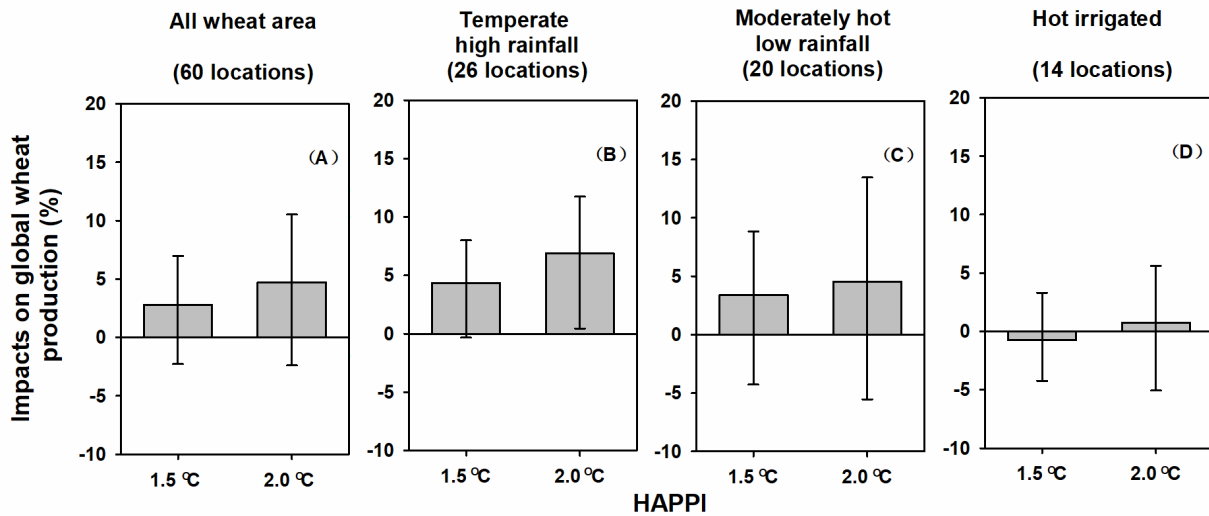


70

71 **Fig. S9. Simulated global impacts of climate change under 1.5 and 2.0 scenario on wheat production from**
 72 **different environments.** (A) All wheat area (60 locations). (B) Temperate high rainfall environment (26 locations).
 73 (C) Moderately hot low rainfall environment (20 locations). (D) Hot irrigated environment (14 locations). Impacts
 74 from the 60 global locations were weighted by FAO production area. Bars are ensemble **medians** of 31 crop
 75 models and five GCMs for 1.5 and 2.0 scenarios (HAPPI), including changes in temperature, rainfall and
 76 atmospheric CO₂ concentration, and mean of 30 years using region-specific soils, cultivars, and crop management.
 77 Error bars indicate the 25th and 75th percentiles across 31 crop models and five GCMs.

78

79 **Note: Similar with Fig.S9, but show the means across crop models and GCMs.**

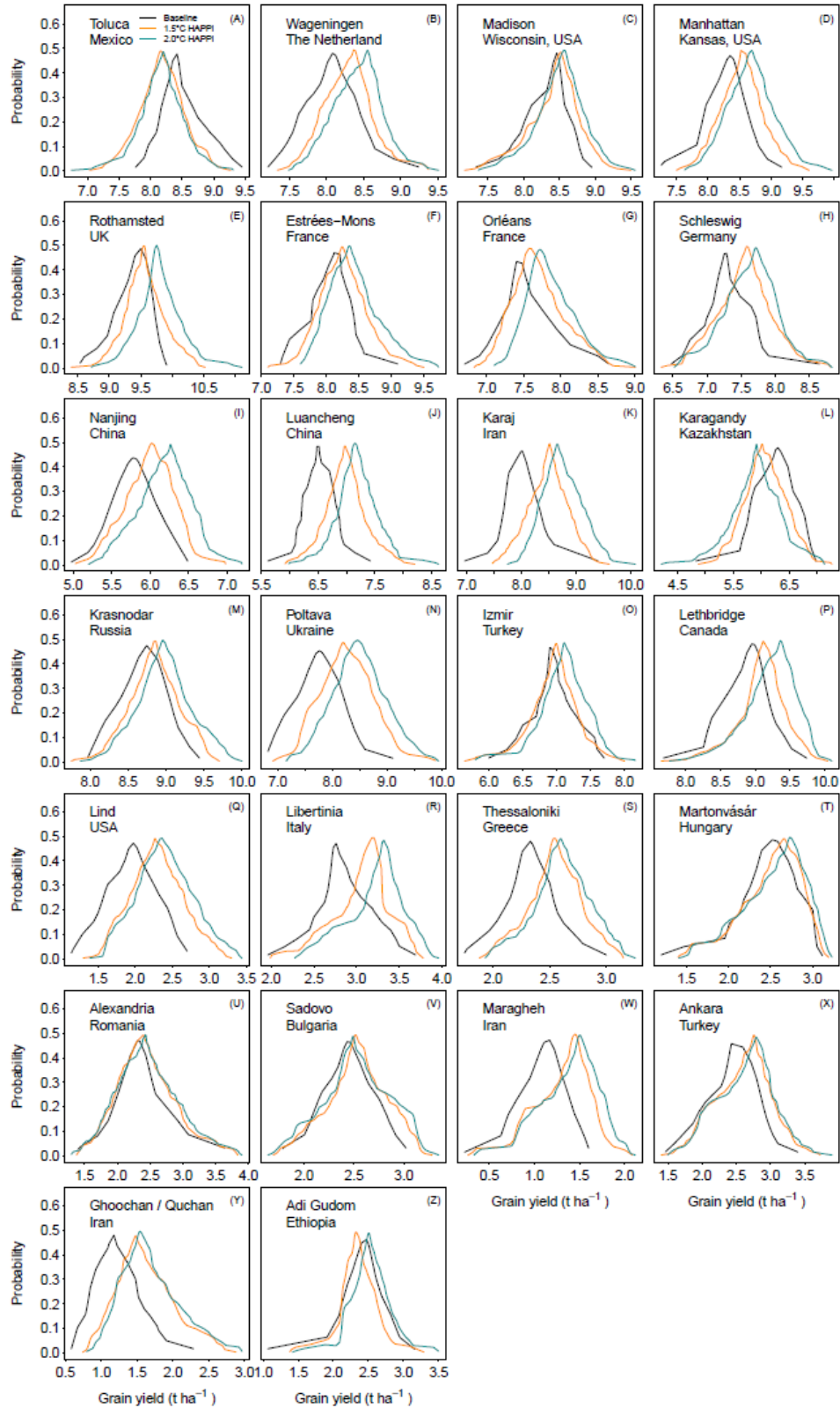


80

81 **Fig. S10. Simulated global impacts of climate change under 1.5 and 2.0 scenario on wheat production from**
82 **different environments.** (A) All wheat area (60 locations). (B) Temperate high rainfall environment (26 locations).
83 (C) Moderately hot low rainfall environment (20 locations). (D) Hot irrigated environment (14 locations). Impacts
84 from the 60 global locations were weighted by FAO production area. Bars are ensemble **means** of 31 crop models
85 and five GCMs for 1.5 and 2.0 scenarios (HAPPI), including changes in temperature, rainfall and atmospheric CO₂
86 concentration, and mean of 30 years using region-specific soils, cultivars, and crop management. Error bars
87 indicate the 25th and 75th percentiles across 31 crop models and five GCMs.

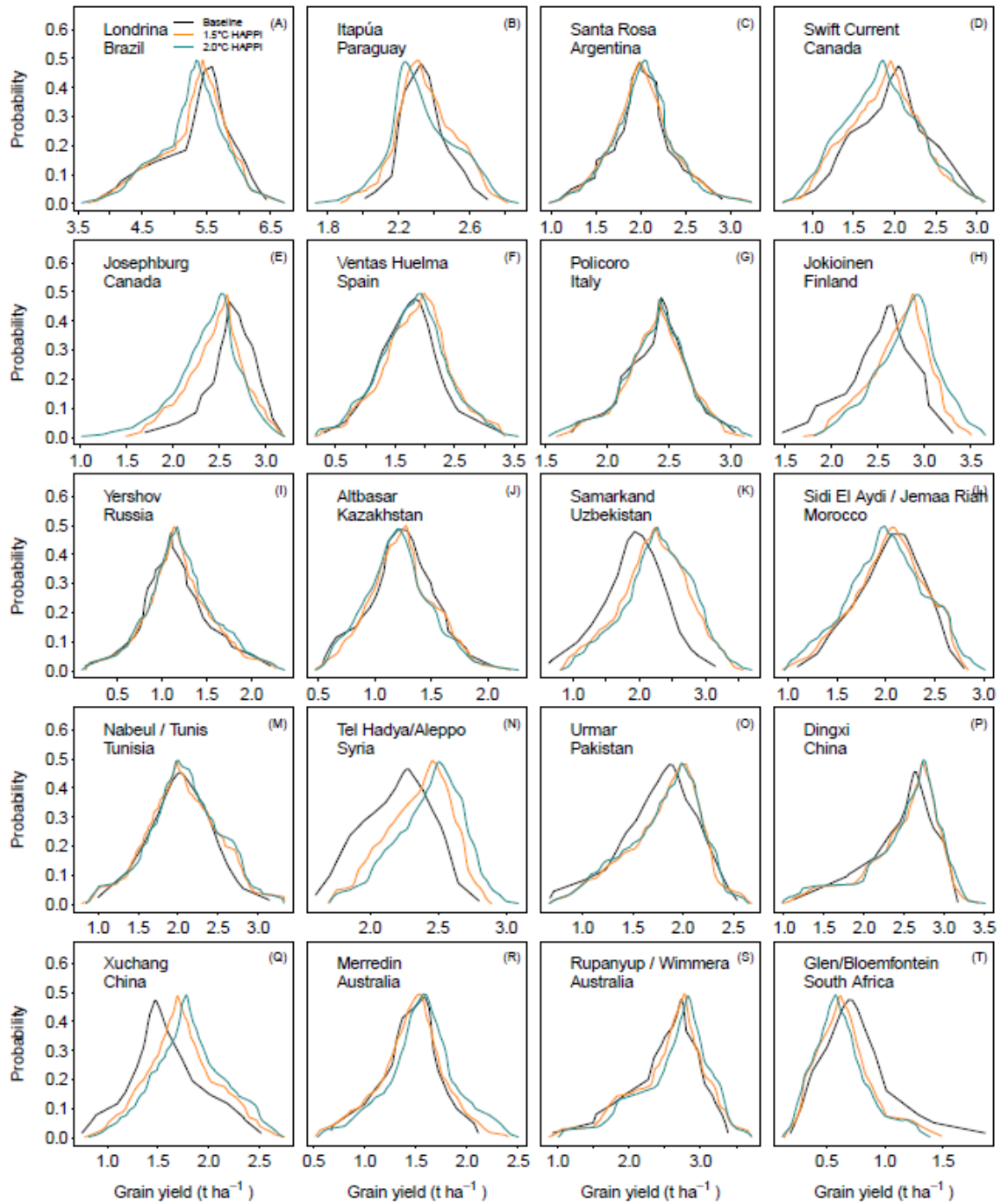
88

89



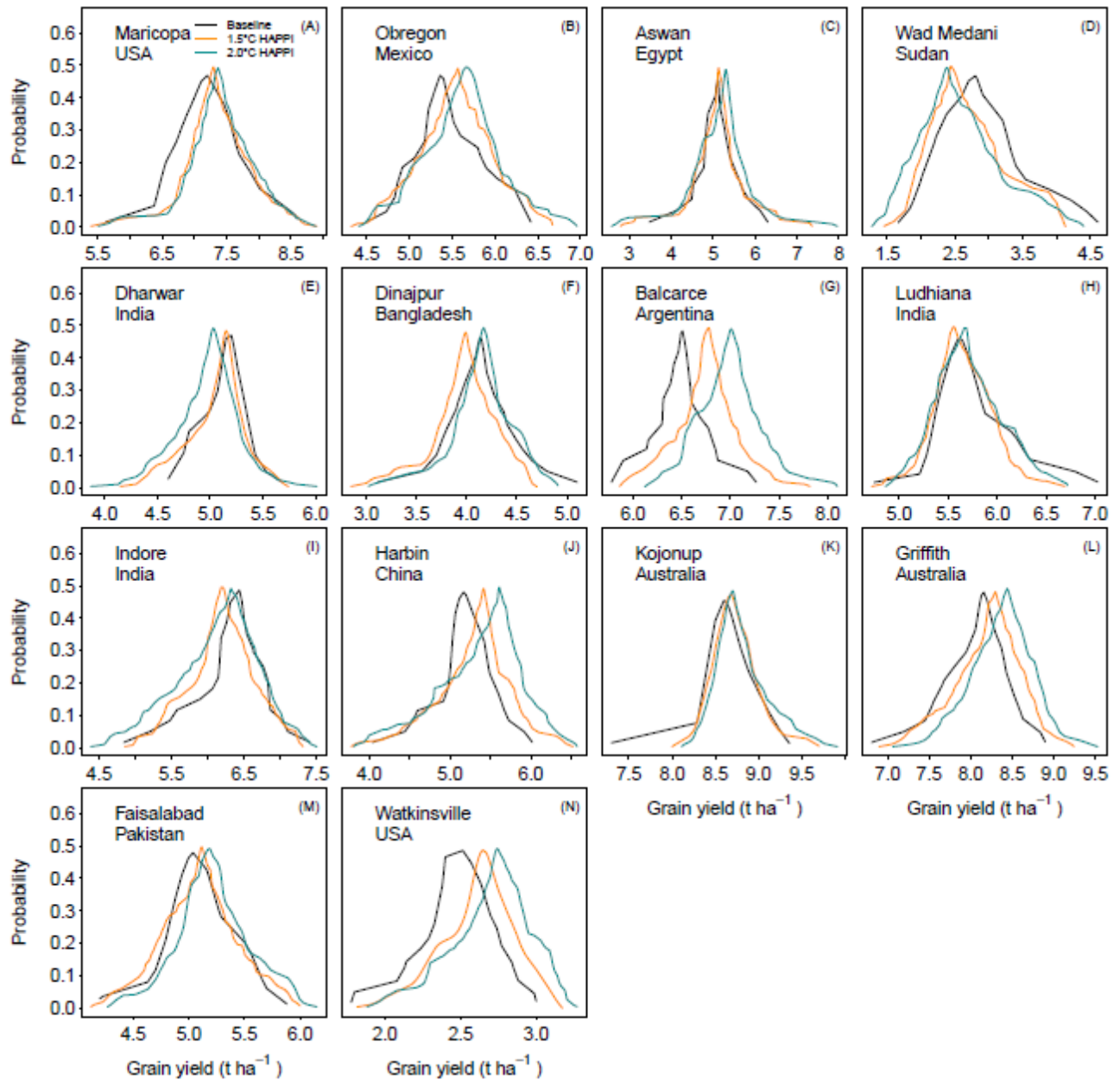
90

91 **Fig. S11.** Yield distribution for the 26 temperate high rainfall global locations for the 1981-2010 baseline and under
 92 1.5 and 2.0 scenarios (including changes in temperature, rainfall and atmospheric CO₂ concentration).



93

94 **Fig. S12.** Yield distribution at 20 moderately hot low rainfall global locations for the 1981-2010 baseline and under
 95 1.5 and 2.0 scenarios (including changes in temperature, rainfall and atmospheric CO₂ concentration).

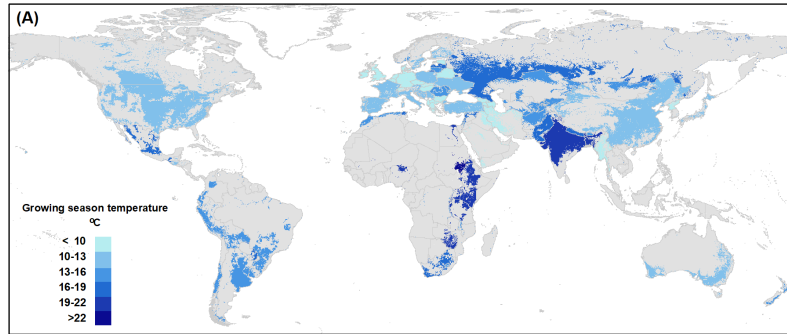


96

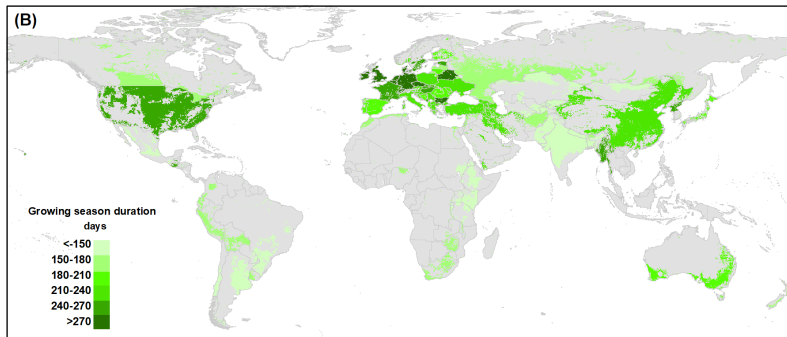
97 **Fig. S13.** Yield distribution at 14 hot irrigated global locations for the 1981-2010 baseline and under 1.5 and 2.0
 98 scenarios (including changes in temperature, rainfall and atmospheric CO₂ concentration).

99

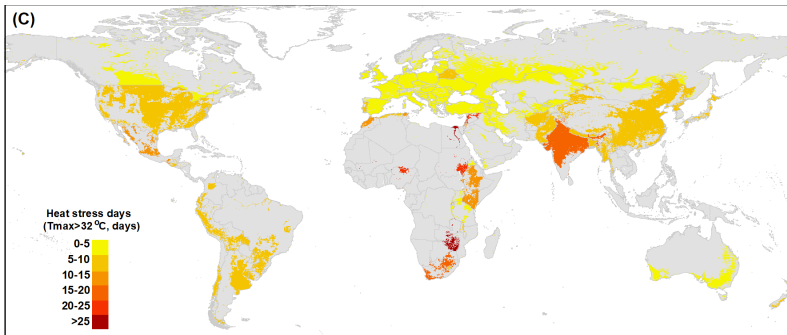
100



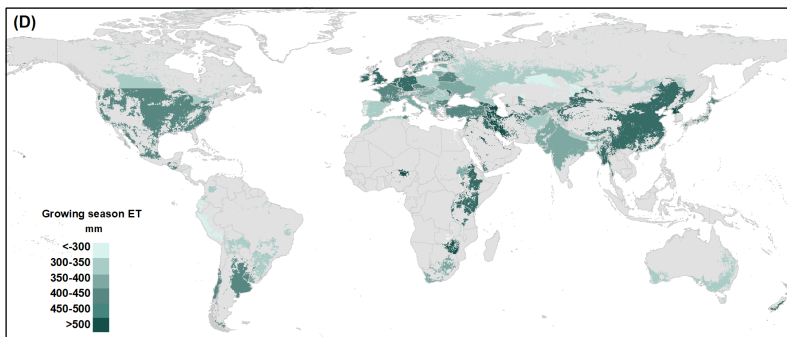
101



102

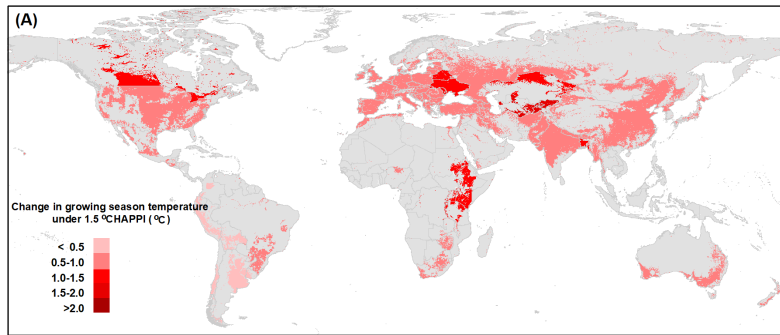


103

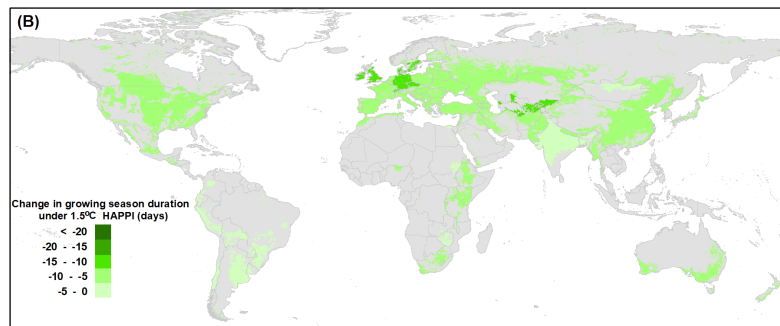


104 **Fig. S14. Simulated multi-model ensemble median of growing season (sowing to maturity) variables by country**
105 **for the 1981-2010 baseline.** (A) Growing season mean temperature. (B) Growing season duration. (C) Heat stress
106 days from anthesis to maturity (daily maximum temperature > 32°C). (D) Growing season evapotranspiration (ET).
107 All growing season variables were calculated from simulated growing season variables at the 60 corresponding
108 locations.

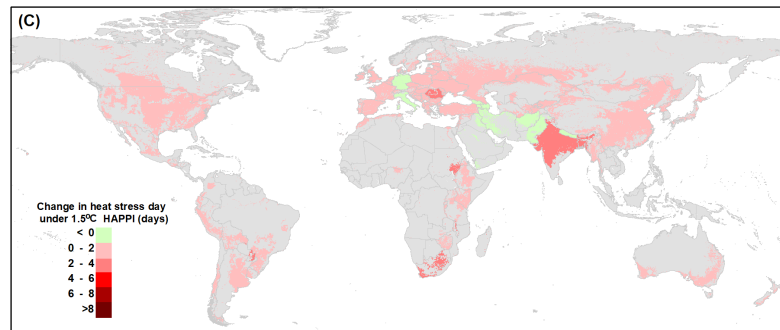
109



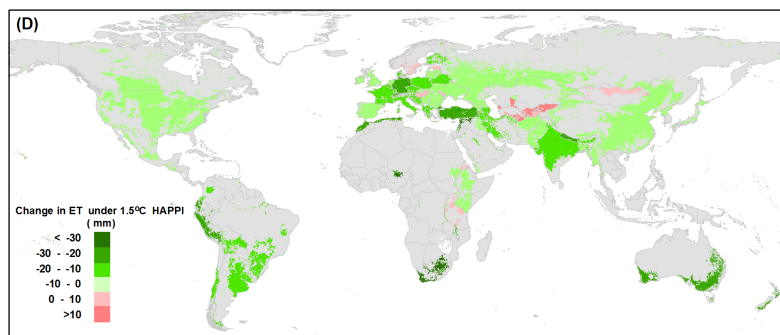
110



111



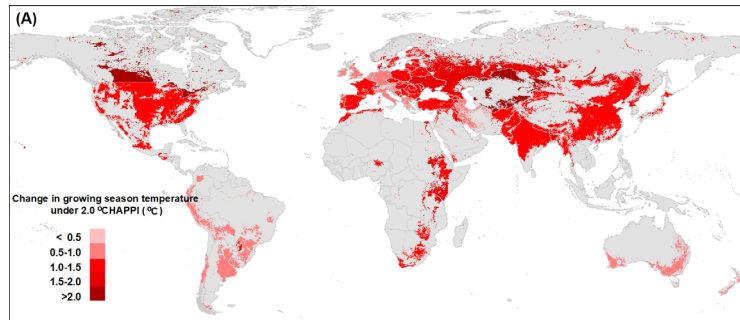
112



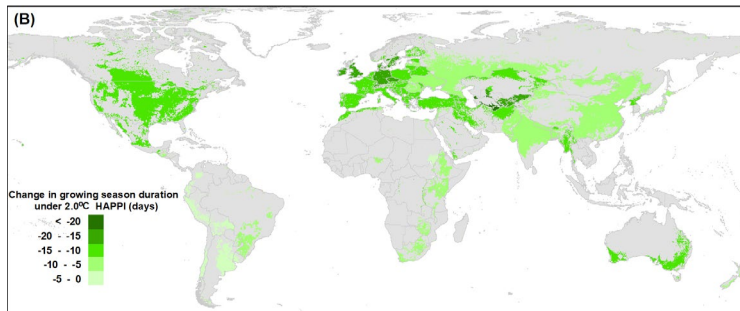
113

114 **Fig. S15. Simulated multi-model ensemble median of changes in growing season (sowing to maturity) variables**
115 **by country under 1.5 scenario.** (A) Growing season mean temperature. (B) Growing season duration. (C) Heat
116 stress days from anthesis to maturity (daily maximum temperature > 32°C). (D) Growing season evapotranspiration
117 (ET). All growing season variables were calculated from simulated growing season variables at the 60
118 corresponding locations.

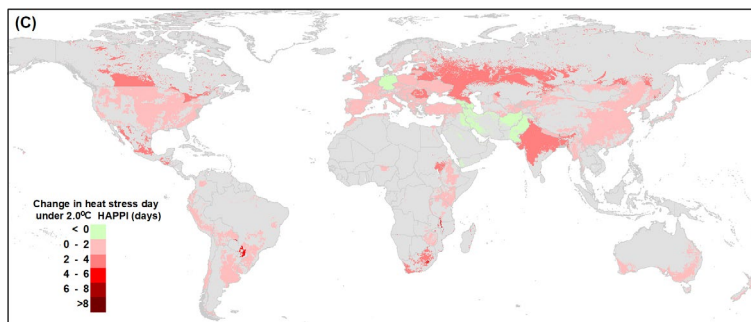
119



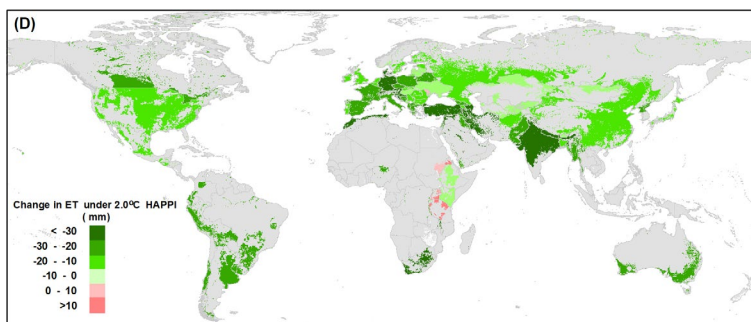
120



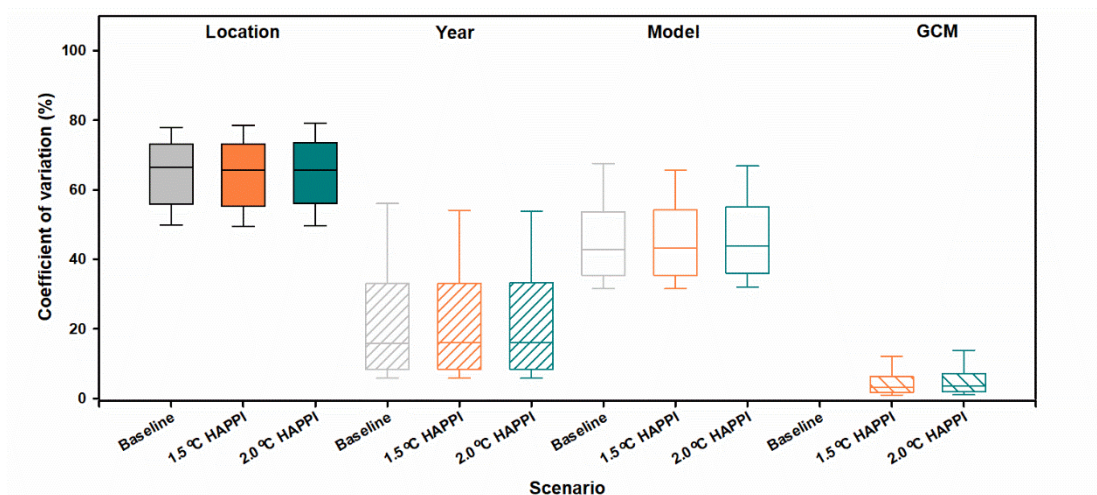
121



122



123 **Fig. S16. Simulated multi-model ensemble median of changes in growing season (sowing to maturity) variables**
124 **by country under 2.0 scenario.** (A) growing season mean temperature, (B) growing season duration, (C) heat stress
125 days from anthesis to maturity (daily maximum temperature >32°C), and (D) growing season evapotranspiration
126 (ET). All growing season variables were calculated from simulated growing season variables at the 60
127 corresponding locations.

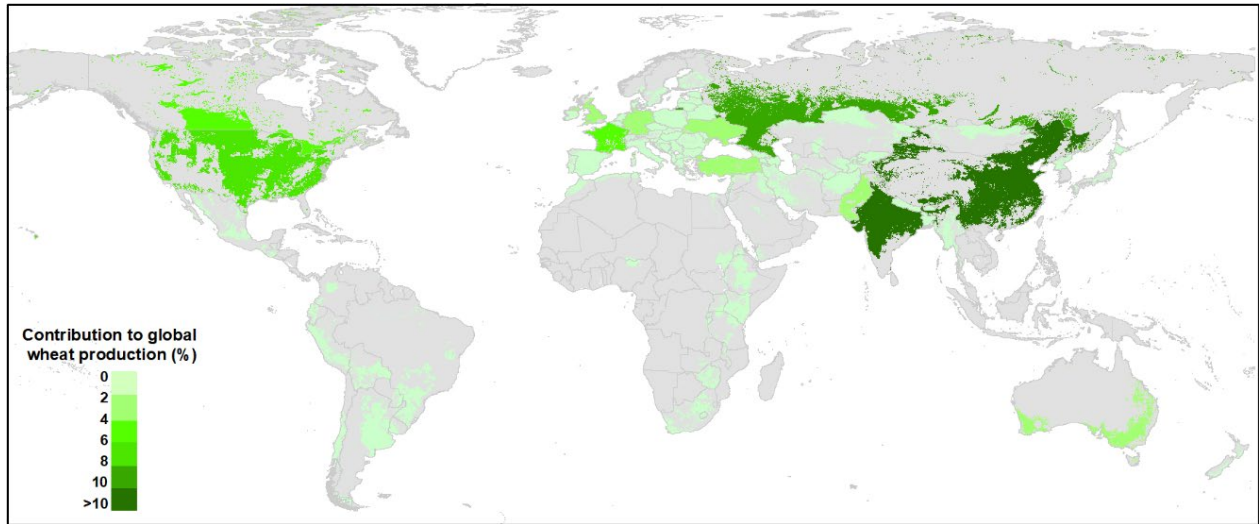


129

130 **Fig. S17. Coefficient of variation (CV) of simulated wheat grain yields for the 1981-2010 baseline (grey)**
 131 **and 1.5 and (orange) and 2.0 (blue) scenarios.** The distribution of CV for ‘Location’ shows the CVs of
 132 simulated wheat grain yields from the 60 global locations within each combination of crop model, year,
 133 and GCM. The distribution of CV for ‘Year’ shows the CVs of simulated wheat grain yields from the 30
 134 years within each combination of crop model, location, and GCM. The distribution of CV for ‘Model’
 135 shows the CVs of simulated wheat grain yields from the 31 crop models within each combination of
 136 location, year, and GCM. The distribution of CV for ‘GCM’ shows the CVs of simulated wheat grain yields
 137 from the five GCMs within each combination of location, crop model, and year. In each box plot,
 138 horizontal lines represent, from top to bottom, the 10th percentile, 25th percentile, median, 75th
 139 percentile, and 90th percentile of the simulations.

140

141

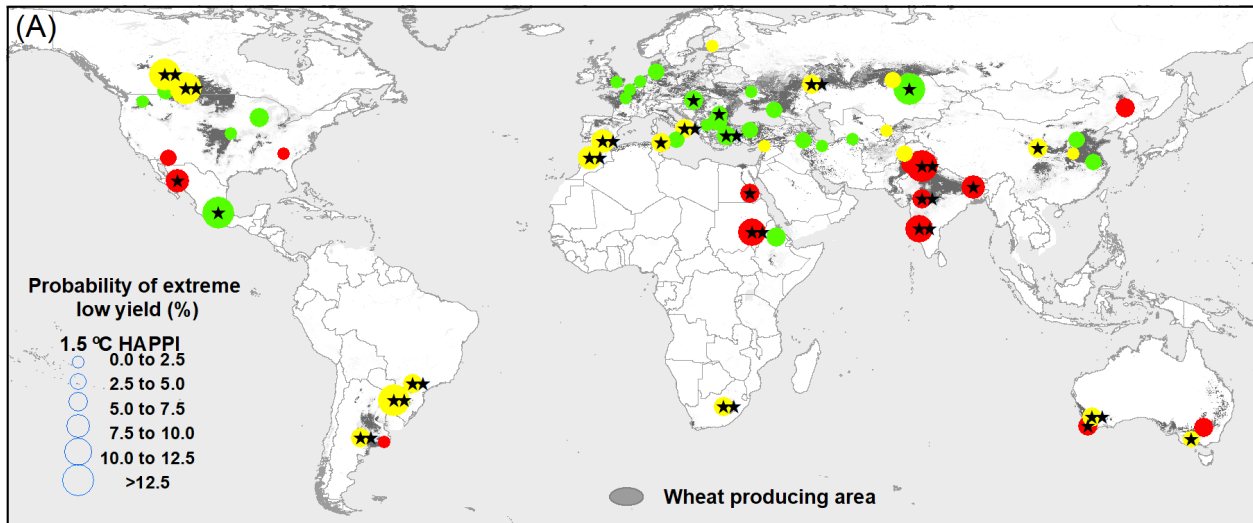


142

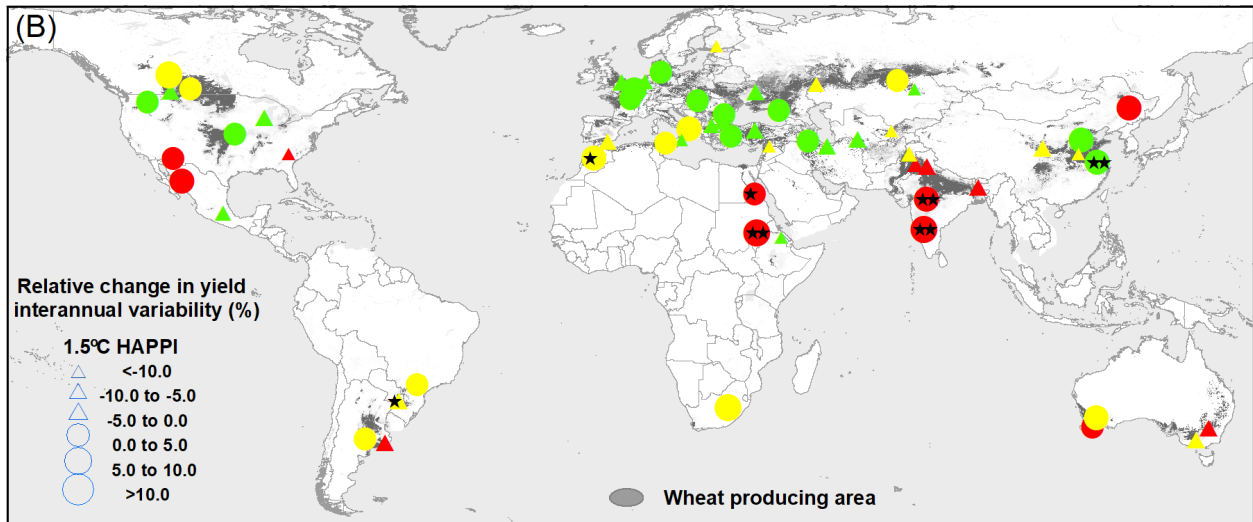
143 **Fig. S18. Contribution of national wheat production from 122 wheat producing countries to global wheat**
144 **production based on 2014 FAO statistical data.**

145

146



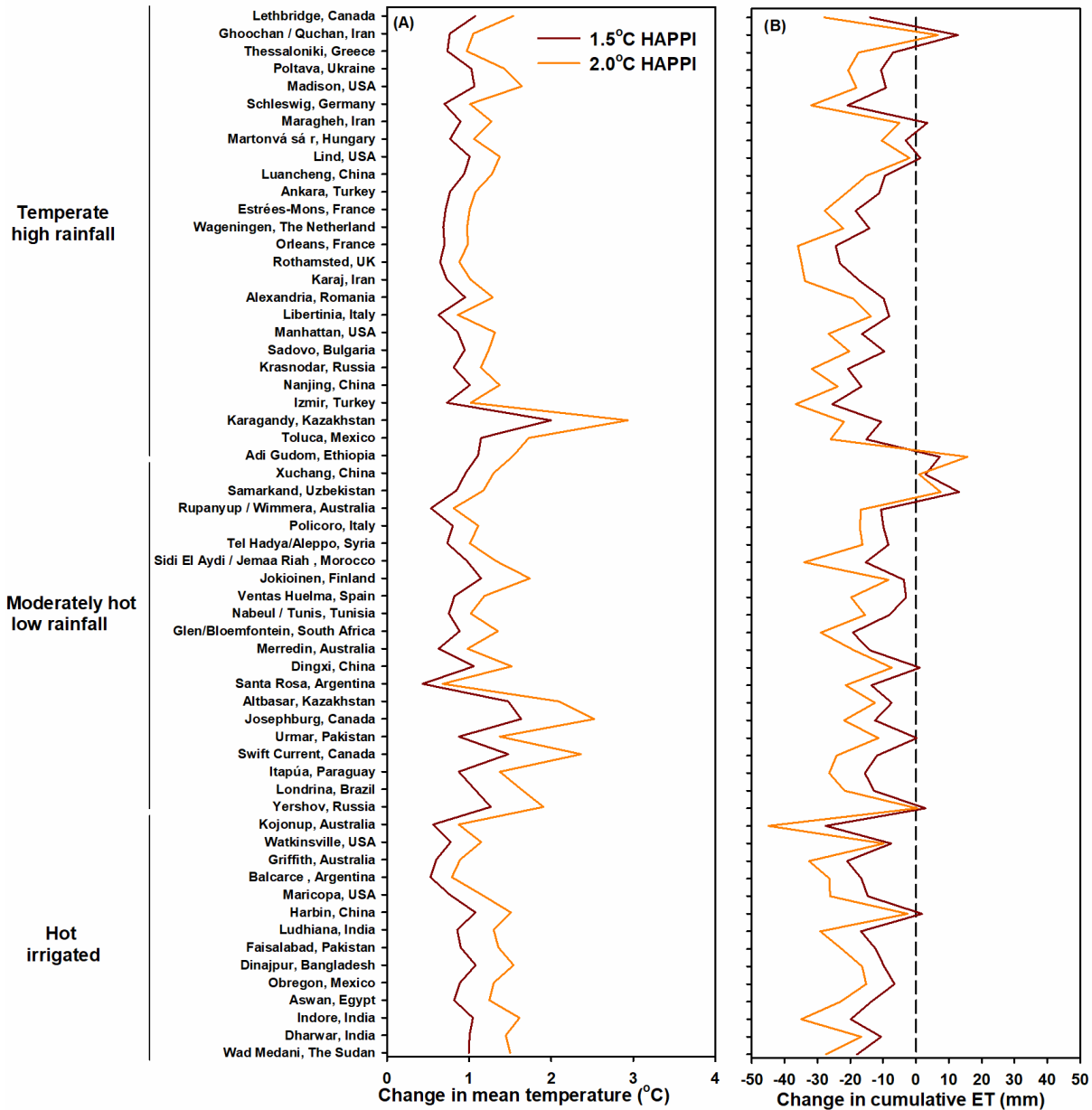
147



148 **Fig. S19. Projected impacts of the 1.5 scenario on the probability of extreme low wheat yields**
149 **(A) and wheat yield interannual variability (B)** at 60 representative global wheat growing
150 locations for clusters of temperate high rainfall or irrigated locations (dark green; 26 locations),
151 moderately hot low rainfall locations (dark yellow; 20 locations), and hot irrigated locations
152 (dark red; 14 locations). In (A and B), ★ and ★★ indicates the low yield probability and
153 interannual yield variability between warming scenario and baseline was significant at $p < 0.05$
154 and $p < 0.01$, respectively. In (B), the circles and triangles showed increased and decreased
155 interannual variability, respectively.

156

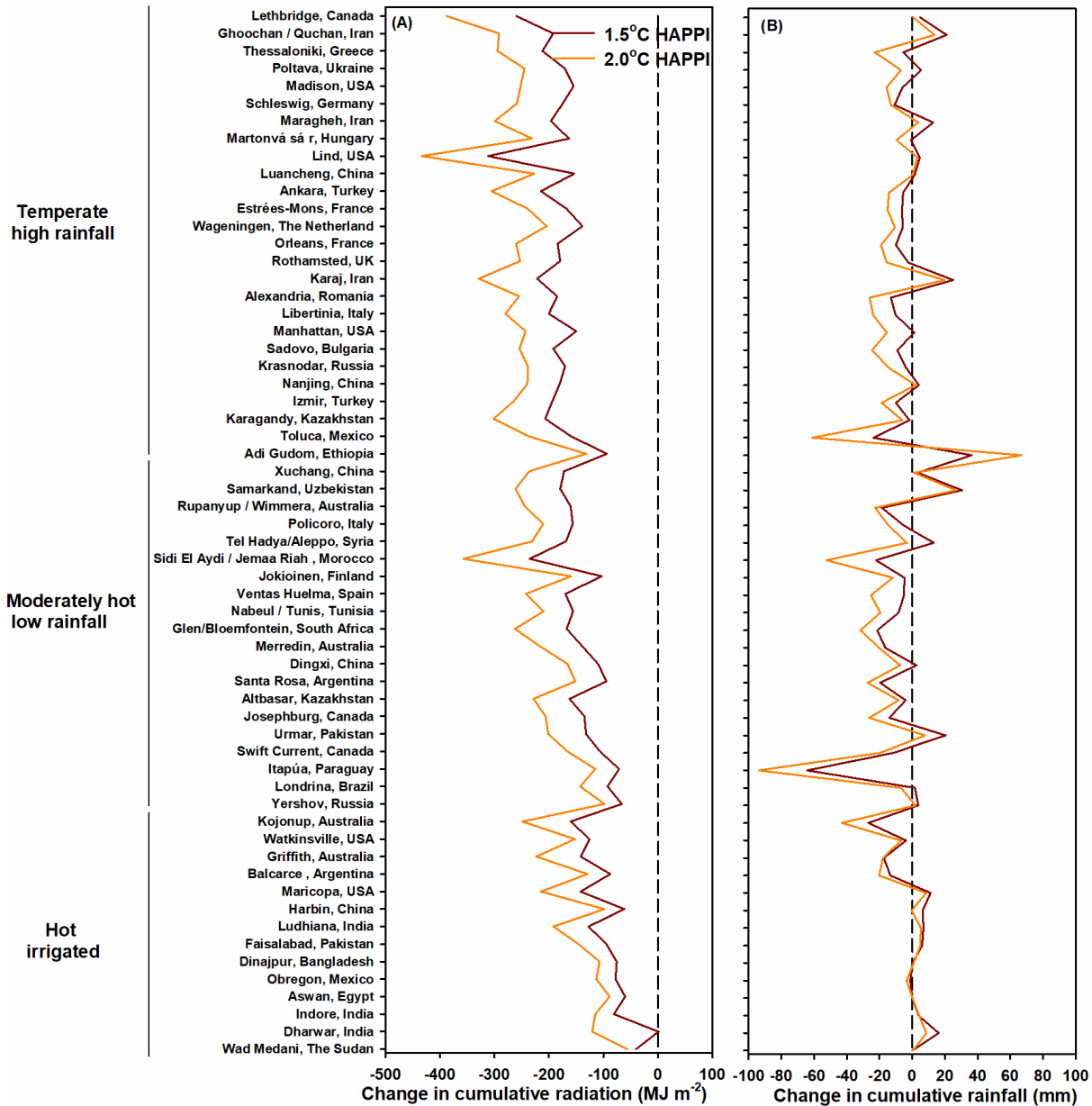
157



158

159 **Fig. S20. Projected changes in growing season (sowing to maturity) mean temperature (A) and cumulative ET**
 160 **(B) for the 60 representative global wheat growing locations under 1.5 and 2.0 scenarios (HAPPI).** The locations
 161 in each environment type were ordered by the growing season mean temperature for the baseline period. All the
 162 changes here were the median of 31 crop models and mean of 30 years and the five global climate models (GCMs).

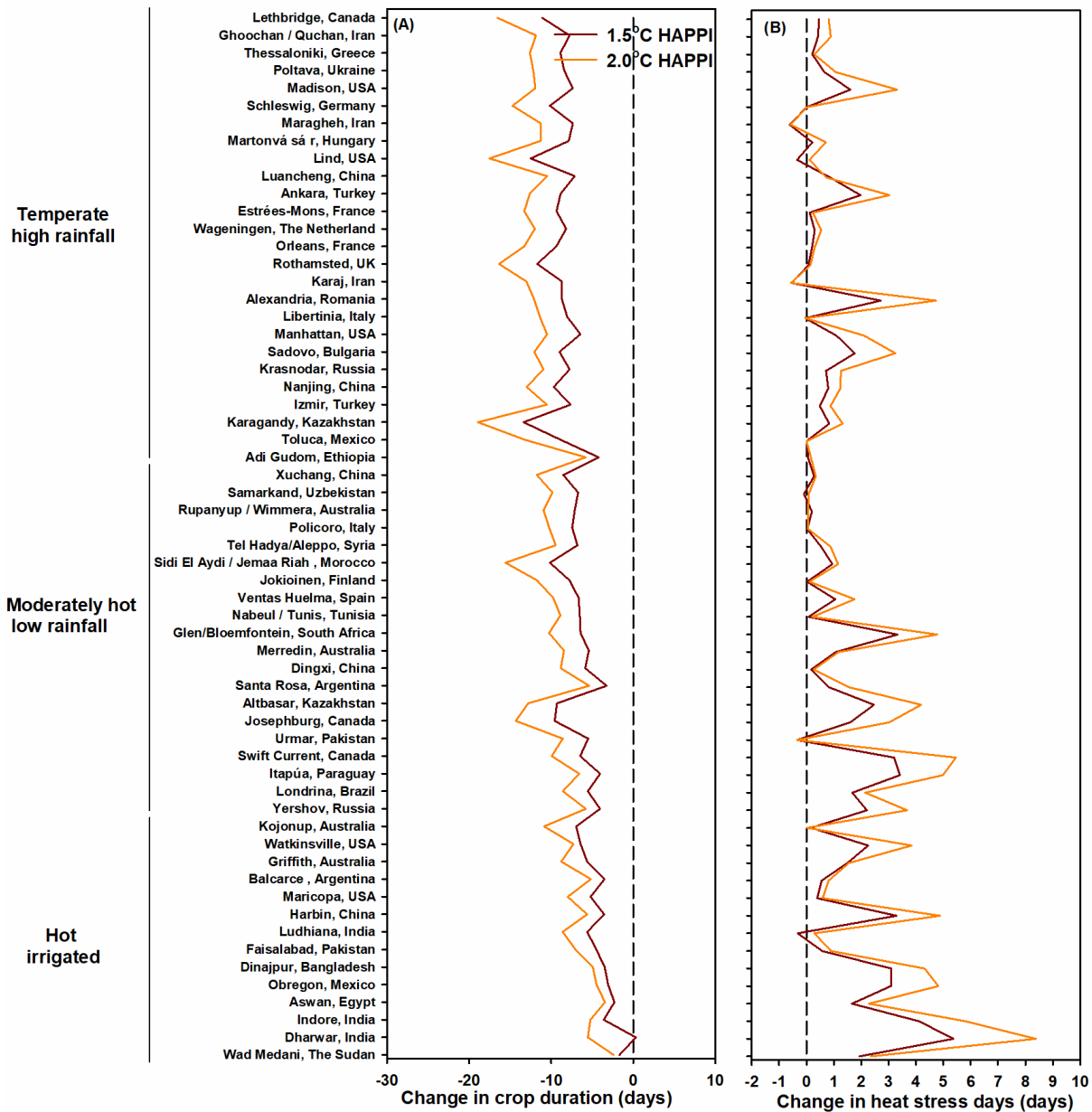
163



164
 165 **Fig. S21. Projected changes in growing season (sowing to maturity) cumulative solar radiation (A) and**
 166 **cumulative rainfall (B) for the 60 representative global wheat growing locations under 1.5 and 2.0 scenarios**
 167 **(HAPPI). The locations in each environment type were ordered by the growing season mean temperature for the**
 168 **baseline period. All the changes here were the median of 31 crop models and mean of 30 years and the five global**
 169 **climate models (GCMs).**

170

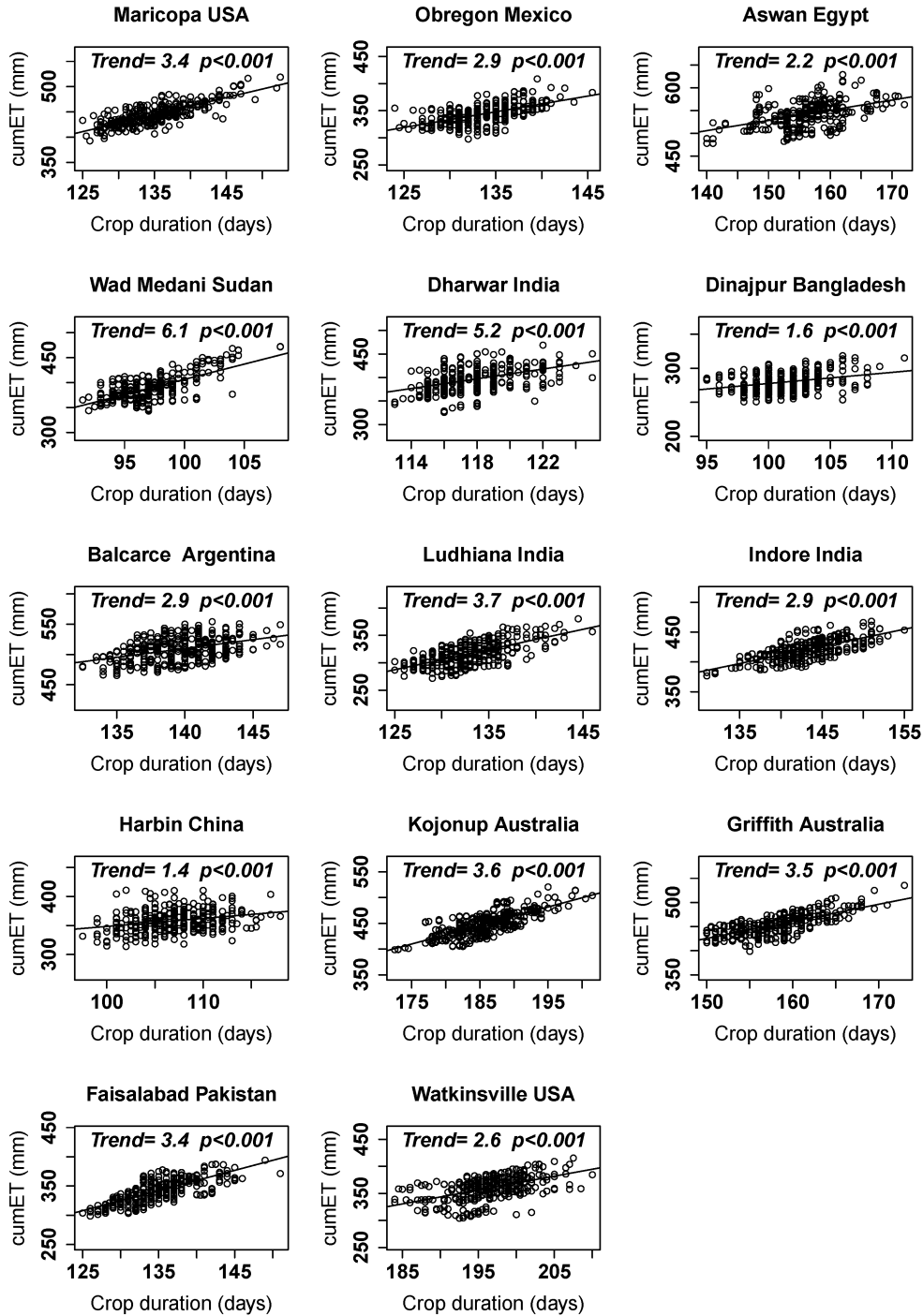
171



172

173 **Fig. S22. Projected changes in growing season (sowing to maturity) duration (A) and heat stress days (B) for the**
 174 **60 representative global wheat growing locations under 1.5 and 2.0 scenarios (HAPPI).** The locations in each
 175 environment type were ordered by the growing season mean temperature for the baseline period. All the changes
 176 here were the median of 31 crop models and mean of 30 years and the five global climate models (GCMs).

177



178

179 **Fig.S23. Relationship between projected growing season (sowing to maturity) cumulative ET and duration for**
 180 **the 14 hot irrigated locations for the 30 growing seasons under different climate scenarios.** The locations in each
 181 environment type were ordered by the growing season mean temperature for the baseline period. All the
 182 simulated data here were the medians of 31 crop models.

183

184 **Table S4 Slopes of linear regression between simulated grain yield and growing season (sowing to maturity) climate variables and growing season duration**
185 **for the 60 global locations under different climate scenarios.** Before conducting the regression, we tested whether there were significant differences between
186 the responses of simulated grain yield to climate variables and growing season duration under three different climate scenarios. If there were no significant
187 differences between different climate scenarios, the regressions were conducted with the simulated data from the 30 growing seasons under baseline and two
188 HAPPI warming scenarios together. And no regressions were conducted when there were significant differences in the responses of simulated grain yield to
189 climate variables and growing season duration between different climates scenarios, which only happened in few locations, as shown as NA in the table below.
190 GST: growing season mean temperature, ET: growing season cumulative evapotranspiration, GSD: growing season duration, HSD: heat stress days during grain
191 filling period, SRAD: growing season cumulative solar radiation, RAIN: growing season cumulative rainfall. All the simulated data used for regressions here were
192 the medians of 31 crop models. *** indicates $p < 0.001$, ** indicates $p < 0.01$, * indicates $p < 0.05$.

Environment type	Location	City	Country	GST (t. ha ⁻¹ . °C ⁻¹)	ET (t. ha ⁻¹ . mm ⁻¹)	GSD (t. ha ⁻¹ . d ⁻¹)	HSD ^a (t. ha ⁻¹ . d ⁻¹)	SRAD (t. ha ⁻¹ ./(MJ.m ²))	RAIN ^b (t. ha ⁻¹ . mm ⁻¹)
Temperate high rainfall	3	Toluca	Mexico	-0.321***	0.01***	na	na	0.003***	
	9	Wageningen	The Netherland	-0.047	0.009***	0.009**	-0.124***	0.001***	
	13	Madison	USA	-0.056*	0.006***	-0.001	-0.004	0.001***	
	14	Manhattan	USA	0.173***	0.003**	-0.003	-0.024***	0.001**	
	15	Rothamsted	UK	na	0.004***	na	-0.037	na	
	16	Estrées-Mons	France	0.033	0.007***	0.01**	na	0.001***	
	17	Orleans	Central France	-0.166***	0.008***	0.015***	-0.074**	0.001***	
	18	Schleswig	Germany	-0.161***	0.008***	0.011***	na	0.001***	
	19	Nanjing	China	0.081*	0.006***	-0.008*	0.077***	0.001***	
	20	Luancheng	China	0.208***	0.005***	-0.021***	0.008	0.001***	
	24	Karaj	Iran	0.374***	-0.006***	-0.015***	-0.075***	-0.0004**	
	26	Karagandy	Kazakhstan	na	0.012***	na	-0.138***	0.002***	
	27	Krasnodar	Russia	-0.01	0.007***	0.011**	-0.034***	0.001***	
	28	Poltava	Ukraine	0.243***	0.012***	0.013**	-0.051***	0.001***	
	29	Izmir	Turkey	-0.126**	0.005***	0.013**	-0.033***	0.001***	
	30	Lethbridge	Canada	0.002	0.008***	0.003	-0.041***	0.001***	
	34	Lind	USA	0.307***	0.011***	0.006**	-0.081***	0.0003*	0.007***
	39	Libertinia	Italy	0.348***	0.01***	0.005	-0.056	-0.001***	0.002***
	40	Thessaloniki	Greece	0.162***	0.008***	-0.001	-0.088***	0.0002*	-0.001***

	41	Martonvásár	Hungary	-0.077**	0.012***	0.016***	-0.062***	-0.001***	0.005***
	42	Alexandria	Romania	0.041	0.01***	0.004	-0.032***	-0.001***	0.006***
	43	Sadovo	Bulgaria	-0.049	0.009***	0.007***	-0.009*	-0.0003*	0.005***
	51	Maragheh	Iran	0.05	0.006***	0.007***	-0.043***	-0.0002	0.004***
	52	Ankara	Turkey	0.087*	0.009***	0.0001	-0.037***	-0.0002*	0.007***
	53	Ghoochan / Quchan	Iran	0.184***	0.009***	0.013***	-0.022	-0.0004*	0.008***
	59	Adi Gudom	Ethiopia	-0.043*	0.005***	0.009**	na	0.0003*	0.001***
	4	Londrina	Brazil	-0.356***	0.014***	0.06***	na	0.004***	
	31	Itapúa	Paraguay	-0.104***	0.008***	0.019***	-0.022***	0.001***	0.001***
	32	Santa Rosa	Argentina	-0.116***	0.008***	0.01***	-0.049***	0.0003	0.004***
	35	Swift Current	Canada	-0.252***	0.016***	na	-0.065***	0.003***	0.009***
	36	Josephburg	Canada	-0.164***	0.012***	na	-0.065***	0.001***	0.005***
	37	Ventas Huelma	Spain	-0.393***	0.011***	0.051***	-0.069***	-0.002***	0.006***
	38	Policoro	Italy	-0.058*	0.007***	0.009***	na	-0.0001	0.001***
	44	Jokioinen	Finland	-0.189***	0.016***	na	na	0.002***	0.003***
	45	Yershov	Russia	-0.198***	0.011***	0.049***	-0.028***	0.001***	0.009***
	46	Altbasar	Kazakhstan	-0.087***	0.011***	0.017***	-0.048***	0.0004***	0.008***
	47	Samarkand	Uzbekistan	0.038	0.011***	0.01**	-0.07***	-0.001***	0.007***
	48	Sidi El Aydi / Jemaa Riah	Morocco	-0.202***	0.012***	0.024***	-0.04**	-0.0003*	na
	49	Nabeul / Tunis	Tunisia	-0.244***	0.013***	0.042***	-0.107***	-0.0003	0.006***
	50	Tel Hadya/Aleppo	Syria	0.052	0.007***	0.002	-0.036***	-0.001***	0.002***
	54	Urmar	Pakistan	-0.13***	0.008***	0.018***	-0.014***	-0.001***	0.004***
	55	Dingxi	China	-0.189***	0.011***	0.03***	-0.1***	0.001***	0.008***
	56	Xuchang	China	-0.092**	0.011***	0.001	-0.047***	-0.001***	0.006***
	57	Merredin	Australia	-0.244***	0.008***	0.024***	-0.079***	-0.0005*	0.007***
	58	Rupanyup / Wimmera	Australia	-0.247**	0.011***	0.026***	-0.111***	-0.00003	0.006***
	60	Glen/Bloemfontein	South Africa	-0.033*	0.006***	0.001	-0.031***	0.00001	0.004***
Hot irrigated	1	Maricopa	USA	-0.55***	0.02***	0.074***	-0.102***	0.003***	

2	Obregon	Mexico	-0.427***	0.017***	na	-0.029***	0.002***
5	Aswan	Egypt	-0.315***	na	0.051***	-0.068***	0.001***
6	Wad Medani	Sudan	-0.53***	0.02***	na	-0.116***	0.007***
7	Dharwar	India	-0.364***	0.003***	0.085***	-0.016***	0.001***
8	Dinajpur	Bangladesh	-0.268***	0.006***	0.064***	-0.039***	0.003***
10	Balcarce	Argentina	-0.129**	0.007***	0.033***	-0.051***	0.001***
11	Ludhiana	India	-0.286***	0.012***	0.043***	-0.005	0.002***
12	Indore	India	na	0.02***	0.104***	-0.059***	0.003***
21	Harbin	China	-0.268***	0.007***	0.042***	-0.051***	0.002***
22	Kojonup	Australia	-0.29***	0.004***	0.025***	na	0.001***
23	Griffith	Australia	-0.444***	0.008***	0.047***	-0.067***	0.001***
25	Faisalabad	Pakistan	-0.337***	0.011***	0.047***	-0.036***	0.002***
33	Watkinsville	USA	0.076**	0.009***	0.01**	-0.029***	-0.00003

193 **Notes:**

194 a: **na** indicate no regression conducted due to no heat stress days during wheat growing season.

195 b: no data was shown for Loc1-30 as automatic irrigation was applied in all the simulations at these locations.

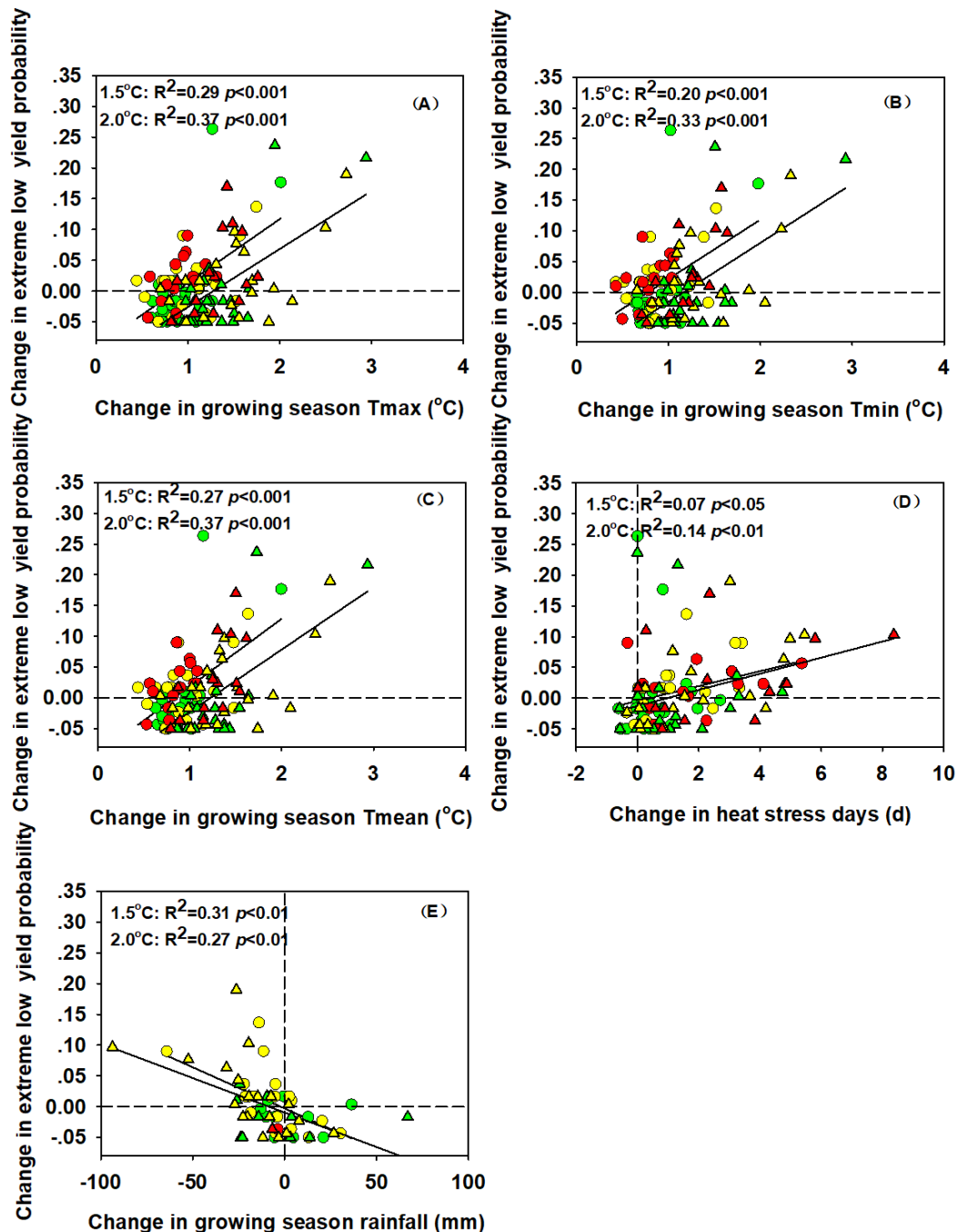
196

197

198

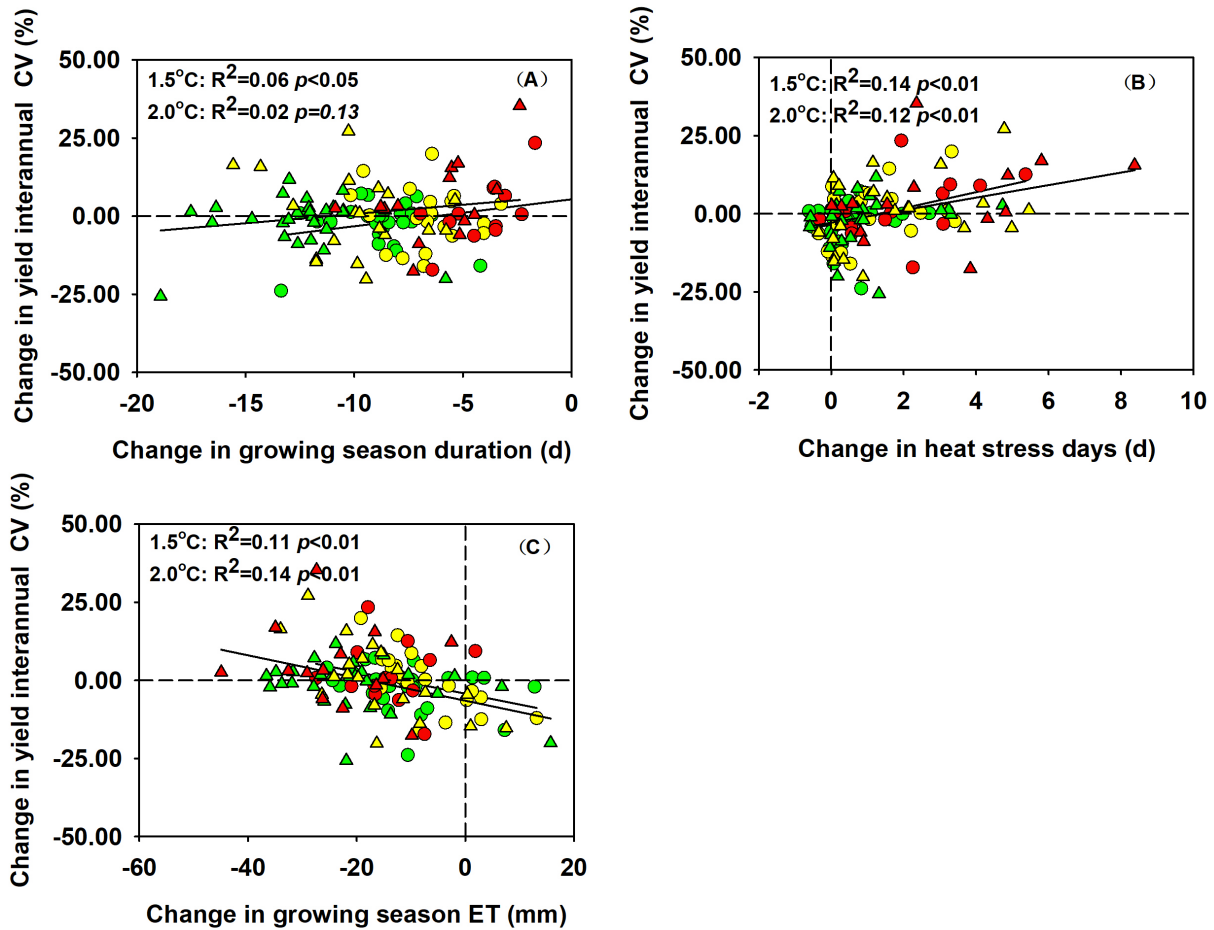
199

200



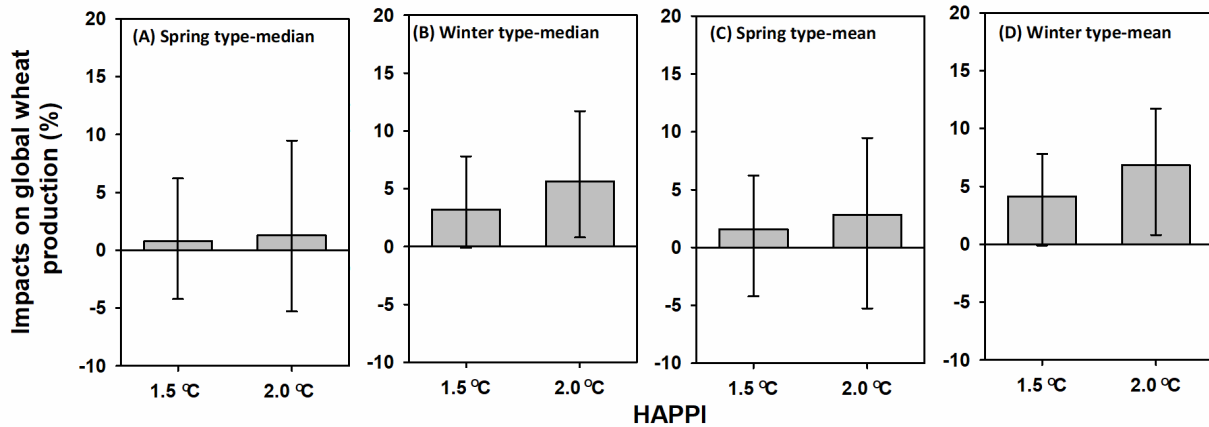
201

202 **Fig.S24. Relationship between changes in extreme low yield probability and changes in growing season variables**
 203 **under two warming scenarios at 60 representative global wheat growing locations for clusters of temperate high**
 204 **rainfall or irrigated locations (green; 26 locations), moderately hot low rainfall locations (yellow; 20 locations),**
 205 **and hot irrigated locations (red; 14 locations). (A) Growing season maximum temperature (°C), (B) Growing**
 206 **season minimum temperature (°C), (C) Growing season mean temperature (°C), (D) Growing season heat stress**
 207 **days (d), (E) Growing season cumulative rainfall (mm). Circles and triangles indicate changes under 1.5 scenario**
 208 **and 2.0 scenario, respectively. In (E), 30 locations (Loc1-30) where automatic irrigation was used in the simulations**
 209 **were not shown.**



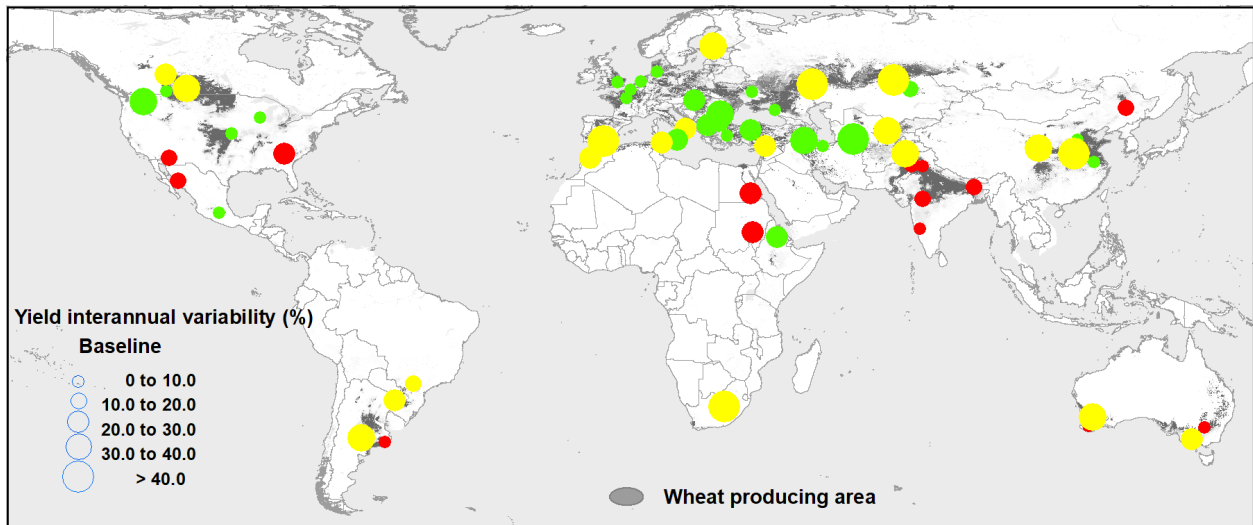
210

211 **Fig.S25. Relationship between relative changes in yield interannual variability (CV) and changes in growing**
 212 **season variables under two warming scenarios at 60 representative global wheat growing locations for clusters**
 213 **of temperate high rainfall or irrigated locations (green; 26 locations), moderately hot low rainfall locations**
 214 **(yellow; 20 locations), and hot irrigated locations (red; 14 locations). (A) Growing season duration (days), (B)**
 215 **Growing season heat stress days (d), (C) Growing season cumulative evapotranspiration (ET, mm). Circles and**
 216 **triangles indicate changes under 1.5 scenario and 2.0 scenario, respectively.**



217

218 **Fig. S26. Simulated global impacts of climate change under 1.5 and 2.0 scenario on wheat production from**
 219 **different wheat types.** (A) Spring type wheat from model ensemble medians (39 locations). (B) Winter type wheat
 220 from model ensemble medians (21 locations). (C) Spring type wheat from model ensemble means. (D) Winter type
 221 wheat from model ensemble means. Impacts from the 60 global locations were weighted by FAO production area.
 222 Bars are ensemble **medians or means** of 31 crop models and five GCMs for 1.5 and 2.0 scenarios (HAPPI), including
 223 changes in temperature, rainfall and atmospheric CO₂ concentration, and mean of 30 years using region-specific
 224 soils, cultivars, and crop management. Error bars indicate the 25th and 75th percentiles across 31 crop models and
 225 five GCMs.



226

227 **Fig.S27 Simulated interannual yield variability (coefficient of variation) during the 1981-2010 baseline period at**
 228 **60 representative global wheat growing locations for clusters of temperate high rainfall or irrigated locations**
 229 **(green; 26 locations), moderately hot low rainfall locations (yellow; 20 locations), and hot irrigated locations**
 230 **(red; 14 locations).**

231

232

233 Reference

- 234 Aggarwal P, Banerjee B, Daryaei M *et al.* (2006) InfoCrop: A dynamic simulation model for the
235 assessment of crop yields, losses due to pests, and environmental impact of agro-ecosystems in
236 tropical environments. II. Performance of the model. *Agricultural Systems*, **89**, 47-67.
- 237 Allen MR, Ingram WJ (2002) Constraints on future changes in climate and the hydrologic cycle. *Nature*,
238 **419**, 224-232. doi:10.1038/nature01092
- 239 Al-Mulla Y, Wu J, Singh P, Flury M, Schillinger W, Huggins D, Stockle C (2009) Soil water and temperature
240 in chemical versus reduced-tillage fallow in a Mediterranean climate. *Applied Engineering in*
241 *Agriculture*, **25**, 45.
- 242 Angulo C, Rötter R, Lock R, Enders A, Fronzek S, Ewert F (2013) Implication of crop model calibration
243 strategies for assessing regional impacts of climate change in Europe. *Agricultural and Forest*
244 *Meteorology*, **170**, 32-46.
- 245 Araya T, Nyssen J, Govaerts B, Deckers J, Cornelis WM (2015) Impacts of conservation agriculture-based
246 farming systems on optimizing seasonal rainfall partitioning and productivity on vertisols in the
247 Ethiopian drylands. *Soil and Tillage Research*, **148**, 1-13.
- 248 Asseng S (2004) *Wheat Crop Systems: A Simulation Analysis*, Melbourne, Australia, CSIRO Publishing.
- 249 Asseng S, Ewert F, Martre P *et al.* (2015) Rising temperatures reduce global wheat production. *Nature*
250 *Climate Change*, **5**, 143-147.
- 251 Asseng S, Martre P, Maiorano A *et al.* (2018) Climate change impact and adaptation for wheat protein.
252 *Global Change Biology*, Accepted.
- 253 Asseng S, Keating BA, Fillery IRP *et al.* (1998) Performance of the APSIM-wheat model in Western
254 Australia. *Field Crops Research*, **57**, 163-179.
- 255 Asseng S, Travasso MI, Ludwig F, Magrin GO (2013) Has climate change opened new opportunities for
256 wheat cropping in Argentina? *Climatic change*, **117**, 181-196.
- 257 Balkovič J, van der Velde M, Schmid E *et al.* (2013) Pan-European crop modelling with EPIC:
258 Implementation, up-scaling and regional crop yield validation. *Agricultural Systems*, **120**, 61-75.
- 259 Balkovič J, van der Velde M, Skalský R *et al.* (2014) Global wheat production potentials and management
260 flexibility under the representative concentration pathways. *Global and Planetary Change*, **122**,
261 107-121.
- 262 Bannayan M, Sanjani S, Alizadeh A, Lotfabadi SS, Mohamadian A (2010) Association between climate
263 indices, aridity index, and rainfed crop yield in northeast of Iran. *Field Crops Research*, **118**, 105-
264 114.
- 265 Basso B, Cammarano D, Troccoli A, Chen D, Ritchie J (2010) Long-term wheat response to nitrogen in a
266 rainfed Mediterranean environment: Field data and simulation analysis. *European Journal of*
267 *Agronomy*, **33**, 132-138.
- 268 Beringer T, Lucht W, Schaphoff S (2011) Bioenergy production potential of global biomass plantations
269 under environmental and agricultural constraints. *Global Change Biology Bioenergy*, **3**, 299-312.
- 270 Berzsenyi Z, Győrffy B, Lap D (2000) Effect of crop rotation and fertilisation on maize and wheat yields
271 and yield stability in a long-term experiment. *European Journal of Agronomy*, **13**, 225-244.
- 272 Biernath C, Gayler S, Bittner S, Klein C, Hogy P, Fangmeier A, Priesack E (2011) Evaluating the ability of
273 four crop models to predict different environmental impacts on spring wheat grown in open-top
274 chambers. *European Journal of Agronomy*, **35**, 71-82.
- 275 Bondeau A, Smith PC, Zaehle S, Schaphoff S, Lucht W, Cramer W, Gerten D (2007) Modelling the role of
276 agriculture for the 20th century global terrestrial carbon balance. *Global Change Biology*, **13**,
277 679-706.
- 278 Boogaard H, Kroes J (1998) Leaching of nitrogen and phosphorus from rural areas to surface waters in
279 the Netherlands. *Nutrient Cycling in Agroecosystems*, **50**, 321-324.

- 280 Brisson N, Gary C, Justes E *et al.* (2003) An overview of the crop model STICS. *European Journal of*
 281 *Agronomy*, **18**, 309-332.
- 282 Brisson N, Mary B, Ripoche D *et al.* (1998) STICS: a generic model for the simulation of crops and their
 283 water and nitrogen balances. I. Theory and parameterization applied to wheat and corn.
 284 *Agronomie*, **18**, 311-346.
- 285 Cao W, Liu T, Luo W, Wang S, Pan J, Guo W (2002) Simulating organic growth in wheat based on the
 286 organ-weight fraction concept. *Plant Production Science*, **5**, 248-256.
- 287 Cao W, Moss DN (1997) Modelling phasic development in wheat: a conceptual integration of
 288 physiological components. *Journal of Agricultural Science*, **129**, 163-172.
- 289 Challinor A, Wheeler T, Craufurd P, Slingo J, Grimes D (2004) Design and optimisation of a large-area
 290 process-based model for annual crops. *Agricultural and Forest Meteorology*, **124**, 99-120.
- 291 Chen C, Wang E, Yu Q (2010) Modeling Wheat and Maize Productivity as Affected by Climate Variation
 292 and Irrigation Supply in North China Plain. *Agronomy Journal*, **102**, 1037-1049.
- 293 Cuculeanu V, Marica A, Simota C (1999) Climate change impact on agricultural crops and adaptation
 294 options in Romania. *Climate Research*, **12**, 153-160.
- 295 Donaldson E, Schillinger WF, Dofing SM (2001) Straw production and grain yield relationships in winter
 296 wheat. *Crop Science*, **41**, 100-106.
- 297 Fader M, Rost S, Muller C, Bondeau A, Gerten D (2010) Virtual water content of temperate cereals and
 298 maize: Present and potential future patterns. *Journal of Hydrology*, **384**, 218-231.
- 299 FAO (2010) *Asian wheat producing countries-Uzbekistan-Central Zone*,
 300 http://www.fao.org/ag/agp/agpc/doc/field/Wheat/asia/Uzbekistan/agroeco_central.htm (last
 301 visited: 09.22.2015).
- 302 FAO (2014) *Asian wheat producing countries-Uzbekistan-Central Zone*,
 303 http://www.fao.org/ag/agp/agpc/doc/field/Wheat/asia/Uzbekistan/agroeco_central.htm (last
 304 visited: 09.22.2015).
- 305 Ferrise R, Triossi A, Stratonovitch P, Bindi M, Martre P (2010) Sowing date and nitrogen fertilisation
 306 effects on dry matter and nitrogen dynamics for durum wheat: An experimental and simulation
 307 study. *Field Crops Research*, **117**, 245-257.
- 308 Franzluebbbers AJ, Stuedemann JA (2014) Crop and cattle production responses to tillage and cover crop
 309 management in an integrated crop–livestock system in the southeastern USA. *European Journal*
 310 *of Agronomy*, **57**, 62-70.
- 311 Gaiser T, Perkons U, Küpper PM *et al.* (2013) Modeling biopore effects on root growth and biomass
 312 production on soils with pronounced sub-soil clay accumulation. *Ecological Modelling*, **256**, 6-15.
- 313 Gbegbelegbe S, Cammarano D, Asseng S *et al.* (2017) Baseline simulation for global wheat production
 314 with CIMMYT mega-environment specific cultivars. *Field Crops Research*, **202**, 122-135.
- 315 Gerten D, Schaphoff S, Haberlandt U, Lucht W, Sitch S (2004) Terrestrial vegetation and water balance -
 316 hydrological evaluation of a dynamic global vegetation model. *Journal of Hydrology*, **286**, 249-
 317 270.
- 318 Goudriaan J, Van Laar HH (eds) (1994) *Modelling Potential Crop Growth Processes. Textbook With*
 319 *Exercises*, Dordrecht, The Netherlands, Kluwer Academic Publishers.
- 320 He J, Stratonovitch P, Allard V, Semenov MA, Martre P (2010) Global Sensitivity Analysis of the Process-
 321 Based Wheat Simulation Model SiriusQuality1 Identifies Key Genotypic Parameters and Unravels
 322 Parameters Interactions. *Procedia - Social and Behavioral Sciences*, **2**, 7676-7677.
- 323 Heng LK, Asseng S, Mejahed K, Rusan M (2007) Optimizing wheat productivity in two rain-fed
 324 environments of the West Asia–North Africa region using a simulation model. *European Journal*
 325 *of Agronomy*, **26**, 121-129.
- 326 Hoogenboom G, White J (2003) Improving physiological assumptions of simulation models by using
 327 gene-based approaches. *Agronomy Journal*, **95**, 82-89.

328 Hu J, Cao W, Zhang J, Jiang D, Feng J (2004) Quantifying responses of winter wheat physiological
329 processes to soil water stress for use in growth simulation modeling. *Pedosphere*, **14**, 509-518.

330 Hu W, Schoenau JJ, Cutforth HW, Si BC (2015) Effects of row-spacing and stubble height on soil water
331 content and water use by canola and wheat in the dry prairie region of Canada. *Agricultural
332 Water Management*, **153**, 77-85.

333 Huang G, Zhang R, Li G *et al.* (2008) Productivity and sustainability of a spring wheat–field pea rotation
334 in a semi-arid environment under conventional and conservation tillage systems. *Field Crops
335 Research*, **107**, 43-55.

336 Hunt LA, Pararajasingham S (1995) CROPSIM-wheat - a model describing the growth and development
337 of wheat. *Canadian Journal of Plant Science*, **75**, 619-632.

338 Ilbeyi A, Ustun H, Oweis T, Pala M, Benli B (2006) Wheat water productivity and yield in a cool highland
339 environment: Effect of early sowing with supplemental irrigation. *Agricultural Water
340 Management*, **82**, 399-410.

341 Iqbal M, Akhter J, Mohammad W, Shah S, Nawaz H, Mahmood K (2005) Effect of tillage and fertilizer
342 levels on wheat yield, nitrogen uptake and their correlation with carbon isotope discrimination
343 under rainfed conditions in north-west Pakistan. *Soil and Tillage Research*, **80**, 47-57.

344 Islam T (1991) Water use of a winter wheat cultivar (*Triticum aestivum*). *Agricultural Water
345 Management*, **19**, 77-84.

346 Izaurrealde R, Solberg E, Nyborg M, Malhi S (1998) Immediate effects of topsoil removal on crop
347 productivity loss and its restoration with commercial fertilizers. *Soil and Tillage Research*, **46**,
348 251-259.

349 Izaurrealde R, Williams JR, McGill WB, Rosenberg NJ, Jakas MQ (2006) Simulating soil C dynamics with
350 EPIC: Model description and testing against long-term data. *Ecological Modelling*, **192**, 362-384.

351 Izaurrealde RC, McGill WB, Williams JR (2012) Development and application of the EPIC model for carbon
352 cycle, greenhouse-gas mitigation, and biofuel studies. In: *Managing agricultural greenhouse
353 gases: Coordinated agricultural research through GRACEnet to address our changing climate*.
354 (eds Liebig MA, Franzluebbers AJ, Follett RF) pp Page. Amsterdam, Elsevier.

355 Jamieson P, Semenov M (2000) Modelling nitrogen uptake and redistribution in wheat. *Field Crops
356 Research*, **68**, 21-29.

357 Jamieson P, Semenov M, Brooking I, Francis G (1998) Sirius: a mechanistic model of wheat response to
358 environmental variation. *European Journal of Agronomy*, **8**, 161-179.

359 Jones J, Hoogenboom G, Porter C *et al.* (2003) The DSSAT cropping system model. *European Journal of
360 Agronomy*, **18**, 235-265.

361 Kassie BT, Asseng A, Porter CH, Royce F (2016) Performance of DSSAT-Nwheat across a wide range of
362 current and future growing conditions. *Field Crops Research*, **81**, 27-36.

363 Keating BA, Carberry PS, Hammer GL *et al.* (2003) An overview of APSIM, a model designed for farming
364 systems simulation. *European Journal of Agronomy*, **18**, 267-288.

365 Kersebaum K (2007) Modelling nitrogen dynamics in soil-crop systems with HERMES. *Nutrient Cycling in
366 Agroecosystems*, **77**, 39-52.

367 Kersebaum KC (2011) Special features of the HERMES model and additional procedures for
368 parameterization, calibration, validation, and applications. *Ahuja, L.R. and Ma, L. (eds.).
369 Methods of introducing system models into agricultural research. Advances in Agricultural
370 Systems Modeling Series 2, Madison (ASA-CSSA-SSSA)*, 65-94.

371 Kiniry JR, Williams J, Major D *et al.* (1995) EPIC model parameters for cereal, oilseed, and forage crops in
372 the northern Great Plains region. *Canadian Journal of Plant Science*, **75**, 679-688.

373 Latiri K, Lhomme J-P, Annabi M, Setter TL (2010) Wheat production in Tunisia: progress, inter-annual
374 variability and relation to rainfall. *European Journal of Agronomy*, **33**, 33-42.

375 Latta J, O'Leary G (2003) Long-term comparison of rotation and fallow tillage systems of wheat in
376 Australia. *Field Crops Research*, **83**, 173-190.

377 Lawless C, Semenov M, Jamieson P (2005) A wheat canopy model linking leaf area and phenology.
378 *European Journal of Agronomy*, **22**, 19-32.

379 Le S, Josse J, F. H (2008) FactoMineR: An R Package for Multivariate Analysis. *Journal of Statistical*
380 *Software*, **25**, 1-18.

381 Li C, Cao W, Zhang Y (2002) Comprehensive Pattern of Primordium Initiation in Shoot Apex of Wheat.
382 *ACTA Botanica Sinica*, 273-278.

383 Li S, Wheeler T, Challinor A, Lin E, Xu Y, Ju H (2010) Simulating the Impacts of Global Warming on Wheat
384 in China Using a Large Area Crop Model. *Acta Meteorologica Sinica*, **24**, 123-135.

385 Lithourgidis A, Damalas C, Gagianas A (2006) Long-term yield patterns for continuous winter wheat
386 cropping in northern Greece. *European Journal of Agronomy*, **25**, 208-214.

387 Liu B, Asseng S, Muller C *et al.* (2016) Similar estimates of temperature impacts on global wheat yield by
388 three independent methods. *Nature Clim. Change*, **6**, 1130-1136.

389 Müller C, Eickhout B, Zaehle S, Bondeau A, Cramer W, Lucht W (2007) Effects of changes in CO₂, climate,
390 and land use on the carbon balance of the land biosphere during the 21st century. *Journal of*
391 *Geophysical Research-Biogeosciences*, **112**.

392 Maiorano A, Martre P, Asseng S *et al.* (2017) Crop model improvement reduces the uncertainty of the
393 response to temperature of multi-model ensembles. *Field Crops Research*, **202**, 5-20.

394 Martre P, Jamieson PD, Semenov MA, Zyskowski RF, Porter JR, Triboi E (2006) Modelling protein content
395 and composition in relation to crop nitrogen dynamics for wheat. *European Journal of*
396 *Agronomy*, **25**, 138-154.

397 Mitchell D, Achutarao K, Allen M *et al.* (2017) Half a degree additional warming, prognosis and projected
398 impacts (HAPPI): background and experimental design. *Geoscientific Model Development*, **10**,
399 571-583.

400 Nendel C, Berg M, Kersebaum K *et al.* (2011) The MONICA model: Testing predictability for crop growth,
401 soil moisture and nitrogen dynamics. *Ecological Modelling*, **222**, 1614-1625.

402 O'Leary G, Connor D (1996a) A simulation model of the wheat crop in response to water and nitrogen
403 supply .1. Model construction. *Agricultural Systems*, **52**, 1-29.

404 O'Leary G, Connor D (1996b) A simulation model of the wheat crop in response to water and nitrogen
405 supply .2. Model validation. *Agricultural Systems*, **52**, 31-55.

406 O'Leary G, Connor D, White D (1985) A simulation-model of the development, growth and yield of the
407 wheat crop. *Agricultural Systems*, **17**, 1-26.

408 Pan J, Zhu Y, Cao W (2007) Modeling plant carbon flow and grain starch accumulation in wheat. *Field*
409 *Crops Research*, **101**, 276-284.

410 Pan J, Zhu Y, Jiang D, Dai TB, Li YX, Cao WX (2006) Modeling plant nitrogen uptake and grain nitrogen
411 accumulation in wheat. *Field Crops Research*, **97**, 322-336.

412 Pavlova VN, Varcheva SE, Bokusheva R, Calanca P (2014) Modelling the effects of climate variability on
413 spring wheat productivity in the steppe zone of Russia and Kazakhstan. *Ecological Modelling*,
414 **277**, 57-67.

415 Pecetti L, Hollington P (1997) Application of the CERES-Wheat simulation model to durum wheat in two
416 diverse Mediterranean environments. *European Journal of Agronomy*, **6**, 125-139.

417 Porter J (1984) A model of canopy development in winter wheat. *The Journal of Agricultural Science*,
418 **102**, 383-392.

419 Porter JR (1993) AFRCWHEAT2: a model of the growth and development of wheat incorporating
420 responses to water and nitrogen. *European Journal of Agronomy*, **2**, 69-82.

421 Portmann FT, Siebert S, Döll P (2010) MIRCA2000—Global monthly irrigated and rainfed crop areas
422 around the year 2000: A new high - resolution data set for agricultural and hydrological
423 modeling. *Global biogeochemical cycles*, **24**.

424 Priesack E, Gayler S, Hartmann H (2006) The impact of crop growth sub-model choice on simulated
425 water and nitrogen balances. *Nutrient Cycling in Agroecosystems*, **75**, 1-13.

426 R Core Team (2017) R: A language and environment for statistical computing. R Foundation for
427 Statistical Computing. Vienna, Austria. <https://www.R-project.org/>

428 Rötter RP, Palosuo T, Kersebaum KC *et al.* (2012) Simulation of spring barley yield in different climatic
429 zones of Northern and Central Europe: a comparison of nine crop models. *Field Crops Research*,
430 **133**, 23-36.

431 Ramirez-Rodrigues MA, Asseng S, Fraise C, Stefanova L, Eisenkolbi A (2014) Tailoring wheat
432 management to ENSO phases for increased wheat production in Paraguay. *Climate Risk*
433 *Management*, **3**, 24-38.

434 Ritchie JT, Godwin DC, Otter-Nacke S (1985) *CERES-wheat: A user-oriented wheat yield model.*
435 *Preliminary documentation.*

436 Ritchie S, Nguyen H, Holaday A (1987) Genetic diversity in photosynthesis and water-use efficiency of
437 wheat and wheat relatives. *Journal of Cellular Biochemistry*, 43-43.

438 Romero CC, Hoogenboom G, Baigorria GA, Koo J, Gijsman AJ, Wood S (2012) Reanalysis of a global soil
439 database for crop and environmental modeling. *Environmental Modelling & Software*, **35**, 163-
440 170.

441 Rost S, Gerten D, Bondeau A, Lucht W, Rohwer J, Schaphoff S (2008) Agricultural green and blue water
442 consumption and its influence on the global water system. *Water Resources Research*, **44**.

443 Royo C, Villegas D, Rharrabti Y, Blanco R, Martos V, García del Moral L (2006) Grain growth and yield
444 formation of durum wheat grown at contrasting latitudes and water regimes in a Mediterranean
445 environment. *Cereal Research Communications*, **34**, 1021-1028.

446 Ruane AC, Goldberg R, Chryssanthacopoulos J (2015) Climate forcing datasets for agricultural modeling:
447 Merged products for gap-filling and historical climate series estimation. *Agricultural and Forest*
448 *Meteorology*, **200**, 233-248.

449 Ruane AC, Phillips MM, Rosenzweig C (2018) Climate shifts for major agricultural seasons in +1.5 and
450 +2.0°C worlds: HAPPI projections and AgMIP modeling scenarios. *Agric. Forest Meteorol.*, **259**,
451 329–344. doi:10.1016/j.agrformet.2018.05.013

452 Schillinger WF, Schofstoll SE, Alldredge JR (2008) Available water and wheat grain yield relations in a
453 Mediterranean climate. *Field Crops Research*, **109**, 45-49.

454 Semenov M, Shewry P (2011) Modelling predicts that heat stress, not drought, will increase vulnerability
455 of wheat in Europe. *Scientific Reports*, **1**.

456 Senthilkumar S, Basso B, Kravchenko AN, Robertson GP (2009) Contemporary Evidence of Soil Carbon
457 Loss in the US Corn Belt. *Soil Science Society of America Journal*, **73**, 2078-2086.

458 Shibu M, Leffelaar P, van Keulen H, Aggarwal P (2010) LINTUL3, a simulation model for nitrogen-limited
459 situations: Application to rice. *European Journal of Agronomy*, **32**, 255-271.

460 Singels A, De Jager J (1991) Determination of optimum wheat cultivar characteristics using a growth
461 model. *Agricultural Systems*, **37**, 25-38.

462 Soltani A, Maddah V, Sinclair T (2013) SSM-Wheat: a simulation model for wheat development, growth
463 and yield. *International Journal of Plant Production*, **7**, 711-740.

464 Sommer R, Pignin C, Haddad A, Hajdibo A, Hayek P, Khalil Y (2012) Simulating the effects of zero tillage
465 and crop residue retention on water relations and yield of wheat under rainfed semiarid
466 Mediterranean conditions. *Field Crops Research*, **132**, 40-52.

467 Spitters CJT, Schapendonk AHCM (1990) Evaluation of breeding strategies for drought tolerance in
468 potato by means of crop growth simulation. *Plant and Soil*, **123**, 193-203.

469 Steduto P, Hsiao T, Raes D, Fereres E (2009) AquaCrop-The FAO Crop Model to Simulate Yield Response
470 to Water: I. Concepts and Underlying Principles. *Agronomy Journal*, **101**, 426-437.

471 Steduto P, Pocuca V, Caliandro A, Debaeke P (1995) An evaluation of the crop-growth simulation
472 submodel of epic for wheat grown in a Mediterranean climate with variable soil-water regimes.
473 *European Journal of Agronomy*, **4**, 335-345.

474 Stenger R, Priesack E, Barkle G, Sperr C (1999) Expert-N A tool for simulating nitrogen and carbon
475 dynamics in the soil-plant-atmosphere system. pp Page, New Zealand, Land Treatment
476 collective proceedings Technical Session.

477 Stockle C, Donatelli M, Nelson R (2003) CropSyst, a cropping systems simulation model. *European
478 Journal of Agronomy*, **18**, 289-307.

479 Tao F, Yokozawa M, Zhang Z (2009a) Modelling the impacts of weather and climate variability on crop
480 productivity over a large area: A new process-based model development, optimization, and
481 uncertainties analysis. *Agricultural and Forest Meteorology*, **149**, 831-850.

482 Tao F, Zhang Z (2010) Adaptation of maize production to climate change in North China Plain: Quantify
483 the relative contributions of adaptation options. *European Journal of Agronomy*, **33**, 103-116.

484 Tao F, Zhang Z (2013) Climate change, wheat productivity and water use in the North China Plain: A new
485 super-ensemble-based probabilistic projection. *Agricultural and Forest Meteorology*, **170**, 146-
486 165.

487 Tao F, Zhang Z, Liu J, Yokozawa M (2009b) Modelling the impacts of weather and climate variability on
488 crop productivity over a large area: A new super-ensemble-based probabilistic projection.
489 *Agricultural and Forest Meteorology*, **149**, 1266-1278.

490 Tavakkoli AR, Oweis TY (2004) The role of supplemental irrigation and nitrogen in producing bread
491 wheat in the highlands of Iran. *Agricultural Water Management*, **65**, 225-236.

492 van Rees H, McClelland T, Hochman Z, Carberry P, Hunt J, Huth N, Holzworth D (2014) Leading farmers in
493 South East Australia have closed the exploitable wheat yield gap: Prospects for further
494 improvement. *Field Crops Research*, **164**, 1-11.

495 Wang E, Engel T (2000) SPASS: a generic process-oriented crop model with versatile windows interfaces.
496 *Environmental Modelling & Software*, **15**, 179-188.

497 Wang E, Martre P, Zhao Z *et al.* (2017) The uncertainty of crop yield projections is reduced by improved
498 temperature response functions. *Nat Plants*, **3**, 17102.

499 Wang E, Robertson MJ, Hammer GL *et al.* (2002) Development of a generic crop model template in the
500 cropping system model APSIM. *European Journal of Agronomy*, **18**, 121-140.

501 Webber H, Gaiser T, Oomen R *et al.* (2016) Uncertainty in future irrigation water demand and risk of
502 crop failure for maize in Europe. *Environmental Research Letters*, **11**, 074007.

503 Weir A, Bragg P, Porter J, Rayner J (1984) A winter wheat crop simulation model without water or
504 nutrient limitations. *The Journal of Agricultural Science*, **102**, 371-382.

505 Williams J (1995) *The EPIC model in: Computer Models of Watershed Hydrology*, Water Resources
506 Publications, Highlands Ranch, Colorado, USA.

507 Williams JR, Jones CA, Kiniry JR, Spanel DA (1989) The EPIC crop growth model. *Transactions of the ASAE*,
508 **32**, 497-511.

509 Yan M, Cao W, C. Li ZW (2001) Validation and evaluation of a mechanistic model of phasic and
510 phenological development in wheat. *Chinese Agricultural Science*, **1**, 77-82.

511 Yin X, van Laar HH (2005) *Crop systems dynamics: an ecophysiological simulation model of genotype-by-
512 environment interactions*, Wageningen, The Netherlands, Wageningen Academic Publishers.

513 Zhao C, Liu B, Piao S *et al.* (2017) Temperature increase reduces global yields of major crops in four
514 independent estimates. *Proceedings of the National Academy of Sciences of the United States of
515 America*, **114**, 9326-9331.

